Universidade do Minho
Escola de Engenharia

Ana Catarina Rodrigues Milho

Control of Salmonella Enteritidis biofilms present on different food contact surfaces using bacteriophages

fevereiro de 2019

Universidade do Minho
Escola de Engenharia

Ana Catarina Rodrigues Milho

Control of Salmonella Enteritidis biofilms present on different food contact surfaces using bacteriophages

Tese de Doutoramento em Engenharia Química e Biológica

Trabalho efectuado sob a orientação de
Professora Doutora Sanna Maria Sillankorva
Professora Doutora Joana Cecília Valente de Rodrigues Azeredo

fevereiro de 2019

DECLARAÇÃO DE INTEGRIDADE

Declaro ter atuado com integridade na elaboração da presente tese. Confirmo que em todo o trabalho conducente à sua elaboração não recorri à prática de plágio ou a qualquer forma de falsificação de resultados. Mais declaro que tomei conhecimento integral do Código de Conduta Ética da Universidade do Minho.

Universidade do Minho, fevereiro de 2019

_____

Acknowledgments

Gostaria de agradecer a todos aqueles que, através do seu apoio e carinho, possibilitaram a concretização desta tese de doutoramento.

Antes de mais, gostaria de agradecer à Sanna, minha orientadora e amiga, que sempre me apoiou, e acreditou em mim e na minha capacidade de trabalho. Juntas, atravessámos tempestades, e juntas, conseguimos vencê-las. Estarás para sempre no meu coração.

À professora Joana, minha co-orientadora, por me ter dado a oportunidade de entrar para o seu grupo de trabalho e confiado em mim para desenvolver o tema da minha tese no seu laboratório. Ficar-lhe-ei eternamente agradecida por isso.

Aos meus colegas do LPhage, por me terem recebido de braços abertos quando cheguei a Braga; ao Henrique e ao Rodrigo, pela amizade e pelas belas gargalhadas que me proporcionaram desde que se juntaram ao nosso grupo, tornando o meu dia-a-dia no laboratório mais alegre; e ao Hugo, meu amigo do coração, pelos conselhos, relativos ao trabalho mas não só, pelas risadas, e por sempre me ter apoiado e acreditado em mim.

Aos meus amigos do LMaS, Di, Susana, Daniela, Ângela, Fernando, foi com muito gosto que a partir de janeiro de 2018 comecei a partilhar o espaço de trabalho convosco. Funcionamos na perfeição! O meu muito obrigada por me proporcionarem um ambiente de trabalho tão funcional e divertido.

Aos meus cúmplices da hora de almoço, hora do lanche e outras horas que tais: Pedro, Tina, Cláudia, Sara, Aloia, Chema, Beatriz, Elisa, Lina e Gabi. Obrigada por serem meus amigos e me deixarem almoçar e lanchar convosco. Sem vocês, a minha vida seria bem mais triste. Convosco, é uma alegria pegada!

Aos meus queridos amigos Cebianos Nuno, Di, Paula, Isa e Eva, por me aturarem durante estes cinco anos, e por terem estado sempre comigo nos bons e maus momentos. Por ouvirem as minhas lamúrias sem se queixarem disso, dando-me sempre apoio, força e carinho, sem os quais não teria sido capaz de terminar esta etapa da minha vida. Ficarei para sempre agradecida de vos ter conhecido.

Aos meus amigos da Margem Sul, alguns dos quais conheço há quase 30 anos... Bruno, Roberto, Ricardo, Natália, Alex, Carina, Valter, Fernanda: obrigada por serem o meu porto de abrigo sempre que vou a casa. Convosco estou de volta às minhas origens, com histórias e gargalhadas, como se voltássemos a ter 15 anos... Para sempre juntos!

Aos meus amigos de Lisboa: Vilma e Carolina, as minhas melhores amigas; Sara, Irina, Filipe, Joana, Nuno, Maria, meus amigos e antigos colegas de laboratório; André, Sara, Cátia e Lídia,

meus amigos da borga até às 7 da manhã. A todos vós, muito obrigada por fazerem parte da minha vida e me deixarem fazer parte da vossa. Sei que posso contar convosco, para o que der e vier.

À minha querida amiga Maria João, não só pela amizade e apoio, mas também pelas dicas de trabalho essenciais, sem as quais não teria sido capaz de terminar esta tese.

Ao meu namorado Carlos, pelo apoio, amor e carinho. Por felizmente perceberes muito mais de computadores que eu e me ajudares sempre que eu preciso de alguma coisa relacionada com informática (sou uma naba!). Por seres atencioso e me fazeres rir quando estou em baixo. Por me teres aturado nestes últimos dias de escrita da tese em que me tornei numa ermita. Finalmente, obrigada a ti, Carlos, por teres aparecido na minha vida no momento certo e me teres feito sentir que a tua família é a minha segunda família. Amo-te muito!

Aos meus queridos pais, Florinda e Armindo, e à chata da minha irmã, Telma: obrigada por serem a minha família, não queria outra. Obrigada pelo amor e apoio incondicionais que sempre demonstraram. Por acreditarem sempre em mim e nas minhas capacidades para enfrentar adversidades, mesmo quando eu não acreditava. Obrigada por serem quem são. Amo-vos do fundo do meu coração. Esta tese é-vos dedicada.

This study was supported by the Portuguese Foundation for Science and Technology (FCT) under the scope of the strategic funding of UID/BIO/04469 unit and COMPETE 2020 (POCI-01-0145-FEDER-006684) and BioTecNorte operation (NORTE-01-0145-FEDER-000004) funded by the European Regional Development Fund under the scope of Norte2020 - Programa Operacional Regional do Norte; by BioHealth - Biotechnology and Bioengineering approaches to improve health quality (NORTE-07-0124-FEDER-000027), under the scope of Programa Operacional Regional do Norte; by PSEUDOMONAL - Development of an anti-pseudomonal product with genetically modified phages to control biofilms formed by *Pseudomonas aeruginosa* (PTDC/EBB-BIO/114760/2009), under the scope of PIDDAC and COMPETE (FCOMP-01-0124-FEDER-014759); by FCT (IF/01413/2013) under the scope of Investigador FCT. The author also acknowledges FCT for the attribution of the PhD grant SFRH/BD/94434/2013.

Abstract

Salmonella, a human pathogenic bacterium, is still, nowadays, one of the main causes of food-related outbreaks, that result in thousands of illnesses and hospitalizations each year, around the globe. Contaminated poultry, fruit, and fresh vegetables are the key vehicles of human contamination, which could be prevented by the application of good processing practices and appropriate washing of food products. Besides this, the fact that *Salmonella* can form biofilms on food working surfaces and equipments, makes this microorganism even more difficult to eliminate with the commonly used chemical and physical cleaning procedures. Hence, the development of new *Salmonella* control strategies is imperative. Virulent bacterio(phages), viruses that exclusively infect bacteria, resulting in their lysis, are regarded as good alternatives for the elimination of *Salmonella* biofilms and adhered cells from contaminated surfaces and food products. Therefore, the main objective if this thesis was the application of phages for the control of *S.* Enteritidis biofilms formed on different food contact surfaces.

In this work, a *Salmonella* phage, named PVP-SE2, was genomically analysed, and based on the nowadays gene information available in databases, this phage does not encode for known toxins or antibiotic resistance, making it a great candidate for the biocontrol of *Salmonella*. Other characterizations were also completed, such as determination of its growth parameters and phage infectivity towards *S.* Enteritidis biofilm communities after artificial contamination of surfaces (e.g. polystyrene, stainless steel, and poultry skins). Results showed that this phage was capable of reducing the number of *Salmonella* cells adhered to these surfaces, and also of significantly reducing the bacterial loads present in the formed biofilms. These results reaffirmed PVP-SE2 potential to be used in the control of this pathogen.

Like most phage genomes, PVP-SE2 genome presented many open reading frames (ORFs) that encoded for proteins with unknown function. This comes as an obstacle since some of these ORFs may encode for proteins with toxic or other undesired properties. To be accepted in a possible phage-based product, the deletion of all of the ORFs with unknown and unnecessary functions would be ideal. Therefore, a strategy was designed: to use Bacteriophage Recombineering of Electroporated DNA to create a phage genome devoid of the ORFs with unknown and unnecessary functions. The first ORF with unknown function considered for deletion was Orf_01, which was successfully achieved. The stability of this mutation was evaluated, and the results showed that Orf_01 deletion was stable for at least 11 generations. The new recombinant phage, named PVP-SE2ΔOrf_01, was characterized regarding its replication parameters and ability to infect *S.* Enteritidis planktonic cells in the exponential and stationary phases. It was shown that, although

PVP-SE2ΔOrf_01's kinetics of infection were substatially different from the wild type phage, the reductions of *Salmonella* planktonic cells in both exponential and stationary phases were identical to the ones obtained for PVP-SE2, most likely due to the faster latent period of this phage compared to its parental phage. This work showed that BRED is a suitable method to genetically modify phages, and also that Orf_01 is not essential for PVP-SE2 replication and infection abilities.

Escherichia coli, another human pathogen commonly related to foodborne outbreaks, was previously shown to be present together with *Salmonella* in food processing facilities. This information led to the idea that these two bacteria could be forming mixed biofilms when contaminating food working surfaces. Hence, the last chapter of this thesis was dedicated to the study of interactions found to happen between *E. coli* and *S.* Enteritidis when forming dual-species biofilms, and how this relationship could affect the ability of a cocktail composed by two phages, DaIca, an *E. coli* phage, and φ135, a *Salmonella* phage, to control these mixed biofilm populations. First, kinetics formation of mono- and dual-species biofilms were characterized, showing that both bacteria grew more when alone than in mixed biofilms. Then, confocal laser microscopy imaging was used to characterize spatial distribution of both species when forming single and mixed biofilms, which showed that spatial distribution of cells in dual-species biofilms resembles the distribution of *E. coli* and *S.* Enteritidis, when in single biofilms. FTIR-ATR biofilm extracellular polymeric substances (EPS) matrices analyses were performed and showed that the EPS spectra of mixed species biofilms can either be a mixture of both species EPS, or that the EPS of one strains predominates. DaICa and φ135 phages were used to challenge both mono- and dual-species biofilms, and results showed that both phages had a better antibiofilm capacity against *E. coli* and *S.* Enteritidis, respectively, when these species formed single-species biofilms, rather than mixed biofilms. This could be explained by the alterations in biofilm structure, EPS composition when the two species are forming a mixed biofilm, by the differences in phage growth characteristics in the two strains of each species tested, and also the distinct growth characteristics of the strains used in this work.

In conclusion, this work has emphasized the importance of the control of *S.* Enteritidis biofilms using phages as an alternative to the usually used cleaning processes so cross-contamination of food products does not occur. However, it has been shown that, although phages can effectively reduce the number of viable cells present on different types of food contact surfaces, this is not enough. Therefore, the need to genetically modify phages so that they become more effective towards biofilms, which can be accomplished by the insertion, for example, of genes encoding for

enzymes with antibiofilm properties, or genome engineered phages that contain only essential genes for their replication and infectivity, so they become safer to be used in a possible phage-based product, is a reality and it should be pursued. Furthermore, since biofilms in nature are rarely composed just by one bacterial species, more studies of species-species interactions that can influence phage's antibiofilm properties must be done in a more exhaustive manner.

Sumário

Salmonella, uma bactéria patogénica para os humanos, continua a ser, nos dias de hoje, uma das principais causadoras de surtos relacionados com alimentos, que resultam em milhares de pessoas doentes e até mortes, por ano, em todo o mundo. Carne de aves, fruta e vegetais frescos são os principais veículos de contaminação de humanos, o que poderia ser evitado pela aplicação de boas práticas de processamento e de lavagem dos alimentos. Para além disso, o facto de *Salmonella* ter a capacidade de formar biofilmes em superfícies e equipamentos de processamento de alimentos, torna este microrganismo ainda mais difícil de eliminar com os procedimentos químicos e físicos normalmente usados na limpeza. Por isso, é imperativo o desenvolvimento de estratégias alternativas de controlo de *Salmonella*. Os (bacterió)fagos, vírus que infetam exclusivamente bactérias, são vistos como boas alternativas para a eliminação de biofilmes e células aderidas de *Salmonella* presentes em superfícies e alimentos contaminados. Deste modo, o principal objetivo do trabalho desenvolvido nesta tese foi a aplicação de fagos para o controlo de biofilmes de *Salmonella* Enteritidis formados em diferentes superfícies que periodicamente se encontram em contacto com alimentos.

No presente trabalho, o genoma do fago PVP-SE2, específico para *S.* Enteritidis, foi analisado, e os resultados obtidos demonstraram que não codifica para genes de toxinas nem genes de resistência a antibióticos conhecidos, tornando este fago um ótimo candidato para o biocontrolo deste agente patogénico. De seguida, os parâmetros de replicação do fago PVP-SE2 foram caracterizados para avaliar e confirmar a sua capacidade de infetar e replicar em células de *S.* Enteritidis, o microrganismo modelo usado neste estudo. Posteriormente, diferentes superfícies, como o polistireno, aço inoxidável, e pele de galinha, foram artificialmente contaminados com *S.* Enteritidis, durante várias horas, e tratadas com o fago PVP-SE2. Os resultados desta experiência mostraram que este fago foi capaz de reduzir o número de células de *S.* Enteritidis aderidas às superfícies descritas, e também de reduzir significativamente os níveis de bactérias presentes nos biofilmes formados. Estes resultados reafirmam o potencial do fago PVP-SE2 para ser usado no controlo de *Salmonella*.

Como a maioria dos genomas de fagos, o genoma do PVP-SE2 é constituído por várias *open reading frames* (*ORFs*) que codificam para proteínas de função desconhecida. Esta característica surge como um obstáculo porque algumas destas *ORFs* podem codificar para proteínas com propriedades tóxicas ou outras propriedades indesejadas. Para que seja aceite para um possível produto à base de fagos, a deleção de todas as *ORFs* com funções desconhecidas e desnecessárias à replicação do fago no seu hospedeiro seria a uma hipótese a ter em conta. Por

isso, uma estratégia foi definida: usar a técnica de *Bacteriophage Recombineering of Electroporated DNA* para criar um genoma livre de *ORFs* com funções desconhecidas e desnecessárias. A primeira *ORF* com função desconhecida que foi considerada para deleção foi a Orf_01, tarefa que foi concluída com sucesso. A estabilidade desta mutação foi avaliada e os resultados obtidos mostraram que a deleção da Orf_01 mantave-se estável durante pelo menos 11 gerações. O novo fago recombinante, nomeado PVP-SE2ΔOrf_01, foi caracterizado tendo em conta os seus parâmetros de replicação e a sua capacidade de infeção de células planctónicas de *S.* Enteritidis nas fases exponencial e estacionária. Neste trabalho, foi demonstrado que, apesar de o fago PVP-SE2ΔOrf_01 apresentar uma cinética de infeção bastante diferente daquela apresentada pelo fago selvagem, as reduções de células de *Salmonella* nas fases exponencial e estacionária foram idênticas às obtidas com o fago PVP-SE2. Este estudo mostra que a técnica de *Bacteriophage Recombineering of Electroporated DNA* é adequada à modificação genética de fagos, e simultaneamente que a Orf_01 não é essencial à replicação e capacidade de infeção do fago PVP-SE2.

Escherichia coli, outra bactéria patogénica para os humanos comummente relacionada com surtos de origem alimentar, foi já previamente isolada juntamente com *Salmonella* em instalações de processamento de alimentos. Esta informação levou à dedução de que estas duas espécies bacterianas poderiam formar biofilmes mistos em superfícies de processamento alimentar. Assim, o último capítulo desta tese foi dedicado ao estudo das interações que surgem entre *E. coli* e *S.* Enteritidis quando estas formam biofilmes mistos, e como esta relação poderia afetar a capacidade de um cocktail fágico, composto pelos fagos Dalca, de *E. coli*, e φ135, de *S.* Enteritidis, de controlar estes biofilmes. Primeiramente, as cinéticas de formação dos biofilmes simples e mistos foram caracterizadas, mostrando que ambas as espécies crescem melhor em biofilmes simples do que em mistos. De seguida, a tecnologia de microscopia confocal a laser foi utilizada para caracterizar a distribuição espacial de ambas as espécies ao formarem biofilmes simples e mistos, o que revelou que a distribuição das células em biofilmes mistos se assemelha à distribuição de *E. coli* e *S.* Enteritidis em biofilmes simples. A técnica de espetroscopia de infravermelho com transformada de Fourier com refletância total atenuada foi usada para analisar as matrizes de substâncias poliméricas extracelulares dos biofilmes estudados, revelando que os espectros destas em biofilmes mistos podem ser, por um lado, uma mistura de substâncias poliméricas extracelulares de ambas as espécies, ou por outro, que as substâncias poliméricas extracelulares

de uma espécie são predominantes. Os fagos Dalca e φ135 foram aplicados em biofilmes simples e mistos, sendo que os resultados obtidos mostraram que ambos os fagos apresentam uma capacidade anti-biofilme mais elevada contra *E. coli* e *S.* Enteritidis, respetivamente, quando estas se encontram em biofilmes simples do que quando se apresentam em biofilmes mistos. Estes resultados podem ser explicados pelas alterações sofridas na estrutura dos biofilmes e composição das suas substâncias poliméricas extracelulares quando as duas espécies estão presentes num biofilme misto.

Em conclusão, esta tese enfatiza a importância do controlo de biofilmes de *S.* Enteritidis usando fagos como alternativa aos usuais procedimentos de limpeza de forma a que a contaminação cruzada de alimentos não ocorra. Contudo, ficou demostrado que, apesar de os fagos terem a capacidade de reduzirem o número de células viáveis presentes em diferentes tipos de superfícies que se encontram em contacto com produtos alimentares, esta redução não é suficiente. Desta forma, a necessidade de adotar novas estratégias de controlo de biofilmes de *Salmonella*, como o uso de fagos geneticamente modificados com capacidade aumentada de diminuir o número de células bacterianas presentes nos biofilmes, pela inserção, por exemplo, de genes que codifiquem para enzimas com ação contra os biofilmes, ou desenvolver fagos geneticamente modificados para conter apenas genes essenciais para a sua replicação e capacidade de infeção, de modo a que se tornem mais seguros para serem usados num possível produto baseado em fagos, é uma realidade e deve ser tida em conta. Para além disso, uma vez que, na natureza, os biofilmes são raramente constituídos por uma única espécie bacteriana, estudos mais aprofundados das interações espécie-espécie que podem influenciar as propriedades anti-biofilme dos fagos devem ser levados a cabo.

Table of Contents

Table of Contents

CHAPTER I - General Introduction

CHAPTER II - Control of *Salmonella* Enteritidis on Food Contact Surfaces with Bacteriophage PVP-SE2

List of Figures

List of Tables

List of Abbreviations, Acronyms and Symbols

AA	Amino acids
BRED	Bacteriophage Recombineering of Electroporated DNA
bp	base pairs
BSA	Bovine serum albumin
CDC	Centers for Disease Control and Prevention
CDS	Coding sequence
CFU	Colony forming unit
CI	Competitive index
CLSM	Confocal laser scanner microscopy
CRISPR/Cas	Clustered Regularly Interspaced Short Palindromic Repeats/ CRISPR associated
DNA	Deoxyribonucleic acid
DSB	Double-strand break
EC 434	*Escherichia coli* 434 strain
EC 515	*Escherichia coli* 515 strain
EDTA	Ethylenediamine tetraacetic acid
EFSA	European Food Safety Authority
EPS	Extracellular polymeric substances
ETN	Ethanolamine
EU	European Union
FAS	Ferric ammonium sulphate
FDA	Food and Drug Administration
FTIR-ATR	Fourie transformed infrared-attenuated total reflectance
Gal	Galactose
Glc	Glucose
GlcNac	N-Acetylglucosamine
GMPs	Good Manufacturing Practices
HACCP	Hazard Analysis and Critical Control Points
HDR	Homology-directed repair
Hep	Heptose
h	hour
IPTG	Isopropyl β-D-1-thiogalactopyranoside
KDO	3-deoxy-D-manno-2-octulosonic acid
LB	Luria-Bertani medium
LEDS	Laboratory-based Enteric Disease Surveillance system
LOD	Limit of detection
LPS	Lipopolysaccharide
MAGE	Multiplex Automated Genomic Engineering

min	minute
MLST	Multilocus sequence typing
MOI	Multiplicity of infection
NARMS	National Antimicrobial Resistance Monitoring System
NCBI	National Center for Biotechnology Information
NHEJ	Non-homologous end-joining
OD_{620}	Optical density at 620 nm
ORF	Open reading frame
PCA	Principal component analysis
PCR	Polymerase chain reaction
PEEC	Pathogen-elicited epithelial chemoattractant
PFGE	Pulse-field gel electrophoresis
PFU	Plaque forming unit
Phages	Bacteriophages
PMN	Polymorphonuclear leukocytes
PT	Phage typing
RIR	Relative increase ratio
RNA	Ribonucleic acid
SCV	*Salmonella*-containing vacuole
SD	Standard deviation
SDS	Sodium dodecyl sulphate
SE 269	*Salmonella* Enteritidis 269 strain
SE EX2	*Salmonella* Enteritidis EX2 strain
SEM	Scanning electron microscope
sec	second
sfGFP	Superfolder green fluorescent protein
SIF	*Salmonella* induced filaments
SM buffer	Sodium chloride/magnesium sulphate buffer
SNV	Standard normal variate
SPI-I	*Salmonella* pathogenicity island I
SPI-II	*Salmonella* pathogenicity island II
T3SS	Type-III secretion system
T3SS-I	Type-III secretion system I
T3SS-II	Type-III secretion system II
TALEN	Transcription activator-like effector nuclease
T	Temperature
t_d	Doubling time

Tm	Melting temperature
TEM	Transmission electron microscopy
USDA	United States Department of Agriculture
WHO	World Health Organization
ZFN	Zinc-finger nuclease
μ_{max}	Specific growth rate
2D	Two dimensions
3D	Three dimensions

Papers in peer-reviewed international journals

Milho C, Silva MD, Melo L, Santos S, Azeredo J, Sillankorva S. **Control of *Salmonella* Enteritidis on food contact surfaces with bacteriophage PVP-SE2.** 2018. Biofouling (30:1-16; doi: 10.1080/08927014.2018.1501475).

Papers under preparation

Milho C, Azeredo J, Sillankorva S. **Using synthetic biology tools to engineer *Salmonella* phage PVP-SE2: mutation stability and infectivity characterization (submitted).**

Milho C, Silva MD, Alves D, Oliveira H, Sousa C, Azeredo J, Sillankorva S. **Interspecies interactions of *Escherichia coli* and *Salmonella* Enteritidis in dual-species biofilms and their control by phages (submitted).**

Book chapters

Milho C, Silva MD, Sillankorva M. **Biofilm applications of bacteriophages *In* Bacteriophages - Biology, Technology, Therapy.** 2019. Eds. Harper D, Abedon S, Burrowes B, McConville M. Springer International Publishing (ISBN 978-3-319-41985-5).

Costa AR, Milho C, Azeredo J, Pires DP. **Synthetic biology to engineer bacteriophage genome *In* Bacteriophage Therapy.** 2018. Eds. Azeredo J, Sillankorva S. Humana Press (ISBN 978-1-4939-7395-8; doi: 10.1007/978-1-4939-7395-8).

Abstracts and proceedings in international conferences

Milho C, Silva MD, Alves DF, Azeredo J, Sillankorva S. **Interspecies interactions of *Salmonella* Enteritidis and *Escherichia coli* in dual-species biofilms and their control by bacteriophages.** Viruses of Microbes 2018 (EMBO Workshop) - Abstract Book, (414), 298, 2018, Wrocław, Poland.

Milho C, Silva MD, Alves DF, Azeredo J, Sillankorva S. **Interspecies interactions and bacteriophage control in *S.* Enteritidis and *E. coli* mixed biofilms.** Microbiotec'17 - Congress of Microbiology and Biotechnology 2017, (P-225), 342, 2017, Porto, Portugal.

Milho C, Silva MD, Melo L, Santos S, Azeredo J, Sillankorva S. **Control of *Salmonella* Enteritidis on food contact surfaces with bacteriophage PVP-SE2.** Phages in Medicine, Food and Biotechnology, 13-14 September 2017, Oxford, United Kingdom.

Milho C, Nogueira M, Simões C, Ackermann H, Kropinski AM, Azeredo J, Sillankorva S. **Use of bacteriophages to prevent *Salmonella* Enteritidis biofilm formation on poultry skins at refrigerated temperatures.** Biofilms 7, 26-28 June 2016, Porto, Portugal.

List of Publications

Milho C, Sillankorva S. **Prevention and control of *Salmonella* Enteritidis on poultry skins at refrigerated and room temperatures using φ38 phage.** Phages in Interaction IV, Leuven, Belgium, September 2015.

Chapter I

General Introduction

This chapter was based on the following book chapters:

Milho C, Silva MD, Sillankorva S. Biofilm applications of bacteriophages *In* Bacteriophages - Biology, Technology, Therapy. 2019. Eds. Harper D, Abedon S, Burrowes B, McConville M. Springer International Publishing (ISBN 978-3-319-41985-5)

Rita Costa A, Milho C, Azeredo J, Pires DP. Synthetic biology to engineer bacteriophage genomes *In* Bacteriophage Therapy. 2018. Eds. Azeredo J, Sillankorva S. Humana Press (ISBN 978-1-4939-7395-8; doi: 10.1007/978-1-4939-7395-8)

Abstract

Salmonella enterica is one of the major pathogens responsible for outbreaks related to the consumption of contaminated food products. Although some serovars, like *S.* Typhi and *S.* Paratyphi, can cause threatening health issues, infection with most serovars result in symptoms like diarrhea, vomiting, fever and abdominal cramps, which are usually self-limiting. Contaminated water and poultry products are the most common vehicles of human infections. Food products often come into contact with *S. enterica* through cross-contamination from food handling surfaces and utensils, in the case of poultry meat, or through the contact with feces, when considering eggs. The ability of *Salmonella enterica* to form biofilms constitutes one of its many virulence factors. These structured and complex microbial communities contribute largely to the dissemination of *Salmonella*, since, in this state, bacteria become more resistant to most of the control procedures, such as desiccation, chemical treatments, and physical methods, that are typically adopted in food handling facilities. (Bacterio)phages, the natural predators of bacteria, have regained visibility for biofilm control purposes, as bacterial resistance to antimicrobials has become a major problem. However, the use of phages as biocontrol agents is still not a consensual matter, not only because of their narrow host spectrum, but also due to the number of genes present in phage genomes that encode for proteins with unknown function or the development of resistance by bacteria to phages. To overcome these limitations, synthetic biology tools, like BRED and CRISPR/Cas, can be applied to genetically modify phages to make their host spectrum broader or to eliminate genes with unknown and unnecessary function. These and other synthetic biology strategies may be the future for phages to become universally accepted as food biocontrol agents.

Keywords*: Salmonella enterica*; bacteriophages; biofilms; synthetic biology

1.1 *Salmonella*: overview

Salmonella is a genus of Gram-negative, facultative anaerobe enterobacteria, displaying peritrichous flagella and motility [1] . It is constituted by species *S. bongori* and *S. enterica*, being the latter divided into six subspecies: *enterica*, *salamae*, *arizonae*, *diarizonae*, *houtenae*, and *indica* [2]. *S. enterica* comprises more than 2500 serovars, and over 50% of these belong to the *S. enterica* subsp. *enterica*, which, despite of their high genetic similarity, vary greatly in their host range and disease outcome, ranging from enteritis to typhoid fever [3,4]. *S. enterica* subsp. *enterica* members are usually related to warm-blooded vertebrates like livestock animals, which are mainly infected by the ingestion of water or food contaminated by feces containing this bacterium [3].

Salmonella is one of the main causes of zoonotic diseases worldwide. Bacteria belonging to this genus can cause fever, diarrhea, abdominal cramps, and even death, when ingested [5]. Every year, *Salmonella* is estimated to cause 1.2 million illnesses in the United States, with 23,000 hospitalizations and 450 deaths [6]. In the European Union (EU), more than 100,000 new human infections are reported each year, being estimated that the economic burden of salmonellosis in humans can reach 3 billion euros per year [7,8]. The first reported outbreak dates from 1923 due to consumption of unpasteurized apple cider rinsed in a stream contaminated with serovar *S. enterica* subsp. *enterica* serovar Typhi (*S.* Typhi). This pathogen causes enteric fever, an illness that, if left untreated, can lead to death [9,10]. However, this is not the only serovar involved in foodborne illnesses. Currently, the most common *Salmonella* serovars isolated during outbreaks, both in the USA and EU, are *S. enterica* subsp. *enterica* serovar Enteritidis (*S.* Enteritidis) and *S. enterica* subsp. *enterica* serovar Typhimurium (*S.* Typhimurium) [7,11].

Among the different *S. enterica* serovars, *S.* Enteritidis is the most reported serovar in human cases, representing 45.7% of the total number of confirmed cases of salmonellosis in the EU per year, which corresponds to approximately to 43,000 cases [7]. This bacterium causes an acute gastroenteritis, that is characterized by diarrhea, abdominal cramps, fever, nausea and vomiting, but is usually self-limiting [12]. However, invasive infections, like bacteremia and meningitis, can occur, for which antimicrobial therapy is necessary [13].

1.2 Human salmonellosis pathogenesis

Salmonella is acquired by humans usually through the consumption of contaminated water and food, which, eventually, leads to the development of an acute gastroenteritis [12] . To successfully stablish an infection, *Salmonella* has to overcome several stages such as the adhesion to the surface of the host cell, production of virulence factors, which facilitate invasion and multiplication, while simultaneously managing to surpass the host's immune defense mechanisms [14]. After being ingested, *Salmonella* must survive the low pH found in the stomach, so it can proceed to colonize different organs in the human body, such as the small intestine, colon, and cecum [15]. This colonization begins with the adhesion of *Salmonella* to the intestinal surface, process that comprises two stages, namely a reversible and irreversible adhesion [16]. In this way, *Salmonella* interacts with host cells before invasion or when it forms biofilms on the surface of the intestinal epithelium. This interaction is mediated by fimbriae, like type 1 and long polar fimbriae, non-fimbrial adhesins, such as type-I secretion system substrate SiiE protein, flagella, assembled by a flagellar-specific type-III secretion system (T3SS), among other cell components, that are expressed at the bacterial cell surface, to guarantee that the adhesion process is successfully completed [17–19].

Once attached to the intestinal lumen, *Salmonella* must be internalized so it can survive and multiply, and to do that it induces its own phagocytosis by the expression of genes present in *Salmonella* pathogenicity islands (SPI) I and II [20,21]. Among the genes present in the SPI-I are the ones encoding for the type-III secretion system I (T3SS-I), which becomes active upon contact with host cells and translocates effector proteins into them, helping host cell invasion by remodelling the plasma membrane and manipulating signaling host cell pathways [22,23]. SopB is an example of an effector protein secreted by the T3SS-I, and it plays a relevant role in the activation of secretory pathways, inducing inflammation and altering ion balances within cells, leading to secretion of fluids in the gastrointestinal tract and consequent diarrhea [24,25]. Other translocated effectors, like SipA, SipC and SopE, can interact with the actin cytoskeleton, causing the host cell membrane to extend outwards, which facilitates engulfment and internalization of *Salmonella* by the host cell [26–28]. After invasion, *Salmonella* is internalized into an early endosome inside cells such as M cells, which are used as passage to the reticuloendothelial system, epithelial cells, dendritic cells (major antigen presenting cells) and macrophages, that are specialized in the detection, phagocytosis, and destruction of bacteria and also act as reservoir for *Salmonella* (revised in [19]). For this new endosome, named *Salmonella*-containing vacuole (SCV), to mature and enable

survival and replication of bacterial cells, the type-III secretion system II (T3SS-II), encoded by the SPI-II, is expressed, and more than 30 effector proteins are secreted into the lumen of the SCV [29]. Some of these effectors are responsible for the maintenance of the SCV (SifA, SopD2, SseJ and PipB2), its positioning in the juxtanuclear region, near the Golgi apparatus (SseF and SseG), modulation of the host immune system (SpvC, SspH1 and SseL), and also for interactions with the host cytoskeleton (SteC, SpvB, SspH2 and SrfH) [29]. As the SCV matures and is surrounded by actin polymerization events, it migrates from the intestinal luminal border to the basal membrane, thus avoiding degradation by phagolysosomes [30]. *Salmonella* evades these organelles by increasing phosphatidylinositol-3-phosphate levels on the SCV and creating a compartment with characteristics of late endosome, with the presence of, for example, EEA1 protein, involved in the fusion of early and late endosomes, SCV lumen acidification, and acquisition of several lysosomal proteins [31]. However, SCV content differs from the phagolysosome lumen as it does not contain lysosomal hydrolases [32]. After SCV reaches its appropriate position, *Salmonella* cells begin to replicate, and *Salmonella* induced filaments (SIF) start to form by the action of several T3SS-II effectors, which promote the maintenance of the integrity of SCV [33]. These effectors may be also responsible for the delivery of nutrients to the SCV, thus helping bacterial multiplication [14]. While these events occur, other processes are simultaneously taking place that lead to the appearance of salmonellosis symptoms. For example, the previously mentioned SopB protein is responsible for the increase of Ins(1,4,5,6)P4 concentration, which can antagonize the closure of chloride channel, leading to electrolyte imbalance and fluid secretion [34]. Also, epithelial cells infected with *Salmonella* secrete chemokines [35] and prostaglandins [36], which results in the recruitment to the infection locus of inflammatory cells that interact with *Salmonella*. This interaction promotes the release of proinflammatory cytokines, intensifying the inflammatory response [37]. Then, infected epithelial cells deliver the pathogen-elicited epithelial chemoattractant (PEEC) through the apical membrane, stimulating the transepithelial migration of polymorphonuclear leukocytes (PMNs) between epithelial cells [38], and are responsible for the phagocytosis and killing of *Salmonella* cells [39]. Epithelial cells infected with *Salmonella* that escaped the immune system become extruded from the intestinal villus surface, resulting in the releasing of infected cells into the intestinal lumen and in the villus flattening, which ultimately causes loss of absorptive surfaces and subsequently the appearance of diarrhea [25].

1.3 *Salmonella* biofilms: a major virulence factor

Among the different virulence traits displayed by *Salmonella*, the ability to form biofilms on abiotic and biotic surfaces is one of the most important when it comes to food spoilage, disease dissemination and even industrial equipment degradation [40–44]. Furthermore, living in a biofilm state enables *Salmonella* to survive and multiply under harsh conditions such as food industrial plants [45]. In food industrial settings, biofilms may be formed in different types of surfaces (Figure 1.1). Food processing surfaces and utensils are an excellent niche for biofilm formation due to the nutritional richness allied to the suitable conditions of temperature and pH in the environment [46]. Biofilms can also be formed on equipment surfaces, particularly those with high humidity or moisture levels, which do not necessarily contact directly with foods. Cross-contamination, however, is a major cause of food product contamination, for instance, as a result of spread of moisture drops and aerosols formed during cleaning and worker's activity [44].

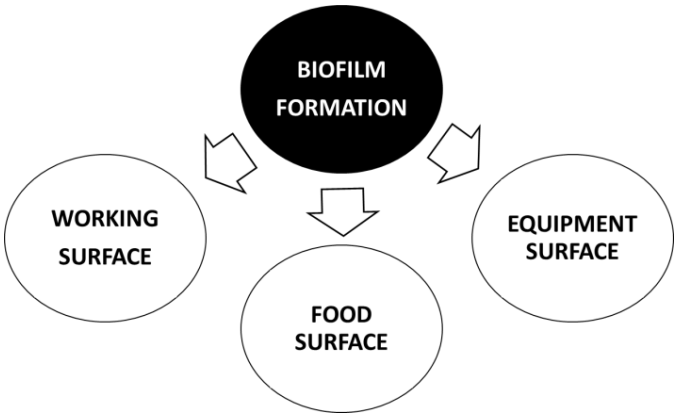

Figure 1.1 - Biofilm formation in food industry surfaces.

There is consensus that biofilm formation involves a series of sequential steps or stages (Figure 1.2). First, a conditioning film is formed on a surface. In food environments, organic and inorganic molecules, including proteins, lipids, nucleic acids, and others, released from foods (such as, milk, meat, fruits, vegetables) adsorb to the surface almost immediately after surfaces come into contact with a liquid phase, forming a layer at the water/solid interface. This results in an increased concentration of nutrients on the surface and also alters the physicochemical properties of the surface [47–49].

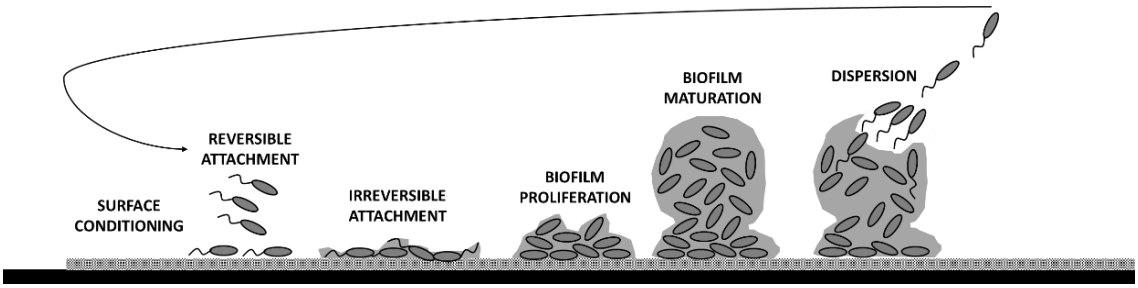

Figure 1.2 - Biofilm formation steps.

The second stage of biofilm formation is the reversible attachment of bacteria to the surface. Bacteria approach the surface either randomly or in a directed manner via chemotaxis and motility, and weak interactions, such as electrostatic forces, van der Waals forces, and hydrophobic interactions, developed between them and the surface. Determination of whether further levels of attachment will occur depends on the net sum of the attractive and repulsive forces that are generated. The physicochemical properties of the surface, the existence of nutrients, the conditions of surrounding environment, the bacterial growth stage and the existence of bacterial structures, such as fimbriae and flagella, also influence bacterial attachment. It is noteworthy that, in this stage, bacteria can easily be detached from the surface if the environment is not favorable [44,47,50].

Once reversibly attached, if conditions are favorable, then bacteria can become irreversibly attached. In this stage, several short-range forces are involved, such as dipole-dipole interactions, hydrogen, ionic and covalent bonding, and hydrophobic interactions. The attachment is reinforced by bacterial surface structures, including receptor-specific ligands located on pili, fimbriae, and fibrillae. The most important characteristic of the irreversible attachment stage is the production of extracellular polymeric substances (EPS), which aid in attachment of the bacterial cell to the surface. EPS consists mainly of polysaccharides, but it also can contain nucleic and amino acids, glycoproteins and phosphoproteins, sugars, phospholipids, uronic acids, and phenolic compounds. In addition to strengthening the attachment, EPS is responsible for a reduction in diffusional transport, which alters the physiological status of the embedded bacterial cells, decreasing their growth and metabolism rates, nutrient storage, and increased resistance to antimicrobial agents. At the end of this stage, bacterial attachment to the surface is irreversible, unless any physical or chemical intervention is applied [44,50].

Following irreversible attachment, bacterial cells grow and divide, intercommunicating through chemical signals. The production of EPS is enhanced, with bacteria multiplying within this structure, which results in the formation of microcolonies. Their continuous growth leads to the formation of a layer of bacterial cells that can cover the entire exposed surface [47,51].

The density and complexity of biofilms increases with the continued attachment and growth of bacteria as well as EPS production, resulting in multi-layers of bacterial cells embedded within the EPS matrix. Within the biofilm, also exist water-filled channels that are responsible for transporting nutrients and removing waste products. Different microorganisms with different nutritional requirements can attach and colonize the surface, contributing to the heterogeneity of the biofilm. At this stage, a mature biofilm with a complex three-dimensional structure has been formed (Figure 1.3) [47,51]. As biofilms mature, cells detach and disperse from the original biofilm. Detachment can be a consequence of nutrient depletion, decreased pH or oxygenation, and accumulation of toxic products. Fluid dynamics and shear forces of the bulk fluid also contribute to the dispersion of biofilm cells. Specific enzymes that degrade the EPS of different microorganisms may be produced, contributing to the detachment of cells from the biofilm. It is thought that biofilm-released cells are phenotypically more similar to planktonic cells than to biofilm cells. The released cells are able to colonize new niches and initiate the formation of new biofilms [47,49,51].

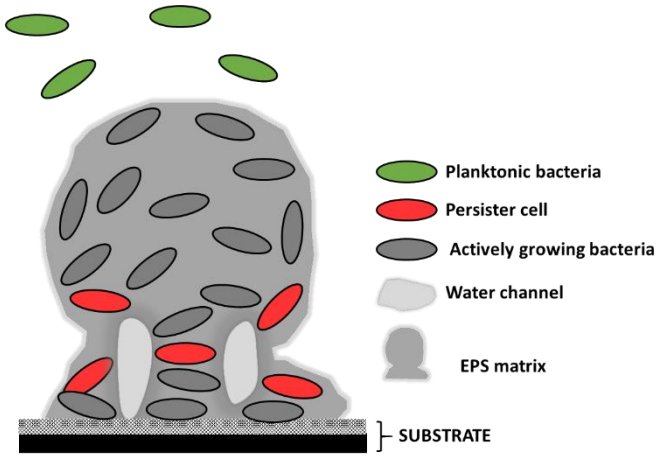

Figure 1.3 - Representation of a mature biofilm.

Bacterial organization into multispecies communities attached to surfaces is common in industry, as in any other natural environment. In fact, life in a multispecies biofilm confers ecological advantages, in comparison to planktonic living or even single-species biofilms. Within the EPS matrix, bacteria are protected from environmental damages [52], host immune defenses, if the pathogens are infecting animals [53], and, most relevantly, from antimicrobial agents [54,55]. Cells

can easily intercommunicate within the biofilm structure and horizontally transfer genes. Furthermore, biofilm formation is associated with an alteration in gene expression, being under the control of a gene regulation system known as quorum sensing. The lower growth rate of bacteria when living as a biofilm is also advantageous, contributing to their increased antimicrobial resistance [56,57]. The presence of persister cells in the biofilm environment, those that are in a state of dormancy, a state in which cells are metabolically inactive, is of utmost importance due to their high tolerance to antimicrobials. It has been suggested that persister cells are the major responsible for the recalcitrance of biofilms to these agents [58,59].

Biofilm formation, particularly of *Salmonella*, has a notable impact in different food industry settings. *Salmonella* biofilms are of special concern in the poultry [60], eggs [61], red meat [62], seafood [63,64], and fresh fruits and vegetable processing industries [65] (Figure 1.4). In this way, biofilms act as reservoir for *Salmonella* to cross-contaminate food products during their processing, which ultimately leads to great economical losses for the producers [66]. Different approaches have been adopted in order to eliminate biofilms from food environments, including the use of chemical sanitizers [67], natural compounds [68], enzymes [69], among others. However, bacterial cells in the biofilm state have increased resistance to the usually used disinfection procedures [52]. On the other hand, *Salmonella* may be found in food processing facilities forming microbial consortia with another highly pathogenic biofilm producer regularly linked to food-related outbreaks, *Escherichia coli* [7]. This relationship has been shown to make these mixed communities even more difficult to eliminate [70]. Hence, the development of new and/ or improved methods for the removal of biofilms from food processing facilities is critical.

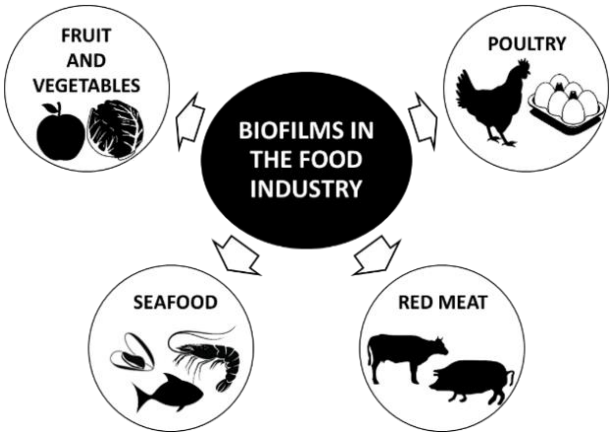

Figure 1.4 - Fields within the food industry with reported problems due to biofilm formation.

1.4 *Salmonella* antibiotic resistance emergence

Antibiotic resistance has been linked to the overuse and misuse of antibiotics in clinical and veterinary medicine, agriculture, including animal production, aquaculture, and horticulture [71]. These malpractices have released significant amounts of antibiotics into the environment, and environmental antibiotic contamination has been recognized as a worldwide phenomenon [72,73], with concentrations found in wastewaters, soils, and sediments ranging from μg/kg to mg/kg. More importantly, the antibiotics in the environment generally resist to biodegradation due to their antimicrobial nature and have, therefore, been classified as emerging pseudo-persistent organic pollutants for their continual input into the environment and permanent presence [74–76]. The same resistance genes found at clinical settings are currently disseminated among pristine ecosystems without any record of antibiotic contamination [77]. Like many other pathogens, the emergence of antibiotic resistance by *S. enterica* serovars is alarming. The Center for Disease Control and Prevention (CDC) reported an eight-year surveillance study categorizing drug-resistant *Salmonella* into ampicillin-only resistance, ceftriaxone/ampicillin resistance, and ciprofloxacin nonsusceptibility [78]. This study was completed by two surveillance systems: The National Antimicrobial Resistance Monitoring System (NARMS); and the Laboratory-based Enteric Disease Surveillance (LEDS) system. LEDS confirmed 369,254 culture-confirmed infections and NARMS confirmed 19,410. Of these samples, on a yearly basis, there were 6,200 resistant culture-confirmed infections: 55% ampicillin-resistant only, 27% ceftriaxone/ampicillin resistant, and 18% ciprofloxacin non-susceptible.

1.5 Bacteriophages and their use in the control of *Salmonella*

(Bacterio)phages are viruses that infect bacteria. They are ubiquitous in the environment, including oceans, soil, deep sea vents, water, and food [79]. It is estimated that phages exist in gigantic amounts that range from 10^{30} to 10^{32} in total, which makes them the most abundant living entities on Earth [80]. They perform very import functions in the regulation of the microbial equilibrium in every ecosystem where this has been investigate [81,82].

Based on their lifestyle, phages can be separated into two different groups: virulent or temperate phages. Virulent phages multiply through a lytic life cycle that ultimately results in the host cell's death. In the lytic life cycle, the phage particle attaches to the host cell surface and introduces its genome. During these first steps, the phage highjacks the host molecular machinery, which

becomes dedicated to the production of new phage particles. Within minutes or hours, depending on the phage growth kinetics, cell lysis occurs, releasing new progeny phages. On the other hand, temperate phages are able to choose the lytic or the lysogenic life cycle. In the lysogenic cycle, the phage genome is injected into the host cell and it can reach a quiescent state, the prophage, which can be integrated into the host genome or maintained as a plasmid. Prophages can remain in this quiescent state by an undetermined time, but eventually, they can end up entering in the lytic cycle [83].

Classification of phages can be done according to their structural, physicochemical, and biological properties. Having or not a tail is one of phages' structural characteristics that are used for their discrimination. Tailed phages (order *Caudovirales*), which contain dsDNA genomes, are the largest and more widespread group of phages, and they are divided into three families: *Myoviridae*, which contain contractile tails; *Siphoviridae*, that present long, noncontractile tails; and *Podoviridae*, which phages comprise short, noncontractile tails [84]. More biological properties can be used for the differentiation of phages, but this is not the focus of this introduction.

Phages have been extensively studied for bacterial control, mainly because of the many advantages they present compared to other biocontrol agents, such as : I) phages are highly specific to their host cells; II) they are self-replicating and self-limiting; III) they show low inherent toxicity; IV) they are cheap and easy to isolate and propagate; V) they are resistant to food processing and environmental stresses; VI) and finally, because phages present a long shelf life [85]. For these reasons, efforts have been made to develop phage-based products to be used in the control of foodborne pathogens. To this moment, the US Food and Drug Administration (FDA) has approved PhageGuard Listex™ (previously known as Listex™ P100), for *Listeria*, PhageGuard S™ (previously known as Salmonelex™), for *Salmonella*, ListShield™, for *Listeria*, EcoShield™, for *E. coli*, and SalmoFresh™, for *Salmonella*. Nevertheless, many report low levels of reduction in meats, ready-to-eat foods, and fresh produce, sometimes leading to less than 1 log of viable cell reductions [86]. The main reason for this to happen is, although phages are effective and quite rapidly lead to a decrease in a major population of the host, the surviving bacteria promptly create phenotypes with altered receptors to which phages can no longer attach [87]. Moreover, above 30% of the genes in phages have unknown function, which causes uneasiness among regulatory agencies regarding the approval of new phage-based products [88].

The emergence of bacterial pathogens resistant to the available antibiotics along with an increase in consumers' disapproval of chemical preservatives in food products emphasizes the need

for adoption of alternative and more natural approaches to diminish the effect of the increase of antibiotic bacterial resistance. One of the possible solutions is the alternative use of phages, since they can infect and multiply within their hosts even if they are antibiotic resistant [89]. Host specificity is generally observed at strain level, species level, or, more rarely, at genus level. Using phages as biocontrol agents in food products and food working and equipment surfaces to control the growth of *Salmonella* has shown very promising results (Figure 1.5). In one study, *Salmonella* Kentucky and *Salmonella* Brandenburg, contaminating stainless steel and glass, were reduced by 2.1-4.3 log with the application of SalmoFresh™ cocktail [90]. In a recent publication [43], the use of phage PVP-SE2 against *S.* Enteritidis artificially contaminating polystyrene and stainless steel surfaces lead to reductions of 2 to 5 log $CFU.cm^{-2}$ at room temperature. Regarding the application of phages to *Salmonella* present in fruit and vegetables, a decrease of 3.5 log at temperatures ranging from 5 °C to 20 °C was obtained when using the SCPLX-1 phage cocktail against *S.* Enteritidis on honeydew melon [91]. Whole cucumbers inoculated with *Salmonella* Newport were treated with SalmoFresh™, and at 22 °C, bacterial numbers declined 1.83 log on the first day of cocktail application [92]. Poultry meat has been responsible for several *Salmonella*-related outbreaks [7]. Several studies have been done for the evaluation of phage efficacy in reducing bacterial levels on *Salmonella*-contaminated chicken meat. For example, a phage cocktail was applied to chicken breasts artificially contaminated with *S.* Enteritidis, and after one day of incubation, bacterial cell numbers were undetectable [93]. In another study, chicken cuts were spiked with *S.* Enteritidis and treated with a phage cocktail, which resulted in a drop by 3.52 log in viable cell number, at 4 °C, and in undetectable levels, at room temperature, after three days [94].

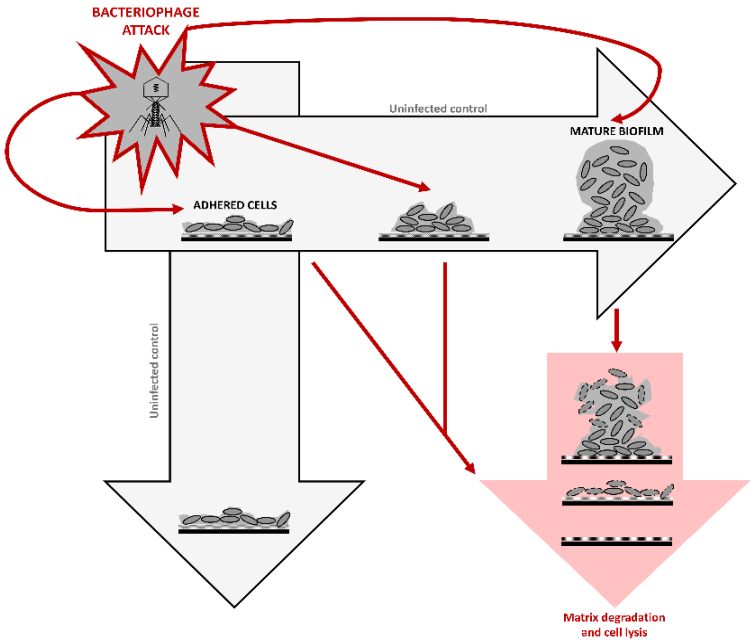

Figure 1.5 - Phage action against bacterial cells present on contaminated food processing surfaces and food products.

1.6 Synthetic biology tools for genome engineering

Phages have played a key role in the birth of molecular biology, and the enthusiasm over phage research endures mostly due to their genome diversity and their overall abundance in nature. We live in a sequencing revolution era where the landmark of over 8000 sequenced phage genomes are available in databases [95]. This genomic information keeps continuously providing new insights into the potential uses of phages, and their derived proteins, in different clinical, industrial, and environmental settings. The term 'synthetic biology' emerged in 1990s with the perception that engineering could be applied to the study of cellular systems and to easily manipulate their genomes to become more productive [96]. Synthetic biology is an emerging field of research which relies on artificially created DNA to create new biochemical systems or organisms with novel or enhanced characteristics [97,98]. It comprises a selection of approaches and methodologies with a focus on engineering biology and biotechnology.

Genome engineering in any organism, from humans to bacteria, relies on the editing of the DNA sequences to be modified. The creation of a DNA double-strand break (DSB) is the first step to perform targeted genome editing at the chosen genomic locus [99]. The reparation of these DSBs can be achieved by one of two different pathways present in almost every organism: non-homologous end-joining (NHEJ) and homology-directed repair (HDR) [100]. NHEJ-mediated repair, which is not dependent on sequence homology, originates the efficient introduction of insertions/

deletions of DNA that alter the genomic sequence, resulting in the disruption of binding sites of trans-acting factors in promoters or enhancers, or in the alteration of the translational reading frame of a determined coding sequence [101]. On the other hand, HDR-mediated repair is used for the insertion of specific point mutations or for the introduction of selected exogenously-provided DNA sequences by homologous recombination with the target locus [102]. Some techniques have been developed to take advantage of nuclease-induced DSBs. In eukaryotes, for example, mega-nucleases [103,104], zinc finger nucleases (ZFNs) [105,106], and transcription activator-like effector nucleases (TALEN) [107–109] have been extensively used for genome engineering.

In prokaryote organisms, mutagenesis techniques either introduce a selection marker in the modified locus or require a two-step process that includes a counter-selection system. Some of the applications include speeding up vaccine development, creating medicines and novel biomaterials, and developing new biofuels as clean energy substitutes for fossil fuels [110]. As an example, genome engineering for industrial acid lactic strains improvement has seen recent advances using traditional and natural genetic mobilization methodologies, such as natural competence [111–113], conjugation [114,115], and phage transduction [116,117]. Phage recombination proteins, like the λ-Red and RecET systems [118], promote homologous recombination between the DNA sequence to be modified and a targeting substrate, and have also been widely used for the genome engineering of several bacterial species, in a process denominated recombineering [119]. However, since there is no selection for mutations, the efficiency of recombineering can be relatively low, which sometimes requires the screening of a great number of colonies [12,13].

In recent years, a new strategy for genome editing has been gaining great visibility, the CRISPR/Cas systems. CRISPR (Clustered Regularly Interspaced Short Palindromic Repeats) Cas (CRISPR associated) modules function as adaptive immune systems against foreign genetic elements like phages and plasmids, and are present in archaea and bacteria [120–123]. However, these systems are being reprogrammed to become incredible genetic tools. Before the discovery of Cas protein functions, the diversity of CRISPR sequences was mainly utilized as a genotyping method known as spacer oligonucleotide typing (spoligotyping) [52,53]. This powerful method has been used to rapidly identify closely related bacterial strains (e.g. *Mycobacterium tuberculosis*). Nowadays, CRISPR/Cas systems are being used for the precise genome editing of different types of cells and organisms. Genome editing carried out by the Cas protein has been used in a variety of fields, such as genome-wide screens to characterize biological functions [124–127], identification and characterization of potential molecules to be used in the treatment of a wide range of

human diseases [128–130], modification of crops to become more resistant to plant diseases [131,132], to correct genetic mutations that cause diseases in humans [133–136], and to make the process for bacterial genome engineering with more fundamental or applied purposes easier and faster [137–144].

Although synthetic biology tools are unanimously considered to be essential for expressive advances in genome engineering, several ethical issues arise regarding the use of such methods. In 2010, a team of researchers created an organism whose genome was totally artificially synthesized in their laboratory [97]. More recently, a research group developed a semi-synthetic organism that was able to store and retrieve increased information from plasmids containing unnatural DNA bases [145]. These authors have been accused of too much interference with nature's course. Hence, several ethical committees and regulatory agencies, such as The European Group on Ethics in Science and New Technologies to the European Commission [146] and the Presidential Commission for the Study of Bioethical Issues [110], became responsible for the regulation of the use synthetic biology tools in the genetic manipulation of organisms.

1.7 Phage genome engineering: state of the art

Currently, phages are regarded as versatile tools that can be used for a varied number of purposes, like the detection of pathogenic bacteria, as antimicrobials in human therapy, and as biocontrol agents of food-contaminating bacteria. However, the application of these viruses presents limitations, such as their narrow host range [147], the emergence of bacterial-phage resistance is a reality [148], their sensitivity to some environmental conditions [149], and the presence in their genome of toxin and antibiotic-resistance genes [150], can discourage more generalized use of phages. To overcome these restrictions, researchers have been resorting to synthetic biology tools for the engineering of phage genomes. Several strategies have been used, like Gibson assembly, where smaller, overlapping, customized DNA fragments are *in vitro* assembled, creating a synthetic phage genome. Then, the genome is rebooted in *E. coli*, for Gram-negative hosts, or in cell-wall deficient L-form bacteria, for Gram-negative hosts [151]. In Bacteriophage Recombineering of Electroporated DNA (BRED), the phage genome DNA and a targeting DNA sequence, directed to the genome region to be modified, are electroporated into bacterial cells that were previously induced for recombineering functions from a plasmid containing, for example, the λ-Red system (Figure 1.6). After homologous recombination between the two DNA molecules, recombinant

phages are obtained [152,153]. The CRISPR/Cas systems are emerging as the best phage genome editing tools. In this technique, the engineered phages, created by homologous recombination, are enriched and selected, since a Cas nuclease selectively cuts the genomes from the non-modified genomes, which will no longer be able to replicate and will not form plaques or these will be present in very low numbers [154]. In table 1 are depicted some examples of phage genome engineering works.

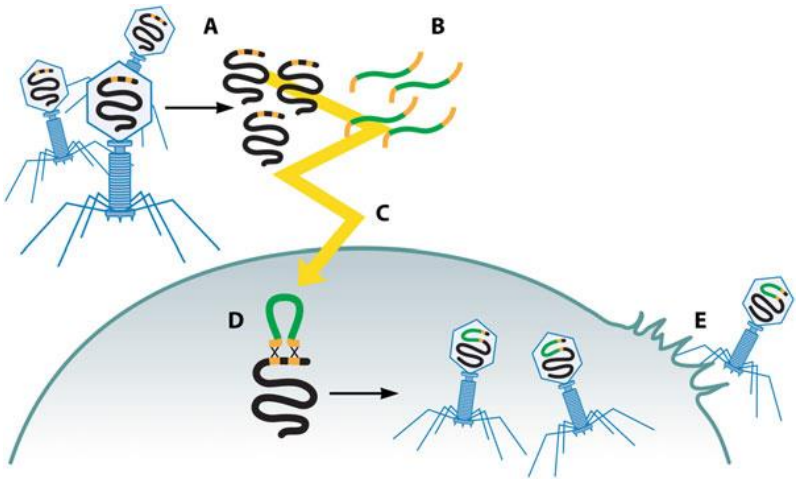

Figure 1.6 - Bacteriophage recombineering of electroporated DNA (BRED). Purified phage DNA (A) and DNA targeting substrates (B) are coelectroporated into cells (C). Recombination between their homologous regions (in orange) (D) results in recombinant phage particles (containing DNA fragments, in green) (E). Adapted from [155].

Table 1 - Examples of phage genome engineering (last 10 years)

Phage	Bacterial host	Genome editing tool	Purpose	Main outcome	Reference
A511	*Listeria monocytogenes*	CRISPR/Cas	Lysostaphin expression	Enhancement of host spectrum	[154] [2018]
phiKpS2	*Klebsiella pneumoniae*	CRISPR/Cas	Gene deletion	Evaluation of gene essentiality	[156] [2018]
vB_BsuP-Goe1	*Bacillus subtilis*	CRISPR/Cas; homologous recombination	Gene deletion and insertion	Evaluation of CRISPR/Cas applicability	[157] [2018]
B025	*L. monocytogenes*	Gibson assembly, L-form bacterium rebbooting	Gene deletion	Genome editing tool development and validation	[151] [2018]
T7	*E. coli*	Cloning	Reporter genes insertion	Insertion of reporter genes in the phage genome for bacterial bioluminescence detection	[158] [2018]
T7	*E. coli*	CRISPR/Cas	Gene deletion	Protocol development and validation	[159] [2017]
Andhra; ISP	*Staphylococcus epidermidis* and *Staphylococcus aureus*	CRISPR/Cas	Gene mutation	Study of CRISPR-Cas10 immunity against virulent staphylococcal phages and demonstration of CRISPR-Cas10 facilitating recombinant phage recovery	[160] [2017]
T4	*E. coli*	CRISPR/Cas	Single and multiple point mutations, insertions and deletions	Evaluation of CRISPR/Cas applicability and gene essentiality	[161] [2017]
p2	*Lactococcus lactis*	CRISPR/Cas	Gene deletions, point mutations and nucleotide insertion	Evaluation of CRISPR/Cas applicability and gene essentiality	[157] [2017]
Y2	*Erwinia amylovora*	Homologous recombination	Gene insertion	Enhancement of phage's killing activity, for bacterial control, and introduction of luciferase reporter gene, for bacterial detection	[162] [2017]
T7	*E. coli*	*In vivo* recombineering	DNA sequence insertion	Protection against acidic environments by display of PhoE signal peptide on the capsid's surface	[163] [2016]

Table 1 - Examples of phage genome engineering (last 10 years) (cont.)

Phage	Bacterial host	Genome editing tool	Purpose	Main outcome	Reference
T7	*E. coli* and *Klebsiella spp.*	Gap repair cloning; yeast rebooting	Modular swapping of phage tail components	Development of a strategy to modulate phage host ranges by engineering phage genomes in *Saccharomyces cerevisiae*	[164] [2015]
2972	*Streptococcus thermophilus*	CRISPR/Cas	DNA point mutations and deletions, gene insertion	Evaluation of CRISPR/Cas applicability and gene essentiality	[165] [2014]
T7	*E. coli*	CRISPR/Cas	Gene deletion	Evaluation of CRISPR/Cas applicability	[166] [2014]
D29	*Mycobacterium smegmatis*	BRED	Gene insertion	Evaluation of BRED applicability	[167] [2013]
P1vir	*E. coli*	BRED	DNA mobile element deletion	Evaluation of BRED applicability and demonstration of non-essentiality of DNA mobile element for lytic replication	[168] [2012]
PBSPCA1	*P. cannabina* pv. *alisalensis* BS91	Homologous recombination	Reporter genes insertion	Insertion of reporter genes in the phage genome for bacterial bioluminescence detection	[169] [2012]
Ms6	*M. smegmatis*	BRED	Gene truncation and tag insertion	Gene functional analysis	[170] [2011]
M13mp18	*E. coli*	Homologous recombination	Gene insertion	Repression of host's SOS DNA Repair System, enhancement of antimicrobial-resistant bacteria killing, and reduction of bacterial resistance development	[171] [2009]
Giles	*M. smegmatis*	BRED	Gene deletions and tag insertions	Genome editing tool development and validation	[152] [2008]
T7	*E. coli*	Cloning	Gene insertion	Phage anti-biofilm ability enhancement	[172] [2007]
PP01	*E. coli*	Homologous recombination	Reporter genes insertion	Insertion of reporter genes in the phage genome for bacterial bioluminescence detection	[173] [2007]

1.8 Concluding remarks and aim of the thesis

Although many efforts have been made to control *Salmonella*-related outbreaks by means of reducing or precluding contamination, like the application of Good Manufacturing Practices (GMPs) and Hazard Analysis and Critical Control Points (HACCP) in the food industry, and the awareness of populations for the risks of eating improperly cooked poultry meat or badly washed fruits and vegetables, each year, hundreds of people still become ill due to the ingestion and consequent infection with this pathogen. *Salmonella's* ability to form biofilms and subsequent increased resistance to disinfection procedures and antimicrobial products has urged researchers to find more efficient ways of eliminating *Salmonella*.

The main objective of the work developed for this thesis was the control of *S.* Enteritidis biofilms present on different food contact surfaces using phages. Phages, being the natural killers of bacteria, have regained attention regarding their application to the control of *Salmonella*, either on contaminated food processing surfaces or food products. It has been shown that these viruses are able to reduce the levels of *Salmonella* bacteria, not only in the biofilm state, but also as superficially attached cells. Nevertheless, phage's narrow host range, the emergence of phage-resistant bacteria, and the difficulty of biofilm removal from some types of surfaces has delayed a more global application of phages as biocontrol agents.

Great synthetic biology tools have been developed in the last years, to facilitate genome engineering of microorganisms for different purposes, such as biological function characterization and enhancement of their natural properties. Tools like CRISPR/Cas and BRED have been used for the genetic modification of phages regarding, for example, the introduction of a gene into a genome to improve its anti-biofilm ability or to diminish the emergence of phage-resistance bacteria, or the deletion of genes to understand their essentiality for the phage replication, all of which showing great results. This information shows that phage genome engineering with synthetic biology tools is imperative for the continuous improvement of phage properties, so their use as biocontrol agents, and not only, gains more recognition and visibility. In this work, the use of BRED allowed the genetic modification of *S.* Enteritidis phage genome, PVP-SE2, in order to increase its safety.

Lastly, since biofilms found in food processing plants have usually a polymicrobial nature, the interactions stablished between *E. coli* and *S.* Enteritidis in dual-species biofilms were investigated to understand their role in the ability of a phage cocktail to control these biofilms.

References

1. Grimont P, Weill F-X. **Antigenic formulae of the *Salmonella* servovars, 9th edition**. WHO. 2007;1–167.

2. Lamas A, Miranda JM, Regal P, Vázquez B, Franco CM, Cepeda A. **A comprehensive review of non-*enterica* subspecies of *Salmonella enterica*.** *Microbiol Res*. 2018;206(October 2017):60–73. doi: 10.1016/j.micres.2017.09.010.

3. Uzzau S, Brown DJ, Wallis T, Rubino S, Leori G, Bernard S et al. **Host adapted serotypes of *Salmonella enterica*.** *Epidemiol Infect*. 2000;125(2):229–55. doi: 10.1017/S0950268899004379.

4. Guibourdenche M, Roggentin P, Mikoleit M, Fields PI, Bockemühl J, Grimont PAD et al. **Supplement 2003-2007 (No. 47) to the White-Kauffmann-Le Minor scheme**. *Res Microbiol*. 2010;161(1):26–9. doi: 10.1016/j.resmic.2009.10.002.

5. Barbara G, Stanghellini V, Berti-Ceroni C, De Giogio R, Salvioli B, Corradi F et al. **Role of antibiotic therapy on long-term germ excretion in faeces and digestive symptoms after *Salmonella* infection.** *Aliment Pharmacol abd Ther*. 2000;14:1127–31.

6. Scallan E, Hoekstra RM, Angulo FJ, Tauxe R V., Widdowson MA, Roy SL et al. **Foodborne illness acquired in the United States-Major pathogens.** *Emerg Infect Dis.* 2011;17(1):7–15. doi: 10.3201/eid1701.P11101.

7. European Food Safety Authority. **The European Union summary report on trends and sources of zoonoses, zoonotic agents and food-borne outbreaks in 2015.** *EFSA J.* 2016;14(12). doi: 10.2903/j.efsa.2016.4634.

8. European Food Safety Authority. **EFSA explains zoonotic diseases: *Salmonella*.** Parma, Italy: European Food Safety Authority; 2014. doi: 10.2805/61217.

9. Paquet P. **Épidémie de fiévre typhoide: Déterminée par la consommation de petit cidre.** *Rev d'Hygíene.* 1923;45:165–9.

10. CDC. **Typhoid Fever and Paratyphoid Fever**. 2018 [accessed 2018 Oct 1]. Available from: https://www.cdc.gov/typhoid-fever/sources.html.

11. Andino A, Hanning I. ***Salmonella enterica*: Survival, Colonization, and Virulence Differences among Serovars.** *Sci World J.* 2015;2015:1–16. doi: 10.1155/2015/520179.

12. CDC. ***Salmonella* - Information for Healthcare Professionals and Laboratories.** 2018 [accessed 2018 Mar 9]. Available from: http://www.cdc.gov/*Salmonella*/general/technical.html.

13. Han J, Gokulan K, Barnette D, Khare S, Rooney AW, Deck J et al. **Evaluation of Virulence and Antimicrobial Resistance in *Salmonella enterica* Serovar Enteritidis Isolates from Humans and Chicken- and Egg-Associated Sources.** *Foodborne Pathog Dis.* 2013;10(12):1008–15. doi: 10.1089/fpd.2013.1518.

14. Wiedemann A, Virlogeux-Payant I, Chaussé A-M, Schikora A, Velge P. **Interactions of *Salmonella* with animals and plants.** *Front Microbiol.* 2015;5(791):1–18. doi: 10.3389/fmicb.2014.00791.

15. Stehr-Green J. ***Salmonella* in the Caribbean.** 2012 [accessed 2018 Nov 5]. Available from: https://www.cdc.gov/epicasestudies/classroom_*Salmonella*.html

16. Cevallos-Cevallos JM, Gu G, Danyluk MD, van Bruggen AHC. **Adhesion and splash dispersal of *Salmonella enterica* Typhimurium on tomato leaflets: Effects of rdar morphotype and trichome density.** *Int J Food Microbiol.* 2012;160(1):58–64. doi: 10.1016/j.ijfoodmicro.2012.09.021.

17. Lahiri A, Lahiri A, Iyer N, Das P, Chakravortty D. **Visiting the cell biology of *Salmonella* infection.** Microbes Infect. 2010;12(11):809–18. doi: 10.1016/j.micinf.2010.05.010.

18. Erhardt M, Dersch P. **Regulatory principles governing *Salmonella* and *Yersinia* virulence.** *Front Microbiol.* 2015;6(SEP):1–20. doi: 10.3389/fmicb.2015.00949.

19. Garai P, Gnanadhas DP, Chakravortty D. ***Salmonella enterica* serovars Typhimurium and Typhi as model organisms.** *Virulence.* 2012;3(4):1–11. doi: 10.4161/viru.21087.

20. Mills DM, Bajaj V, Lee CA. **A 40 kb chromosomal fragment encoding *Salmonella* Typhimurium invasion genes is absent from the corresponding region of the *Escherichia coli* K-12 chromosome.** *Mol Microbiol.* 1995;15(4):749–59. doi: 10.1111/j.1365-2958.1995.tb02382.x.

21. Shea JE, Hensel M, Gleeson C, Holden DW. **Identification of a virulence locus encoding a second type III secretion system in *Salmonella* Typhimurium.** *Proc Natl Acad Sci.* 1996;93(6):2593–7. doi: 10.1073/pnas.93.6.2593.

22. Schlumberger MC, Hardt WD. ***Salmonella* type III secretion effectors: Pulling the host cell's strings.** *Curr Opin Microbiol.* 2006;9(1):46–54. doi: 10.1016/j.mib.2005.12.006.

23. Gal JE. ***Salmonella* interactions with host cells: Type III Secretion at work.** *Annu Rev Cell Dev Biol.* 2001;17:53–86. doi: 10.1146/annurev.cellbio.17.1.53.

24. Norris FA, Wilson MP, Wallis TS, Galyov EE, Majerus PW. **SopB, a protein required for virulence of *Salmonella* Dublin, is an inositol phosphate phosphatase.** *Proc Natl Acad Sci U S A.* 1998;95(24):14057–9.

25. Wallis TS, Galyov EE. **Molecular basis of *Salmonella*-induced enteritis.** *Mol Microbiol.* 2000;36(5):997–1005.

26. Zhou D, Mooseker MS, Galán JE. **An invasion-associated *Salmonella* protein modulates the actin-bundling activity of plastin.** *Proc Natl Acad Sci U S A.* 1999;96(18):10176–81.

27. Kaniga K, Tucker S, Trollinger D, Galan JE. **Homologs of the *Shigella* IpaB and IpaC invasins are required for *Salmonella* Typhimurium entry into cultured epithelial cells.** *J Bacteriol.* 1995;177(14):3965–71.

28. Wood MW, Rosqvist R, Mullan PB, Edwards MH, Galyov EE. **SopE, a secreted protein of *Salmonella Dublin*, is translocated into the target eukaryotic cell via a *sip*-dependent mechanism and promotes bacterial entry.** *Mol Microbiol.* 1996;22(2):327–38. doi: 10.1046/j.1365-2958.1996.00116.x

29. Figueira R, Holden DW. **Functions of the *Salmonella* pathogenicity island 2 (SPI-2) type III secretion system effectors.** *Microbiology.* 2012;158(5):1147–61. doi: 10.1099/mic.0.058115-0.

30. Holden DW. **Trafficking of the *Salmonella* vacuole in macrophages.** *Traffic.* 2002;3(3):161–9.

31. Steele-Mortimer O, Méresse S, Gorvel JP, Toh BH, Finlay BB. **Biogenesis of *Salmonella* Typhimurium-containing vacuoles in epithelial cells involves interactions with the early endocytic pathway.** *Cell Microbiol.* 1999;1(1):33–49.

32. Garvis SG, Beuzón CR, Holden DW. **A role for the PhoP/Q regulon in inhibition of fusion between lysosomes and *Salmonella*-containing vacuoles in macrophages.** *Cell Microbiol.* 2001;3(11):731–44.

33. Fabrega A, Vila J. ***Salmonella enterica* Serovar Typhimurium Skills To Succeed in the Host: Virulence and Regulation.** *Clin Microbiol Rev.* 2013 Apr;26(2):308–41. doi: 10.1128/CMR.00066-12.

34. Eckmann L, Rudolf MT, Ptasznik A, Schultz C, Jiang T, Wolfson N et al. **D-myo-Inositol 1,4,5,6-tetrakisphosphate produced in human intestinal epithelial cells in response to *Salmonella* invasion inhibits phosphoinositide 3-kinase signaling pathways.** *Proc Natl Acad Sci U S A.* 1997;94(26):14456–60.

35. Eckmann L, Kagnoff M, Fierer J. **Epithelial Cells Secrete the Chemokine Interleukin-8 in**

Response to Bacterial Entry. *Infect Immun.* 1993;61(11):4569–74.

36. Eckmann L, Stenson WF, Savidge TC, Lowe DC, Barrett KE, Fierer J et al. **Role of intestinal epithelial cells in the host secretory response to infection by invasive bacteria: Bacterial entry induces epithelial prostaglandin H synthase-2 expression and prostaglandin E2and F(2α) production.** *J Clin Invest.* 1997;100(2):296–309. doi: 10.1172/JCI119535.

37. Bryant C, Mastroeni P. **Cytokines in Salmonellosis.** *EcoSal Plus.* 2004 Dec 29;1(1). doi: 10.1128/ecosalplus.8.8.5

38. Mccormick BA, Parkos CA, Colgan SP, Carnes K, Madara JL, Mccormick BA et al. **Apical Secretion of a Pathogen-Elicited Epithelial Chemoattractant Activity in Response to Surface Colonization of Intestinal Epithelia by *Salmonella* Typhimurium.** *J Immunol.* 1998;160(1):455–566.

39. Pilsczek FH, Nicholson-Weller A, Ghiran I. **Phagocytosis of *Salmonella* Montevideo by Human Neutrophils: Immune Adherence Increases Phagocytosis, whereas the Bacterial Surface Determines the Route of Intracellular Processing.** *J Infect Dis*. 2005 Jul 15;192(2):200–9. doi: 10.1086/430947.

40. Nair A, Rawool DB, Doijad S, Poharkar K, Mohan V, Barbuddhe SB et al. **Biofilm formation and genetic diversity of *Salmonella* isolates recovered from clinical, food, poultry and environmental sources.** *Infect Genet Evol*. 2015;36:424–33. doi: 10.1016/j.meegid.2015.08.012.

41. Cepeda A, Franco CM. **Effect of Food Residues in Biofilm Formation on Stainless Steel and Polystyrene Surfaces by *Salmonella enterica* Strains Isolated from Poultry Houses.** *Foods.* 2017;6(12):106. doi: 10.3390/foods6120106.

42. Borges KA, Furian TQ, de Souza SN, Menezes R, Salle CTP, de Souza Moraes HL et al. **Phenotypic and Molecular Characterization of *Salmonella* Enteritidis SE86 Isolated from Poultry and Salmonellosis Outbreaks.** *Foodborne Pathog Dis*. 2017;14(12):fpd.2017.2327. doi: 10.1089/fpd.2017.2327.

43. Milho C, Silva MD, Melo L, Santos S, Azeredo J, Sillankorva S. **Control of *Salmonella* Enteritidis on food contact surfaces with bacteriophage PVP-SE2.** *Biofouling.* 2018;30:1–16. doi: 10.1080/08927014.2018.1501475.

44. Balamurugan S, Canada A, Khachatourians G, Korber DR. **Food Processing Biofilms and Antimicrobial Agents.** In: Hui YH, Culbertson JD, editors. *Handbook of Food Science, Technology, and Engineering.* CRC Press; 2006. p. 84-1 - 84-15.

45. Galié S, García-Gutiérrez C, Miguélez EM, Villar CJ, Lombó F. **Biofilms in the food industry: Health aspects and control methods.** *Front Microbiol.* 2018;9(MAY):1–18. doi: 10.3389/fmicb.2018.00898.

46. Chmielewski RAN, Frank JF. **Biofilm formation and control in food processing facilities.** *Compr Rev Food Sci Food Saf.* 2003 Jan;2(1):22–32. doi: 10.1111/j.1541-4337.2003.tb00012.x.

47. Kumar CG, Anand S. **Significance of microbial biofilms in food industry: a review.** *Int J Food Microbiol.* 1998 Jun;42(1–2):9–27.

48. Korber DR, Mangalappalli-Illathu AK, Vidović S. **Biofilm formation by food spoilage microorganisms in food processing environments.** In: Fratamico PM, Annous BA, Gunther NW, editors. *Biofilms in the food and beverage industries.* CRC Press; 2009. p. 169–99.

49. Srivastava S, Bhargava A. **Biofilms and human health.** *Biotechnol Lett.* 2016 Jan;38(1):1–22. doi: 10.1007/s10529-015-1960-8.

50. Dunne WM. **Bacterial Adhesion: Seen Any Good Biofilms Lately?** *Clin Microbiol Rev.* 2002;15(2):155–66.

51. Prakash B, Veeregowda BM, Krishnappa G. **Biofilms: A survival strategy of bacteria.** *Curr Sci.*

2003 Jan;85(9):1299–307.

52. Flemming H, Wingender J. **The biofilm matrix.** *Nat Rev Microbiol.* 2010;8(9):623–33. doi: 10.1038/nrmicro2415.

53. Domenech M, Ramos-Sevillano E, García E, Moscoso M, Yuste J. **Biofilm Formation Avoids Complement Immunity and Phagocytosis of *Streptococcus pneumoniae*.** *Infect Immun.* 2013 Jul;81(7):2606–15. doi: 10.1128/IAI.00491-13.

54. Hall CW, Mah TF. **Molecular mechanisms of biofilm-based antibiotic resistance and tolerance in pathogenic bacteria.** *FEMS Microbiol Rev.* 2017;41(3):276–301. doi: 10.1093/femsre/fux010.

55. Singh S, Singh SK, Chowdhury I, Singh R. **Understanding the Mechanism of Bacterial Biofilms Resistance to Antimicrobial Agents.** *Open Microbiol J.* 2017;11(1):53–62. doi: 10.2174/1874285801711010053.

56. Gutiérrez D, Rodríguez-Rubio L, Martínez B, Rodríguez A, García P. **Bacteriophages as weapons against bacterial biofilms in the food industry.** *Front Microbiol.* 2016;7(JUN):1–15. doi: 10.3389/fmicb.2016.00825.

57. Coughlan LM, Cotter PD, Hill C, Alvarez-Ordóñez A. **New weapons to fight old enemies: Novel strategies for the (bio)control of bacterial biofilms in the food industry.** *Front Microbiol.* 2016;7(OCT):1–21. doi: 10.3389/fmicb.2016.01641.

58. Wood TK, Knabel SJ, Kwan BW. **Bacterial persister cell formation and dormancy.** *Appl Environ Microbiol.* 2013;79(23):7116–21. doi: 10.1128/AEM.02636-13.

59. Lewis K. **Persister Cells**. *Annu Rev Microbiol.* 2010;64(1):357–72. doi: 10.1146/annurev.micro.112408.134306.

60. Antunes P, Mourão J, Campos J, Peixe L. **Salmonellosis: The role of poultry meat.** *Clin Microbiol Infect.* 2016;22(2):110–21. doi: 10.1016/j.cmi.2015.12.004.

61. Ricke SC, Dunkley CS, Durant J. **A review on development of novel strategies for controlling *Salmonella* Enteritidis colonization in laying hens: fiber-based molt diets.** *Poult Sci.* 2013;92(2):502–25. doi: 10.3382/ps.2012-02763.

62. Evangelopoulou G, Kritas S, Govaris A, Burriel AR. **Pork meat as a potential source of *Salmonella enterica* subsp. *arizonae* infection in humans.** *J Clin Microbiol.* 2014;52(3):741–4. doi: 10.1128/JCM.02933-13.

63. Heinitz ML, Ruble RD, Wagner DE, Tatini SR. **Incidence of *Salmonella* in fish and seafood.** *J Food Prot.* 2000;63(5):579–92.

64. Wan Norhana MN, Poole SE, Deeth HC, Dykes GA. **The effects of temperature, chlorine and acids on the survival of *Listeria* and *Salmonella* strains associated with uncooked shrimp carapace and cooked shrimp flesh.** *Food Microbiol.* 2010;27(2):250–6. doi: 10.1016/j.fm.2009.10.008.

65. Amrutha B, Sundar K, Shetty PH. **Study on *E. coli* and *Salmonella* biofilms from fresh fruits and vegetables.** *J Food Sci Technol.* 2017;54(5):1091–7. doi: 10.1007/s13197-017-2555-2.

66. Winkelströter LK, Teixeira FB dos R, Silva EP, Alves VF, De Martinis ECP. **Unraveling Microbial Biofilms of Importance for Food Microbiology.** *Microb Ecol.* 2014;68(1):35–46. doi: 10.1007/s00248-013-0347-4.

67. Jahid IK, Ha S-D. **Inactivation kinetics of various chemical disinfectants on *Aeromonas hydrophila* planktonic cells and biofilms.** *Foodborne Pathog Dis.* 2014;11(5):346–53. doi: 10.1089/fpd.2013.1682.

68. Raffaella C, Casettari L, Fagioli L, Cespi M, Bonacucina G, Baffone W. **Activity of essential oil-based microemulsions against *Staphylococcus aureus* biofilms developed on stainless steel surface in different culture media and growth conditions.** *Int J Food Microbiol.* 2017;241:132–40. doi: 10.1016/j.ijfoodmicro.2016.10.021.

69. Lequette Y, Boels G, Clarisse M, Faille C. **Using enzymes to remove biofilms of bacterial isolates sampled in the food-industry.** *Biofouling.* 2010;26(4):421–31. doi: 10.1080/08927011003699535.

70. Wang R, Kalychayanand N, Schmidt JW, Harhay DM. **Mixed Biofilm Formation by Shiga Toxin-Producing *Escherichia coli* and *Salmonella enterica* Serovar Typhimurium Enhanced Bacterial Resistance to Sanitization due to Extracellular Polymeric Substances.** *J Food Prot.* 2013;77(5):805–13. doi: 10.4315/0362-028X.JFP-13-077.

71. Wegener HC. **Antibiotic Resistance-Linking Human and Animal Health.** In: *Improving Food Safety Through a One Health Approach: Workshop Summary.* Washington D.C., USA: The National Academies Press; 2012. p. 331–48.

72. Manzetti S, Ghisi R. **The environmental release and fate of antibiotics.** *Mar Pollut Bull.* 2014 Feb;79(1–2):7–15. doi: 10.1016/j.marpolbul.2014.01.005.

73. Zhang T, Li B. **Occurrence, Transformation, and Fate of Antibiotics in Municipal Wastewater Treatment Plants.** *Crit Rev Environ Sci Technol.* 2011 Apr 26;41(11):951–98. doi: 10.1080/10643380903392692.

74. Knapp CW, Dolfing J, Ehlert PAI, Graham DW. **Evidence of increasing antibiotic resistance gene abundances in archived soils since 1940.** *Environ Sci Technol.* 2010;44(2):580–7. doi: 10.1021/es901221x.

75. Milić N, Milanović M, Letić NG, Sekulić MT, Radonić J, Mihajlović I et al. **Occurrence of antibiotics as emerging contaminant substances in aquatic environment.** *Int J Environ Health Res.* 2013;23(4):296–310. doi: 10.1080/09603123.2012.733934.

76. Forsberg KJ, Reyes A, Wang B, Selleck EM, Sommer MO, Dantas G. **The shared antibiotic resistome of soil bacteria and human pathogens.** *Science.* 2012 Aug 31;337(6098):1107–11. doi: 10.1126/science.1220761.

77. Martinez JL. **Environmental pollution by antibiotics and by antibiotic resistance determinants.** *Environ Pollut.* 2009 Nov;157(11):2893–902. doi: 10.1016/j.envpol.2009.05.051.

78. CDC. **Resistant *Salmonella* causes 6,200 illnesses a year.** 2016 [accessed 2018 Nov 5]. Available from: http://www.cidrap.umn.edu/news-perspective/2016/12/cdc-resistant-*Salmonella*-causes-6200-illnesses-year.

79. Abedon ST. **Bacteriophage: Ecology Population Growth, Evolution, and Impact of Bacterial Viruses Bacteriophages.** Cambridge, UK: Cambridge University Press; 2008. 526 p.

80. Hatfull GF. **Bacteriophage genomics.** *Curr Opin Microbiol.* 2008;11(5):447–53. doi: 10.1016/j.mib.2008.09.004.

81. Danovaro R, Corinaldesi C, Dell'Anno A, Fuhrman JA, Middelburg JJ, Noble RT et al. **Marine viruses and global climate change.** *FEMS Microbiol Rev.* 2011 Nov;35(6):993–1034. doi: 10.1111/j.1574-6976.2010.00258.x.

82. Clokie MRJ, Millard AD, Letarov A V, Heaphy S. **Phages in nature.** *Bacteriophage.* 2011 Jan 22;1(1):31–45. doi: 10.4161/bact.1.1.14942.

83. Guttman B, Raya R, Kutter E. **Basic Phage Biology.** In: Kutter E, Sulakvelidze A, editors. *Bacteriophages: Biology and Applications.* Boca Raton, FL, USA: CRC Press; 2005. p. 29–66.

84. Ackermann HW. **Bacteriophage Classification.** In: Kutter E, Sulakvelidze A, editors. *Bacteriophages: Biology and Applications.* Boca Raton, FL, USA: CRC Press; 2005. p. 67–89.

85. Sillankorva SM, Oliveira H, Azeredo J. **Bacteriophages and their role in food safety.** *Int J Microbiol.* 2012;2012:863945. doi: 10.1155/2012/863945.

86. Moye Z, Woolston J, Sulakvelidze A. **Bacteriophage Applications for Food Production and Processing.** *Viruses.* 2018 Apr 19;10(4):205. doi: 10.3390/v10040205.

87. Pires DP, Dötsch A, Anderson EM, Hao Y, Khursigara CM, Lam JS et al. **A genotypic analysis of five *P. aeruginosa* strains after biofilm infection by phages targeting different cell surface receptors.** *Front Microbiol.* 2017;8(JUN):1–14. doi: 10.3389/fmicb.2017.01229.

88. Hatfull GF, Hendrix RW. **Bacteriophages and their genomes.** *Curr Opin Virol.* 2011;1(4):298–303. doi: 10.1016/j.coviro.2011.06.009.

89. Torres-Barceló C. **The disparate effects of bacteriophages on antibiotic-resistant bacteria.** *Emerg Microbes Infect.* 2018 Dec 10;7(1):168. doi: 10.1038/s41426-018-0169-z.

90. Woolston J, Parks AR, Abuladze T, Anderson B, Li M, Carter C et al. **Bacteriophages lytic for *Salmonella* rapidly reduce *Salmonella* contamination on glass and stainless steel surfaces.** *Bacteriophage.* 2013 Jul 11;3(3):e25697. doi: 10.4161/bact.25697.

91. Leverentz B, Conway W, Alavidze Z, Janisiewicz W, Fuchs Y, Camp M et al. **Examination of Bacteriophage as a Biocontrol Method for *Salmonella* on Fresh-Cut Fruit: A Model Study.** *J Food Prot.* 2001;64(8):1116–21.

92. Sharma M, Dashiell G, Handy ET, East C, Reynnells R, White C et al. **Survival of *Salmonella* Newport on Whole and Fresh-Cut Cucumbers Treated with Lytic Bacteriophages.** *J Food Prot* 2017;80(4):668–73. doi: 10.4315/0362-028X.JFP-16-449.

93. Han H, Wei X, Wei Y, Zhang X, Li X, Jiang J et al. **Isolation, Characterization, and Bioinformatic Analyses of Lytic *Salmonella* Enteritidis Phages and Tests of Their Antibacterial Activity in Food.** *Curr Microbiol.* 2017;74(2):1–9. doi: 10.1007/s00284-016-1169-7.

94. Augustine J, Bhat SG. **Biocontrol of *Salmonella* Enteritidis in spiked chicken cuts by lytic bacteriophages ΦSP-1 and ΦSP-3.** *J Basic Microbiol.* 2015;55(4):500–3. doi: 10.1002/jobm.201400257.

95. NCBI. **Genomes Groups - Viruses of Bacteria Database.** 2018 [accessed 2018 Nov 14]. Available from: https://www.ncbi.nlm.nih.gov/genomes/GenomesGroup.cgi?taxid=10239&host=bacteria

96. Cameron DE, Bashor CJ, Collins JJ. **A brief history of synthetic biology.** *Nat Rev Microbiol.* 2014;12(5):381–90. doi: 10.1038/nrmicro3239.

97. Gibson DG, Glass JI, Lartigue C, Noskov VN, Chuang R-Y, Algire MA et al. **Creation of a Bacterial Cell Controlled by a Chemically Synthesized Genome.** *Science.* 2010 Jul 2;329(5987):52–6. doi: 10.1126/science.1190719.

98. Gibson DG, Smith HO, Hutchison CA, Venter JC, Merryman C. **Chemical synthesis of the mouse mitochondrial genome.** *Nat Methods.* 2010 Nov 10;7(11):901–3. doi: 10.1038/nmeth.1515.

99. Urnov FD, Rebar EJ, Holmes MC, Zhang HS, Gregory PD. **Genome editing with engineered zinc finger nucleases.** *Nat Publ Genet.* 2010;11(9):636–46. doi: 10.1038/nrg2842.

100. Carroll D. **Genome Engineering With Zinc-Finger Nucleases.** *Genetics.* 2011;188(4):773–82. doi: 10.1534/genetics.111.131433.

101. Chapman JR, Taylor MRG, Boulton SJ. **Playing the End Game: DNA Double-Strand Break Repair Pathway Choice.** *Mol Cell.* 2012 Aug;47(4):497–510. doi: 10.1016/j.molcel.2012.07.029.

102. Rong YS, Golic KG. **Gene targeting by homologous recombination in Drosophila.** *Science.* 2000;288(5473):2013–8.

103. Wang L, Smith J, Breton C, Clark P, Zhang J, Ying L et al. **Meganuclease targeting of PCSK9 in**

macaque liver leads to stable reduction in serum cholesterol. *Nat Biotechnol.* 2018;36(8). doi: 10.1038/nbt.4182.

104. Rivière J, Hauer J, Poirot L, Brochet J, Souque P, Mollier K et al. **Variable correction of Artemis deficiency by I-Sce1-meganuclease-assisted homologous recombination in murine hematopoietic stem cells.** *Gene Ther*. 2014 May 13;21(5):529–32. doi: 10.1038/gt.2014.20.

105. Gammage PA, Viscomi C, Simard M-L, Costa ASH, Gaude E, Powell CA et al. **Genome editing in mitochondria corrects a pathogenic mtDNA mutation *in vivo.*** *Nat Med*. 2018 Nov 24;24(11):1691–5. doi: 10.1038/s41591-018-0165-9.

106. Modares Sadeghi M, Shariati L, Hejazi Z, Shahbazi M, Tabatabaiefar MA, Khanahmad H. **Inducing indel mutation in the SOX6 gene by zinc finger nuclease for gamma reactivation: An approach towards gene therapy of beta thalassemia.** *J Cell Biochem*. 2018 Mar;119(3):2512–9. doi: 10.1002/jcb.26412.

107. Shankar S, Prasad D, Sanawar R, Das A V., Pillai MR. **TALEN based HPV-E7 editing triggers necrotic cell death in cervical cancer cells.** *Sci Rep.* 2017 Dec 14;7(1):5500. doi: 10.1038/s41598-017-05696-0.

108. Tanaka Y, Sone T, Higurashi N, Sakuma T, Suzuki S, Ishikawa M et al. **Generation of D1-1 TALEN isogenic control cell line from Dravet syndrome patient iPSCs using TALEN-mediated editing of the SCN1A gene.** *Stem Cell Res.* 2018 Apr;28:100–4. doi: 10.1016/j.scr.2018.01.036.

109. Xu A, Zhou R, Tu J, Huo Z, Zhu D, Wang D et al. **Establishment of a human embryonic stem cell line with homozygous TP53 R248W mutant by TALEN mediated gene editing.** *Stem Cell Res.* 2018 May;29(March):215–9. doi: 10.1016/j.scr.2018.04.013.

110. Presidential Commission for the Study of Bioethical Issues. **New Directions. The Ethics of Synthetic Biology and Emerging Technologies. Executive Summary and Recommendations.** 2012 Jan;16(1):1–192.

111. Dandoy D, Fremaux C, Henry de Frahan M, Horvath P, Boyaval P, Hols P et al. **The fast milk acidifying phenotype of *Streptococcus thermophilus* can be acquired by natural transformation of the genomic island encoding the cell-envelope proteinase PrtS.** *Microb Cell Fac*t. 2011;10(SUPPL.1):S21. doi: 10.1186/1475-2859-10-S1-S21.

112. Mulder J, Wels M, Kuipers OP, Kleerebezem M, Bron PA. **Unleashing natural competence in *Lactococcus lactis* by induction of the competence regulator ComX.** *Appl Environ Microbiol.* 2017;83(20). doi: 10.1128/AEM.01320-17

113. Zaccaria E, van Baarlen P, de Greeff A, Morrison DA, Smith H, Wells JM. **Control of Competence for DNA Transformation in *Streptococcus suis* by Genetically Transferable Pherotypes.** *PLoS One.* 2014 Jun 26;9(6):e99394. doi: 10.1371/journal.pone.0099394.

114. Machielsen R, Siezen RJ, van Hijum SAFT, van Hylckama Vlieg JET. **Molecular Description and Industrial Potential of Tn 6098 Conjugative Transfer Conferring Alpha-Galactoside Metabolism in *Lactococcus lactis*.** *Appl Environ Microbiol*. 2011 Jan 15;77(2):555–63. doi: 10.1128/AEM.02283-10.

115. Cui Y, Hu T, Qu X, Zhang L, Ding Z, Dong A. **Plasmids from food lactic acid bacteria: Diversity, similarity, and new developments.** *Int J Mol Sci.* 2015;16(6):13172–202. doi: 10.3390/ijms160613172.

116. Ravin V, Sasaki T, Räisänen L, Riipinen K-A, Alatossava T. **Effective plasmid pX3 transduction in *Lactobacillus delbrueckii* by bacteriophage LL-H.** *Plasmid.* 2006 May;55(3):184–93. doi: 10.1016/j.plasmid.2005.12.003

117. Ammann A, Neve H, Geis A, Heller KJ. **Plasmid Transfer via Transduction from *Streptococcus thermophilus* to *Lactococcus lactis*.** *J Bacteriol*. 2008 Apr 15;190(8):3083–7. doi:

10.1128/JB.01448-07.

118. Pines G, Freed EF, Winkler JD, Gill RT. **Bacterial Recombineering: Genome Engineering via Phage-Based Homologous Recombination.** *ACS Synth Biol.* 2015; 20;4(11):1176-85. doi: 10.1021/acssynbio.5b00009.

119. Marinelli LJ, Hatfull GF, Piuri M. **Recombineering: A powerful tool for modification of bacteriophage genomes.** *Bacteriophage*. 2012;(March):5–14. doi: 10.4161/bact.18778.

120. Deveau H, Garneau JE, Moineau S. **CRISPR/Cas system and its role in phage-bacteria interactions.** *Annu Rev Microbiol.* 2010 Jan;64:475–93. doi: 10.1146/annurev.micro.112408.134123.

121. Garneau JE, Dupuis M-È, Villion M, Romero D, Barrangou R, Boyaval P et al. **The CRISPR/Cas bacterial immune system cleaves bacteriophage and plasmid DNA.** *Nature.* 2010;468(7320):67–71. doi: 10.1038/nature09523.

122. Koonin E V, Makarova KS. **CRISPR-Cas: an adaptive immunity system in prokaryotes.** *F1000 Biol Rep.* 2009;1(1):1–6. doi: 10.3410/B1-95.

123. Sorek R, Kunin V, Hugenholtz P. **CRISPR–a widespread system that provides acquired resistance against phages in bacteria and archaea.** *Nat Rev Microbiol.* 2008;6(3):181–6. doi: 10.1038/nrmicro1793.

124. Lopes R, Korkmaz G, Agami R. **Applying CRISPR–Cas9 tools to identify and characterize transcriptional enhancers.** *Nat Rev Mol Cell Biol.* 2016 Sep 6;17(9):597–604. doi: 10.1038/nrm.2016.79.

125. Jiang Y, Zhou Y, Bao X, Chen C, Randolph LN, Du J et al. **An Ultrasensitive Calcium Reporter System via CRISPR-Cas9-Mediated Genome Editing in Human Pluripotent Stem Cells.** *iScience.* 2018 Nov;9:27–35. doi: 10.1016/j.isci.2018.10.007.

126. Trubiroha A, Gillotay P, Giusti N, Gacquer D, Libert F, Lefort A et al. **A Rapid CRISPR/Cas-based Mutagenesis Assay in Zebrafish for Identification of Genes Involved in Thyroid Morphogenesis and Function.** *Sci Rep.* 2018;8(1):1–19. doi: 10.1038/s41598-018-24036-4.

127. Chen J, Lai Y, Wang L, Zhai S, Zou G, Zhou Z et al. **CRISPR/Cas9-mediated efficient genome editing via blastospore-based transformation in entomopathogenic fungus *Beauveria bassiana*.** *Sci Rep.* 2017 Dec 3;7(1):45763.doi: 10.1038/srep45763.

128. Neggers JE, Kwanten B, Dierckx T, Noguchi H, Voet A, Bral L et al. **Target identification of small molecules using large-scale CRISPR-Cas mutagenesis scanning of essential genes.** *Nat Commun.* 2018 Dec 5;9(1):502. doi: 10.1038/s41467-017-02349-8.

129. Chu J, Galicia-Vázquez G, Cencic R, Mills JR, Katigbak A, Porco JA et al. **CRISPR-Mediated Drug-Target Validation Reveals Selective Pharmacological Inhibition of the RNA Helicase, eIF4A.** *Cell Rep*. 2016 Jun;15(11):2340–7. doi: 10.1016/j.celrep.2016.05.005.

130. Wong ASL, Choi GCG, Cui CH, Pregernig G, Milani P, Adam M et al. **Multiplexed barcoded CRISPR-Cas9 screening enabled by CombiGEM.** *Proc Natl Acad Sci.* 2016 Mar 1;113(9):2544–9. doi: 10.1007/978-3-319-12850-4.

131. Zhang Y, Bai Y, Wu G, Zou S, Chen Y, Gao C et al. **Simultaneous modification of three homoeologs of TaEDR1 by genome editing enhances powdery mildew resistance in wheat.** *Plant J.* 2017 Aug;91(4):714–24. doi: 10.1111/tpj.13599.

132. Wang F, Wang C, Liu P, Lei C, Hao W, Gao Y et al. **Enhanced Rice Blast Resistance by CRISPR/Cas9-Targeted Mutagenesis of the ERF Transcription Factor Gene OsERF922.** *PLoS One*. 2016 doi: 10.1371/journal.pone.0154027.

133. Tessadori F, Roessler HI, Savelberg SMC, Chocron S, Kamel SM, Duran KJ et al. **Effective CRISPR/Cas9-based nucleotide editing in zebrafish to model human genetic cardiovascular**

disorders. *Dis Model Mech.* 2018 Oct 1;11(10):dmm035469. doi: 10.1242/dmm.035469.

134. de Carvalho TG, Schuh R, Pasqualim G, Pellenz FM, Filippi-Chiela EC, Giugliani R et al. **CRISPR-Cas9-mediated gene editing in human MPS I fibroblasts.** *Gene.* 2018 Dec;678:33–7. doi: 10.1016/j.gene.2018.08.004.

135. Zhang Y, Long C, Li H, McAnally JR, Baskin KK, Shelton JM et al. **CRISPR-Cpf1 correction of muscular dystrophy mutations in human cardiomyocytes and mice.** *Sci Adv.* 2017 Apr 12;3(4):e1602814. doi: 10.1134/S0026893317020066.

136. Long C, Li H, Tiburcy M, Rodriguez-Caycedo C, Kyrychenko V, Zhou H et al. **Correction of diverse muscular dystrophy mutations in human engineered heart muscle by single-site genome editing.** *Sci Adv.* 2018 Jan 31;4(1):eaap9004. doi: 10.1126/sciadv.aap9004.

137. Ram G, Ross HF, Novick RP, Rodriguez-Pagan I, Jiang D. **Conversion of staphylococcal pathogenicity islands to CRISPR-carrying antibacterial agents that cure infections in mice.** *Nat Biotechnol.* 2018; 36(10):971-976. doi: 10.1038/nbt.4203.

138. Chen W, Zhang Y, Zhang Y, Pi Y, Gu T, Song L et al. **CRISPR/Cas9-based Genome Editing in *Pseudomonas aeruginosa* and Cytidine Deaminase-Mediated Base Editing in *Pseudomonas* Species.** *iScience.* 2018 Aug;6:222–31. doi: 10.1016/j.isci.2018.07.024.

139. Leenay RT, Vento JM, Shah M, Martino ME, Leulier F, Beisel CL. **Genome Editing with CRISPR-Cas9 in *Lactobacillus plantarum* Revealed That Editing Outcomes Can Vary Across Strains and Between Methods.** *Biotechnology Journal.* 2018 Aug 29:e1700583. doi: 10.1002/biot.201700583.

140. Dong C, Fontana J, Patel A, Carothers JM, Zalatan JG. **Synthetic CRISPR-Cas gene activators for transcriptional reprogramming in bacteria.** *Nat Commun.* 2018; Jun 27;9(1):2489. doi: 10.1038/s41467-018-04901-6.

141. Wang T, Guan C, Guo J, Liu B, Wu Y, Xie Z et al. **Pooled CRISPR interference screening enables genome-scale functional genomics study in bacteria with superior performance.** *Nat Commun.* 2018; Jun 26;9(1):2475. doi: 10.1038/s41467-018-04899-x.

142. Zhao Y, Li L, Zheng G, Jiang W, Deng Z, Wang Z et al. **CRISPR/dCas9-Mediated Multiplex Gene Repression in *Streptomyces.*** *Biotechnol J.* 2018 Sep;13(9):1800121. doi: 10.1002/biot.201800121.

143. Westbrook AW, Ren X, Oh J, Moo-Young M, Chou CP. **Metabolic engineering to enhance heterologous production of hyaluronic acid in *Bacillus subtilis.*** *Metab Eng.* 2018; May;47:401-413. doi: 10.1016/j.ymben.2018.04.016.

144. Banno S, Nishida K, Arazoe T, Mitsunobu H, Kondo A. **Deaminase-mediated multiplex genome editing in *Escherichia coli.*** *Nat Microbiol.* 2018; Apr;3(4):423-429. doi: 10.1038/s41564-017-0102-6.

145. Zhang Y, Ptacin JL, Fischer EC, Aerni HR, Caffaro CE, San Jose K et al. **A semi-synthetic organism that stores and retrieves increased genetic information.** *Nature.* 2017; Nov 29;551(7682):644-647. doi: 10.1038/nature24659.

146. The European Group on Ethics in Science and New Technologies to the European Commission. **Ethics of synthetic biology.** Salvi M, editor. Luxembourg: Publications Office of the European Union; 2009.

147. Humphrey T. ***Salmonella* stress responses and food safety.** *Nat Rev Microbiol.* 2004;2(6):1–6. doi: 10.1038/nrmicro907.

148. Marti E, Variatza E, Balcázar JL. **Bacteriophages as a reservoir of extended-spectrum β-lactamase and fluoroquinolone resistance genes in the environment.** *Clin Microbiol Infect.* 2014 Jul;20(7):O456-9. doi: 10.1111/1469-0691.12446.

149. Zhang J, Li Z, Cao Z, Wang L, Li X, Li S et al. **Bacteriophages as antimicrobial agents against major pathogens in swine: a review.** *J Anim Sci Biotechnol.* 2015;6(1):39. doi: 10.1186/s40104-015-

0039-7.

150. Rode TM, Axelsson L, Granum PE, Heir E, Holck A, L'Abée-Lund TM. **High stability of Stx2 phage in food and under food-processing conditions.** *Appl Environ Microbiol.* 2011;77(15):5336–41. doi: 10.1128/AEM.00180-11.

151. Kilcher S, Studer P, Muessner C, Klumpp J, Loessner MJ. **Cross-genus rebooting of custom-made, synthetic bacteriophage genomes in L-form bacteria.** *Proc Natl Acad Sci.* 2018 Jan 16;115(3):567–72. doi: 10.1073/pnas.1714658115.

152. Marinelli LJ, Piuri M, Swigoňová Z, Balachandran A, Oldfield LM, van Kessel JC et al. **BRED: A simple and powerful tool for constructing mutant and recombinant bacteriophage genomes.** *PLoS One*. 2008;3(12):3957–75. doi: 10.1371/journal.pone.0003957.

153. Rita Costa A, Milho C, Azeredo J, Pires DP. **Synthetic Biology to Engineer Bacteriophage Genomes.** In: Sillankorva S, Azeredo J, editors. *Bacteriophage Therapy*. New York, NY, USA: Humana Press; 2018. p. 285–300.

154. Hupfeld M, Trasanidou D, Ramazzini L, Klumpp J, Loessner MJ, Kilcher S. **A functional type II-A CRISPR–Cas system from *Listeria* enables efficient genome editing of large non-integrating bacteriophage.** *Nucleic Acids Res.* 2018 Jul 27;46(13):6920–33. doi: 10.1093/nar/gky544.

155. Pires DP, Cleto S, Sillankorva S, Azeredo J, Lu TK. **Genetically Engineered Phages: a Review of Advances over the Last Decade.** *Microbiol Mol Biol Rev.* 2016 Sep 1;80(3):523–43. doi: 10.1128/MMBR.00069-15.

156. Shen J, Zhou J, Chen G-Q, Xiu Z-L. **Efficient Genome Engineering of a Virulent *Klebsiella* Bacteriophage Using CRISPR-Cas9.** *J Virol.* 2018 Jun 13;92(17). doi: 10.1128/JVI.00534-18.

157. Schilling T, Dietrich S, Hoppert M, Hertel R. **A CRISPR-Cas9-Based Toolkit for Fast and Precise *In Vivo* Genetic Engineering of *Bacillus subtilis* Phages.** *Viruses.* 2018 May 4;10(5):241. doi: 10.3390/v10050241.

158. Hinkley TC, Garing S, Singh S, Le Ny A-LM, Nichols KP, Peters JE et al. **Reporter bacteriophage T7 NLC utilizes a novel NanoLuc::CBM fusion for the ultrasensitive detection of *Escherichia coli* in water.** *Analyst.* 2018;143(17):4074–82. doi: 10.1039/c8an00781k.

159. Manor M, Qimron U. **Selection of Genetically Modified Bacteriophages Using the CRISPR-Cas System.** *Bio Protoc.* 2017;7(15). doi: 10.21769/BioProtoc.2431.

160. Bari SMN, Walker FC, Cater K, Aslan B, Hatoum-Aslan A. **Strategies for Editing Virulent *Staphylococcal* Phages Using CRISPR-Cas10.** *ACS Synth Biol.* 2017 Dec 15;6(12):2316–25. doi: 10.1021/acssynbio.7b00240.

161. Tao P, Wu X, Tang W, Zhu J, Rao V. **Engineering of Bacteriophage T4 Genome Using CRISPR-Cas9.** *ACS Synth Biol.* 2017 Oct 20;6(10):1952–61. doi: 10.1021/acssynbio.7b00179.

162. Born Y, Fieseler L, Thöny V, Leimer N, Duffy B, Loessner MJ. **Engineering of Bacteriophages Y2:: dpoL1-C and Y2:: luxAB for Efficient Control and Rapid Detection of the Fire Blight Pathogen, *Erwinia amylovora.*** *Appl Environ Microbiol.* 2017 Jun 15;83(12):1–13. doi: 10.1128/AEM.00341-17.

163. Nobrega FL, Costa AR, Santos JF, Siliakus MF, Van Lent JWM, Kengen SWM et al. **Genetically manipulated phages with improved pH resistance for oral administration in veterinary medicine.** *Sci Rep.* 2016;6(November):1–12. doi: 10.1038/srep39235.

164. Ando H, Lemire S, Pires DP, Lu TK. **Engineering Modular Viral Scaffolds for Targeted Bacterial Population Editing.** *Cell Syst.* 2015;1(3):187–96. doi: 10.1016/j.cels.2015.08.013.

165. Martel B, Moineau S. **CRISPR-Cas: an efficient tool for genome engineering of virulent bacteriophages.** *Nucleic Acids Res.* 2014 Aug;42(14):9504–13. doi: 10.1093/nar/gku628.

166. Kiro R, Shitrit D, Qimron U. **Efficient engineering of a bacteriophage genome using the type I-E CRISPR-Cas system.** *RNA Biol.* 2014 Jan;11(1):42–4. doi: 10.4161/rna.27766.

167. da Silva JL, Piuri M, Broussard G, Marinelli LJ, Bastos GM, Hirata RDC et al. **Application of BRED technology to construct recombinant D29 reporter phage expressing EGFP.** *FEMS Microbiol Lett.* 2013;344(2):166–72. doi: 10.4161/rna.27766.

168. Fehér T, Karcagi I, Blattner FR, Pósfai G. **Bacteriophage recombineering in the lytic state using the lambda red recombinases.** *Microb Biotechnol.* 2012 Jul;5(4):466–76. doi: 10.1111/j.1751-7915.2011.00292.x.

169. Schofield DA, Bull CT, Rubio I, Wechter WP, Westwater C, Molineux IJ. **Development of an Engineered Bioluminescent Reporter Phage for Detection of Bacterial Blight of Crucifers.** *Appl Environ Microbiol.* 2012;78(10):3592–8. doi: 10.1128/AEM.00252-12.

170. Catalão MJ, Milho C, Gil F, Moniz-Pereira J, Pimentel M. **A Second Endolysin Gene Is Fully Embedded In-Frame with the lysA Gene of Mycobacteriophage Ms6.** *PLoS One.* 2011 Jun 9;6(6):e20515. doi: 10.1371/journal.pone.0020515.

171. Lu TK, Collins JJ. **Engineered bacteriophage targeting gene networks as adjuvants for antibiotic therapy.** *Proc Natl Acad Sci U S A.* 2009 Mar 24;106(12):4629–34. doi: 10.1073/pnas.0800442106.

172. Lu TK, Collins JJ. **Dispersing biofilms with engineered enzymatic bacteriophage.** *Proc Natl Acad Sci U S A.* 2007 Jul 3;104(27):11197–202. doi: 10.1073/pnas.0704624104.

173. Brigati JR, Ripp SA, Johnson CM, Iakova PA, Jegier P, Sayler GS. **Bacteriophage-based bioluminescent bioreporter for the detection of *Escherichia coli* 0157:H7.** *J Food Prot.* 2007;70(6):1386–92. doi: 10.4161/rna.27766.

Chapter II

Control of *Salmonella* Enteritidis on Food Contact Surfaces with Bacteriophage PVP-SE2

This chapter was based on the following paper:

Milho C, Silva MD, Melo L, Santos S, Azeredo J, Sillankorva S. Control of *Salmonella* Enteritidis on food contact surfaces with bacteriophage PVP-SE2. 2018. Biofouling (30:1-16; doi: 10.1080/08927014.2018.1501475)

Abstract

Salmonella is one of the worldwide leading foodborne pathogens responsible for illnesses and hospitalizations, and its capacity to form biofilms is one of its many virulence factors. This work evaluated (bacterio)phage control of adhered and biofilm cells of *Salmonella* Enteritidis on three different substrata at refrigerated and room temperatures, and also a preventive approach in poultry skin. PVP-SE2 phage was efficient in reducing both 24- and 48-h old *Salmonella* biofilms from polystyrene and stainless steel, causing 2 to 5 log CFU.cm^{-2}, with higher killing efficiency at room temperature. PVP-SE2 phage application on poultry skins reduced levels of *Salmonella*. Freezing phage-pretreated poultry skin samples had no influence on the viability of phage PVP-SE2 and their *in vitro* contamination with *S.* Enteritidis provided evidence that phages prevented its further growth. Although not all conditions favour phage treatment, this study endorses their use to prevent and control foodborne pathogen colonization of surfaces.

Keywords: *Salmonella*; bacteriophage; biofilm; control; prevention

2.1 Introduction

Foodborne bacteria continue to be a major cause of illnesses in humans around the world, causing severe threats to human health and safety. Two million deaths are estimated to occur annually due to illnesses related to contaminated food and water, according to the World Health Organization (WHO) [1]. Hence, food safety constitutes an increasing worldwide public health concern, in which *Salmonella* remains one of the most common causes of the reported food poisoning events [1,2]. The disease caused by *Salmonella*, salmonellosis, is the result of ingestion of this bacterium, and it shows symptoms such as diarrhea, fever and abdominal pain that occur 12 to 72 h after consumption of contaminated food [3]. The leading identified food sources for human salmonellosis are poultry products, in particular chicken products [4,5]. During the different stages of food processing, from production to consumption, products are susceptible to cross-contamination, particularly in the case of poultry meat products [6] . Improper handling by the consumer can also contribute to the increased rates of infection [7].

The ecology and occurrence of *Salmonella* serovars in poultry comparing to those directly associated with human salmonellosis remain difficult to quantify, owing to serovar variability in culture media recovery [8]. However, *Salmonella enterica* serovar Enteritidis is one of the most reported serovars related to salmonellosis outbreaks [9].

Problems related to *Salmonella* have significantly increased due to the growing antimicrobial resistance, and also because of its inherent capacity to adhere to surfaces and consequently form biofilms [10,11]. Bacteria within biofilms have an increased resistance to antibiotics, disinfectants, surfactants, and other products with antimicrobial activity [12].

Phages are viruses that infect bacterial cells using the host's machinery to create new progeny. Because of their ability to kill bacteria, they appear to be a good alternative to other products usually used for this purpose (antimicrobials, disinfectants) [13]. Phages present many advantages over traditional antibiotics, since they are specific and efficient against their target bacteria, thereby reducing the destruction of the host's normal flora [14]. They are also innocuous for humans, and they persist only as long as the target pathogen is present [15,16].

In food industries, the use of new phages and commercially available phage products has recently increased, specially owing to the good results for pathogen reduction reported by several authors [17–20]. Also, the FDA's first approved phage product, Listex™ P100, to control *Listeria monocytogenes* in foods, was a strong incentive for the scientific community to start applying phages in food products [21]. Currently, there are several phage-based products approved by the

FDA including PhageGuard Listex™ (previously known as Listex™ P100), for *Listeria*, PhageGuard S™ (previously known as Salmonelex™), for *Salmonella*, ListShield™, EcoShield™, and SalmoFresh™. In a previous study, several *Salmonella* phages were isolated and characterized into different groups [22]. Some of these phages were verified to be good candidates for phage biocontrol of contaminated poultry products, including PVP-SE2 phage, previously known as φ38 [22], which was used in the work described herein. The main goal of this work was to evaluate the *in vitro* efficacy of phage PVP-SE2 to infect adhered and biofilm cells of *Salmonella* Enteritidis on different surfaces and minimize *S.* Enteritidis colonization of poultry skin surfaces.

2.2 Materials and methods

2.2.1 Bacteria and phages

Salmonella enterica serovar Enteritidis S1400 was used to propagate phage PVP-SE2 previously known as φ38 [22]. The bacterium was grown at 37 °C in liquid LB medium or in solid LB medium (LB + 1.5% (w.v^{-1}) of agar). The LPS mutants of *Salmonella* enterica serovar Typhimurium LT2 used in this study were obtained from the *Salmonella* Genetic Stock Centre (University of Calgary, AB, Canada).

2.2.2 Phage propagation and titration

Salmonella phage PVP-SE2 was amplified using the plate lysis and elution method [23]. Titration of the phage was performed according to a previously described protocol [24].

2.2.3 Transmission Electron Microscopy

The morphology of phage particles was observed by transmission electron microscopy (TEM), as previously described [25]. Briefly, phage particles were collected after centrifugation (1 h, 25,000 × *g*, 4 °C). The pellet was washed twice in tap water using the same centrifugation conditions. Phages were deposited on copper grids with carbon-coated Formvar films, stained with 2% (w.v^{-1}) uranyl acetate (pH 4.0) and imaged using a Philips EM 300 electron microscope, with magnification being monitored with T4 phage tails [26].

2.2.4 Phage one-step growth characteristics

The one-step growth curve of phage PVP-SE2 was carried out as previously described [27]. Briefly, 10 mL of mid-exponential phase (OD_{620} ≈ 0.5) *S.* Enteritidis S1400 culture were harvested by centrifugation (7,000 × *g*, 5 min, 4 °C) and the pellet ressuspended in 5 mL of fresh LB to obtain an OD_{620} of 1.0. To this suspension, 5 mL of phage were added to have a multiplicity of infection (MOI) of 0.001. Phage PVP-SE2 was allowed to adsorb for 5 min at room temperature. The mixture was centrifuged as described above and the pellet ressuspended in 10 mL of fresh LB. Samples were taken every 5 min until 40 min, and immediately plated.

2.2.5 Phage DNA extraction, genome sequencing and annotation

Phage DNA was extracted essentially as described before [25]. Purified phages were treated with 0.016% ($v.v^{-1}$) L1 buffer [300 mM NaCl, 100 mM Tris/HCl (pH 7.5), 10 mM EDTA, 0.2 $mg.mL^{-1}$ BSA, 20 $mg.mL^{-1}$ RNase A, 6 $mg.mL^{-1}$ DNase I] for 2 h at 37 °C. After a thermal inactivation of the enzymes for 15 min at 70 °C, 50 $\mu g.mL^{-1}$ proteinase K, 20 mM EDTA and 1% ($w.v^{-1}$) SDS were added and proteins were digested for 18 h at 56 °C. This was followed by phenol, phenol:chloroform:isoamyl alcohol (25:24:1, ($v.v^{-1}$)) and chloroform extractions, respectively. DNA was precipitated with isopropanol (100%) and 3 M sodium acetate (pH 4.6), centrifuged (15 min, 7,600 × *g*, 4 °C), and the pellet air-dried and further resuspended in nuclease-free water (Cleaver Scientific, UK). Genome sequencing was performed on a 454 sequencing platform (Plate-forme d′ Analyses Génomiques at Laval University, Québec city, QC, Canada) to 50-fold coverage. Sequence data was assembled using SeqMan NGen4 software (DNASTAR, Madison, WI, USA). The phage genome was autoannotated, using MyRAST [28] and the presence of non-annotated coding DNA sequences (CDSs), along with genes in which the initiation codon was miscalled, were checked manually using Geneious 6.1.6 (Biomatters, Newark, NJ, USA). Potential frameshifts were checked with BLASTX [29], and BLASTP was used to check for homologous proteins [30], with an E-value threshold of $<1 \times 10^{-5}$ and at least 80% query. Pfam [31] and InterProScan [32] were used for protein motif search, with the same cutoff parameters as used with BLASTP. Proteins molecular weight and isoelectric point were determined using ExPASy Compute pI/Mw [33]. The presence of transmembrane domains was predicted operating TMHMM [34] and Phobius [35], and membrane proteins were annotated when both tools were in agreement. The search of tRNA encoding genes was performed using tRNAscan-SE [36]. Putative promoter regions were checked using PromoterHunter from phiSITE [37] and were further manually verified. ARNold [38] was used to predict rho-independent terminators and the energy was calculated using Mfold [39]. The complete genome sequence of PVP-SE2 was submitted to GenBank under the accession number MF431252.

2.2.6 Stability of phage PVP-SE2 at refrigerated and frozen temperatures

Stability of PVP-SE2 on poultry skins was assessed at refrigerated (4 °C) and frozen (-18 °C) temperatures. Briefly, poultry skin samples (1 cm × 1 cm) were disinfected (Table 2.2), and to each skin square 100 µL of phage PVP-SE2 were added at different concentrations (10^4, 10^5 and

10^6 PFU.mL^{-1}). Skins were dried for 30 min and after that they were transferred to the appropriate storage conditions (4 °C and -18 °C). To recover phage PVP-SE2 from the skin squares, samples were immerged in 1 mL of SM buffer (5.8 g.L^{-1} NaCl, 2 g.L^{-1} $MgSO_4$.7 H_2O, 50 mL 1 M Tris, pH 7.5) and vortexed for 30 s. Serial dilutions were done in SM buffer for each phage PVP-SE2 concentration used, and the plaque forming units (PFUs) determined. Samples were stored for 10 days with triplicate samples assessed every day.

2.2.7 Susceptibility of surviving cells and LT2 mutants to phages

Single colonies (n=12) from each of the three independent phage treatments performed were randomly selected from the stainless steel, polystyrene, and skin surfaces. The susceptibility of these colonies to four phages was tested according to a procedure previously described [40]. The phages PVP-SE2, φ68, PVP-SE1, and φ135 have all been previously characterized [22]. PVP-SE2, φ68, PVP-SE1, and φ135 were also plated in *S.* Typhimurium LT2 mutant strains that have different degrees of deletion in the lipopolysaccharide (LPS) chain (Figure 2.10). Briefly, 10 µL of 10-fold serial dilutions of phage starting at 10^9 PFU.mL^{-1} were added to the bacterial lawns of the mutant strains. Plates were incubated overnight at 37 °C, and lytic activity was checked for the formation of lysis areas and phage plaque turbidity.

2.2.8 *S.* Enteritidis colonization of polystyrene and treatment with phage

Biofilms of *S.* Enteritidis S1400 were formed at 22 °C and 4 °C, in 24-well plates (Sarstedt, Inc., Germany), under static conditions and without medium change to better mimic the handling/storage conditions of poultry products. For biofilm formation, 1 mL of *S.* Enteritidis at 1 × 10^4 CFU.mL^{-1} prepared in LB was added to each well. Biofilms were formed for 1, 24, and 48 h at 22 °C, and for 4, 24, 48, and 72 h at 4 °C, washed once with saline solution (NaCl 0.9% (w.v^{-1})) and treated with phage PVP-SE2 at MOIs of 0.1, 1 and 10. For this, 250 µL of LB and 750 µL of phage were added to each well in order to obtain the right MOI. In the negative control, instead of 750 µL of phage, 750 µL of SM buffer were added. At the end of the treatment, biofilms were washed twice and 1 mL of saline solution (NaCl 0.9% (w.v^{-1})) with ferric ammonium sulfate (FAS) at 2 mM was added to each well. Microplates were sonicated (water bath sonicator, Sonic model SC-52, UK) for 6 min, all wells scrapped and the number of viable cells in each well (CFUs) was counted.

2.2.9 *S.* Enteritidis colonization of stainless steel and treatment with phage

Stainless steel coupons (stainless steel S30400) measuring 1 cm × 1 cm were disinfected by soaking in ethanol 96% ($v.v^{-1}$) for 30 min, washed with distilled water, dried for 30 min at 60 °C and autoclaved at 121 °C for 15 min. The coupons were placed in 24-well plates and contaminated with *S.* Enteritidis S1400. For this, 1 mL of *S.* Enteritidis S1400 at 1×10^4 $CFU.mL^{-1}$ prepared in LB was added to each well. 24 and 48 h old biofilms were formed at 4 °C and 22 °C under static conditions. After this, coupons were washed with 1 mL of saline solution (NaCl 0.9% ($w.v^{-1}$)), and to each well 250 µL of LB medium plus 750 µL of phage PVP-SE2 were added. Phage PVP-SE2 was added at different MOIs (0.1, 1 and 10). In the negative control, instead of 750 µL of phage, SM buffer was used. After 2, 5 or 24 h of incubation, the coupons were washed with saline solution (NaCl 0.9% ($w.v^{-1}$)), put in 1 mL of saline solution (NaCl 0.9% ($w.v^{-1}$)) with FAS at 2 mM, sonicated for 6 min (water bath sonicator, Sonic model SC-52, UK) and vortexed for 30 s. To determine the number of viable cells in each coupon, CFUs counts were performed.

2.2.10 Scanning Electron Microscopy

Biofilm samples formed on stainless steel and polystyrene coupons were rinsed by immersion in dH_2O before adding paraformaldehyde 4% for 1 h at 4 °C. Dehydration was carried out with an ethanol series from 30% to 50 % to 70 % to 80 % to 90 % and absolute, at 4 °C. After fixation, samples were characterized using a desktop Scanning Electron Microscope (SEM) (Phenom ProX, Netherlands). All results were acquired using the ProSuite software (ThermoFisher Scientific, MA, USA). Samples were added to aluminium pin stubs with electrically conductive carbon adhesive tape (PELCO Tabs™, Ted Pella, Inc., CA, USA) and coated with 2 nm of Au for improved conductivity. Each aluminium pin stub was then placed inside a Phenom Standard Sample Holder. The analysis was conducted at 5 kV with intensity image.

2.2.11 *S.* Enteritidis colonization of poultry skins and treatment with phage

Poultry skin samples were cut into small squares (1 cm × 1 cm) and immersed in different solutions and/or in an ultrasound bath during distinct periods of time (Table 2.2). This was carried out to ensure that any effect observed was solely due to the added bacteria and not any other microorganisms, which could lead to variations in the interpretation of the results. After each treatment, viable cells were determined by CFUs counts. Complete eradication of *Salmonella* from

the skin samples was achieved after 4 distinct treatments: 1) acetic acid together with ultrasonic bath; 2) acetic acid (45 min, 4 °C); 3) lactic acid (2 min, 22 °C); and 4) ethanol 96% (30 s, 22 °C). Therefore, for all further experiments, the ethanol (96% ($v.v^{-1}$)) treatment was adopted since it was the fastest treatment tested and there was limited residual activity due to evaporation. For this procedure, poultry skin squares (1 cm × 1 cm) were immersed in ethanol 96% ($v.v^{-1}$), washed with sterile distilled water, and frozen until further use. Frozen skin squares were placed in 24-well microplates. Each square was inoculated on top with 100 µL of an overnight culture of *S.* Enteritidis S1400 diluted with fresh LB medium to a final concentration of 10^4 $CFU.mL^{-1}$. The plates were incubated at 4 °C during 4 and 24 h. After incubation, the skin samples were washed twice with saline solution (NaCl 0.9% ($w.v^{-1}$)), and PVP-SE2 (100 µL) was added to the skin squares at MOIs of 10 and 100. Negative control assays were performed with 100 µL of SM buffer instead of phage. Skin samples were incubated at 4 °C and phage infection was carried for 2, 5 and 24 h. After the treatment, skin samples were washed with 1 mL of saline solution (NaCl 0.9% ($w.v^{-1}$)), put in 1 mL of saline solution (NaCl 0.9% ($w.v^{-1}$)) with FAS at 2 mM, vortexed for 30 s and counting of CFUs was performed.

2.2.12 Phage PVP-SE2 pretreatment of poultry skin samples and post-contamination with *S.* Enteritidis

Phage PVP-SE2 solutions (100 µL) with concentrations of 10^4, 10^5 and 10^6 $PFU.mL^{-1}$ were added to disinfected poultry skin squares (1 cm × 1 cm) and incubated for 30 min at 4 °C. After that, *S.* Enteritidis S1400 (100 µL at 10^4 $CFU.mL^{-1}$) was spread on top of the skin samples, which were then incubated at 4 °C during 5, 24 and 48 h. Negative controls were skin squares in which the 100 µL of phage solution were replaced by 100 µL of SM buffer. After incubation, skin samples were washed, vortexed for 30 s in 1 mL of saline solution (NaCl 0.9% ($w.v^{-1}$)) with FAS at 2 mM and CFUs counts were performed.

2.2.13 Statistical analysis

Statistical analysis of the results was performed using GraphPad Prism 6 (GraphPad Software, CA, USA). Mean and standard deviations (SD) were determined for the independent experiments and the results were presented as mean±SD. Results were compared using two-way ANOVA, with Tukey's multiple comparison statistical test. Differences were considered statistically significant if

$p < 0.05$ (95% confidence interval).

2.3 Results

2.3.1 Phage PVP-SE2

Phage PVP-SE2 was previously suggested as a good biocontrol agent due to its broad-host range [22]. The virion particle resembles phages belonging to the Jersey-like genus of the *Siphoviridae* family, having heads of 57 nm, tails of 125 nm in length and 8 nm wide, and a base plate with three or more spikes (Figure 2.1 A). Furthermore, this phage forms clear plaques, 3 mm in diameter, without halo, in bacterial lawns of its host (data not shown). The one-step growth characteristics revealed that the latent period was 15 min, with a rise period of 15 min, thereby giving an average of 202 progeny phages per infected cell (Figure 2.1 B).

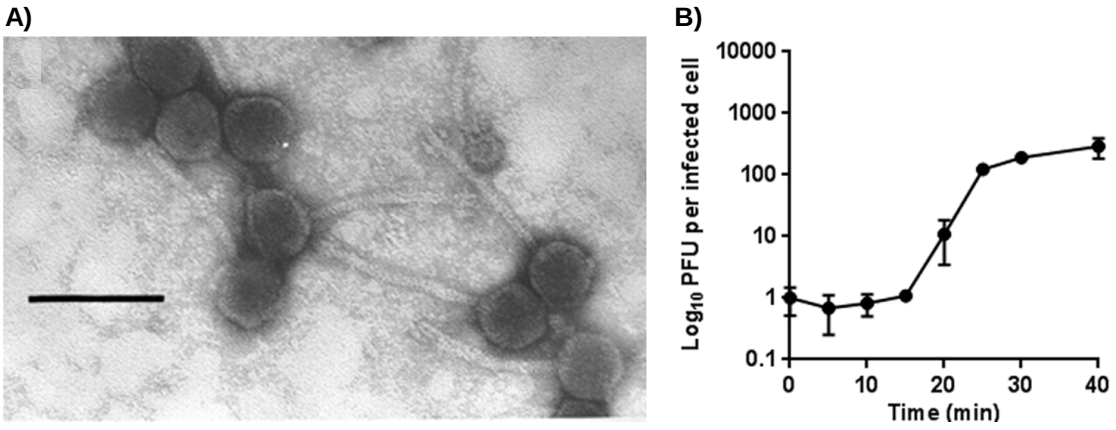

Figure 2.1 - Phage PVP-SE2 characteristics. A) TEM micrograph of phage PVP-SE2. Scale bar represents 100 nm, B) one-step growth curve.

Genome analysis revealed that PVP-SE2 is a virulent phage that does not encode genes related with lysogeny nor known toxins of bacterial origin (Figure 2.2). PVP-SE2 has a linear dsDNA with 42,425 bp with a G + C content of 49.98%. This phage encodes 60 putative coding sequences (CDSs), tightly packed, occupying 92% of its genome (Table 2.1). From the predicted CDSs, 29 had an assigned function, and no unique proteins nor tRNA genes were identified. Fifty-three CDSs possess methionine as a start codon, while four and three CDSs start with GTG and TTG, respectively. Seventeen of the genes are rightward oriented, while 43 are leftward oriented.

Table 2.1 - Features of *S.* Enteritidis phage PVP-SE2 ORFs

ORF	Start	End	Length	AA*	Product	ORF	Start	End	Length	AA*	Product
1	95	325	231	76	hypothetical protein	**30**	23026	23541	516	171	hypothetical protein
2	342	620	279	92	hypothetical membrane protein	**31**	23538	24038	501	166	hypothetical protein
3	638	994	357	118	hypothetical protein	**32**	24040	26373	2334	777	tail tape measure protein
4	991	1146	156	51	hypothetical protein	**33**	26366	26725	360	119	hypothetical protein
5	1143	1301	159	52	hypothetical protein	**34**	26731	27204	474	157	tail assembly chaperone
6	1298	1483	186	61	hypothetical protein	**35**	27317	27496	180	59	superinfection immunity protein
7	1667	2155	489	162	endolysin	**36**	27559	28689	1131	376	hypothetical protein
8	2136	2423	288	95	holin class I	**37**	28686	28916	231	76	hypothetical protein
9	2785	3219	435	144	hypothetical protein	**38**	28884	29030	147	48	hypothetical protein
10	3225	3602	378	125	hypothetical protein	**39**	29029	29700	672	223	DNA-binding protein
11	3605	3808	204	67	hypothetical protein	**40**	29729	30898	1170	389	major tail protein
12	3871	4035	165	54	hypothetical protein	**41**	30898	31317	420	139	hypothetical protein
12A	4230	4337	108	35	hypothetical protein	**42**	31317	31712	396	131	tail protein
13	4405	4581	177	58	hypothetical protein	**43**	31709	32068	360	119	hypothetical protein
14	5476	5646	171	56	DNA-binding HTH domain	**44**	32068	32673	606	201	hypothetical protein
15	5643	5876	234	77	hypothetical protein	**45**	32676	33185	510	169	hypothetical protein
16	5933	8119	2187	728	primase/helicase	**46**	33189	33377	189	62	hypothetical protein
17	8134	8352	219	72	DNA-binding HTH domain	**47**	33414	33764	351	116	Phage neck whiskers
18	8486	9010	525	174	hypothetical protein	**48**	33778	34062	285	94	head protein
19	9054	9536	483	160	HNH endonuclease	**49**	34123	35172	1050	349	coat protein
20	9589	10839	1251	416	hypothetical protein	**50**	35176	35877	702	233	scaffold protein
21	10921	11547	627	208	hypothetical protein	**51**	35962	36087	126	41	i-Spanin
22	11605	14703	3099	1032	DNA polymerase	**52**	36071	36457	387	128	o-Spanin
23	14790	15077	288	95	restriction endonuclease	**53**	36502	36621	120	39	hypothetical protein
24	15109	15300	192	63	hypothetical protein	**54**	36776	37234	459	152	phage neck whiskers
25	15297	17762	2466	821	intein containing helicase	**55**	37237	38280	1044	347	head morphogenesis protein
26	17759	17929	171	56	hypothetical protein	**56**	38457	39107	651	216	amidase
27	18048	20102	2055	684	tailspike protein	**57**	39137	40606	1470	489	portal protein
28	20115	22673	2559	852	tail fiber protein	**58**	40619	41890	1272	423	terminase, large subunit
29	22664	23029	366	121	hypothetical protein	**59**	41880	42386	507	168	terminase, small subunit

*AA - Amino acids.

Overall, 11 promoters and 14 rho-independent terminators were found throughout the genome. Based on the predictions, the genome appeared to be in four functional modules (packaging, structure/morphogenesis, host lysis and replication/regulation), which fits the typical structure of most dsDNA phages (Figure 2.2).

Whole-genome comparison using BLASTN algorithm revealed that PVP-SE2 is highly homologous (>90% coverage, >90% identity and an E-value of 0) to several *Salmonella* siphoviruses, namely of the genus *Jerseyvirus*, indicating that PVP-SE2 belongs to this genus. Overall, the analysis performed herein revealed that this phage is theoretically safe for *Salmonella* control on foods and surfaces.

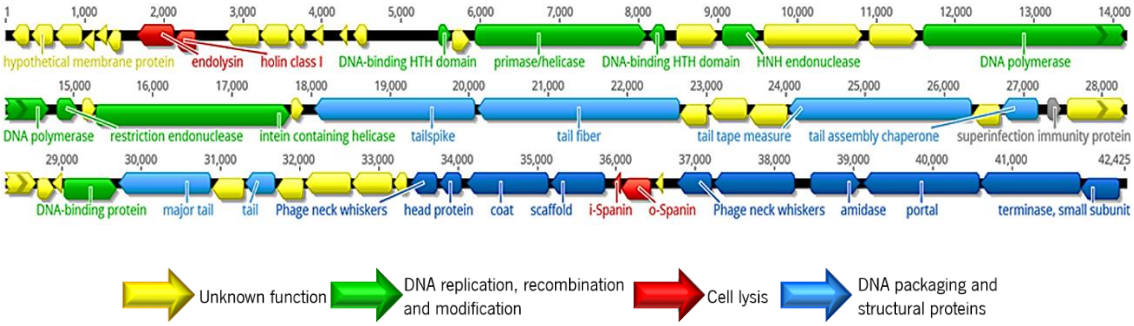

Figure 2.2 - Linear map of phage PVP-SE2 genome sequence. The arrows point the direction of transcription, represent the predicted ORFs and are coloured (blue, green, red and yellow) according to their predicted functions. Major transcriptional units are represented.

2.3.2 PVP-SE2 viability at refrigerated and freezing temperature conditions

The viability and stability of phage PVP-SE2 on poultry skin samples were monitored over a 10-day period at 4 °C and -18 °C, after the disinfection with ethanol 96% ($v.v^{-1}$), a treatment which had no effect on the phage activity, even after five days (data not shown). Test temperatures of 4 °C and -18 °C were chosen as they represent the common temperatures used for storage of poultry meat. The number of PVP-SE2 particles recovered from the samples stored either at 4 °C or -18 °C remained relatively stable after 10 days, and there was no statistically significant loss of activity (Figures 2.3 A and B), which suggests that after defrosting the phages are still capable of actively targeting *Salmonella.*

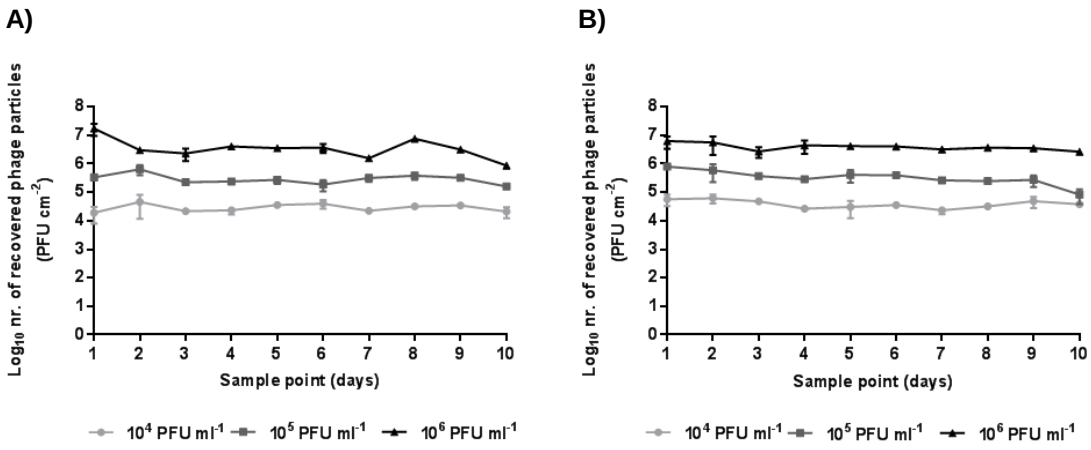

Figure 2.3 - Phage PVP-SE2 viability following storage at A) 4 °C and B) -18 °C for 10 days.

2.3.3 Phage application to *S.* Enteritidis on different contact materials

In food industry environments, *Salmonella* can be found in processing areas, such as walls, floors, pipes and drains, and on food contact surfaces such as stainless steel, aluminum, rubber or polystyrene [12]. To study adhesion and biofilm formation, three surfaces were chosen: polystyrene, stainless steel, and poultry skin. Although the study was designed to evaluate phage control of biofilms, in many circumstances, after *in vitro* contamination of the surfaces with *Salmonella*, cells only adhered and did not increase in number. Therefore, the results of phage control of adhered and biofilm cells are presented herein. At 22 °C, *S.* Enteritidis cells were allowed to adhere for 1 h to polystyrene after which the phage treatment was immediately applied at varied timepoints (Figure 2.4 A). Although phage application for 2 h had no significant effect on cells adhered for 1 h, treatment for 5 and 24 h significantly ($p < 0.05$) reduced the number of viable cells compared to the control samples, that grew 10- to 100-fold in number. In general, these results show that higher reductions were obtained for lower MOIs (0.1 and 1). Phage control of biofilms formed on polystyrene was studied for 24 and 48 h-old *S.* Enteritidis biofilms grown at 22 °C (Figures 2.4 B and C). *Salmonella* levels reached to approximately ≈ 10^6 CFU.cm^{-2} and 10^7 CFU.cm^{-2} in 24 and 48 h-old biofilms, respectively. Treatment of both 24 and 48 h-old biofilms significantly ($p < 0.05$) decreased the number of cells compared to the control samples, regardless of the phage:host ratios applied, with reductions ranging from 1.5 log CFU.cm^{-2} up to 3.4 log CFU.cm^{-2}, for 24 h biofilms (Figure 2.4 B) and from 2.1 up to 5.1 log CFU.cm^{-2}, in 48 h-old biofilms. Overall, the greatest reduction in bacterial numbers was obtained with the lowest MOI used 0.1 (Figure 2.4 C).

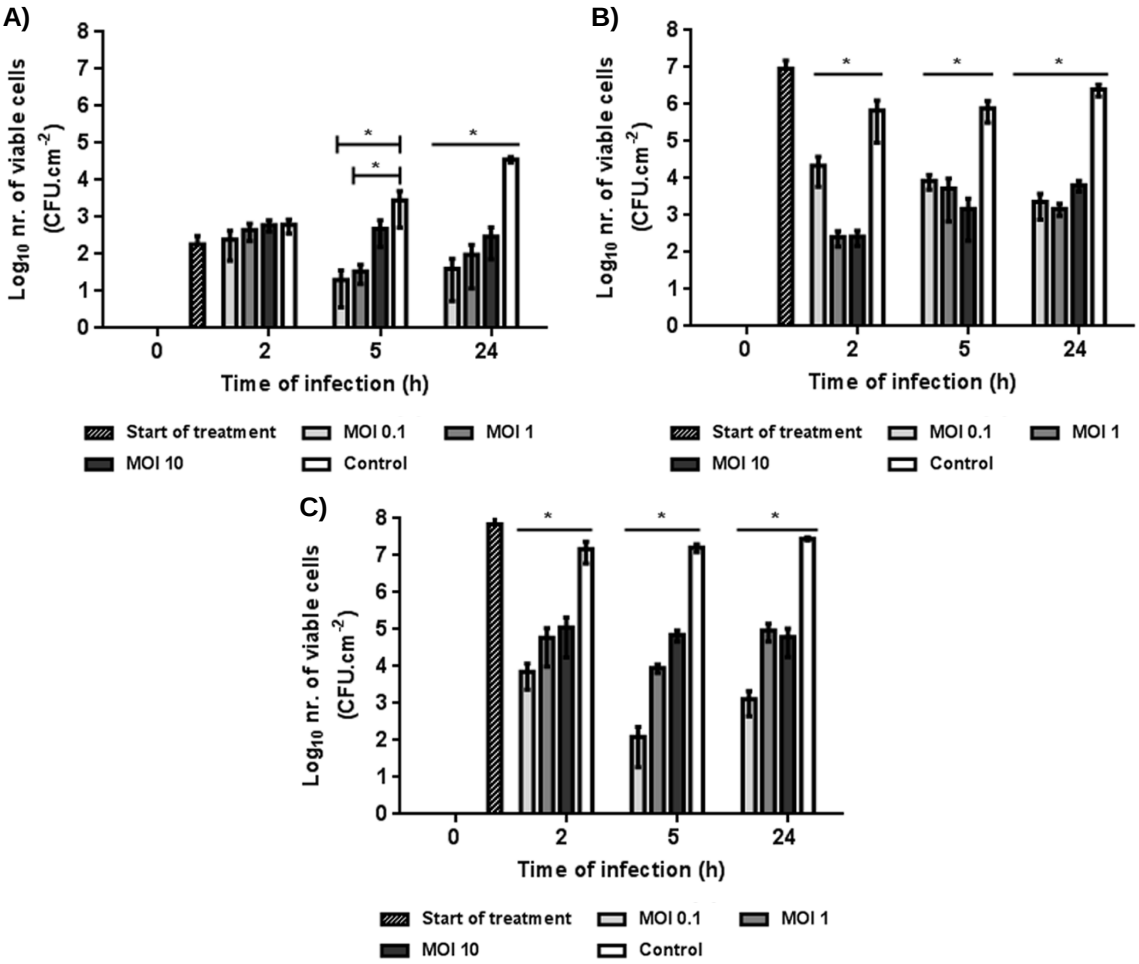

Figure 2.4 - Phage PVP-SE2 control of *S.* Enteritidis S1400 colonizing 24-well polystyrene plates at 22 °C. *S.* Enteritidis colonization during A) 1, B) 24, and C) 48 h and phage treatment during 5, 24 and 24 h. Asterisks (*) indicate significant difference ($p < 0.05$) between PVP-SE2-treated and control samples.

While PVP-SE2 clearly showed promising results at room temperature (22 °C), the same was not evidenced at refrigerated temperatures. At 4 °C, phage control experiments were carried out during 4 h up to 72 h. Even though *Salmonella* is able to grow at refrigerated temperatures, at 4 °C the levels of cells after 4 h were similar to those at 72 h (Figure 2.5) reaching approximately 2.1 log CFU.cm^{-2}. Phage treatment applied to either 48 h or 72 h adhered cells had only a minor effect (Figures 2.5 C and D), which although statistically significant ($p < 0.05$) resulted only in a maximum of 0.5 log CFU.cm^{-2} reduction.

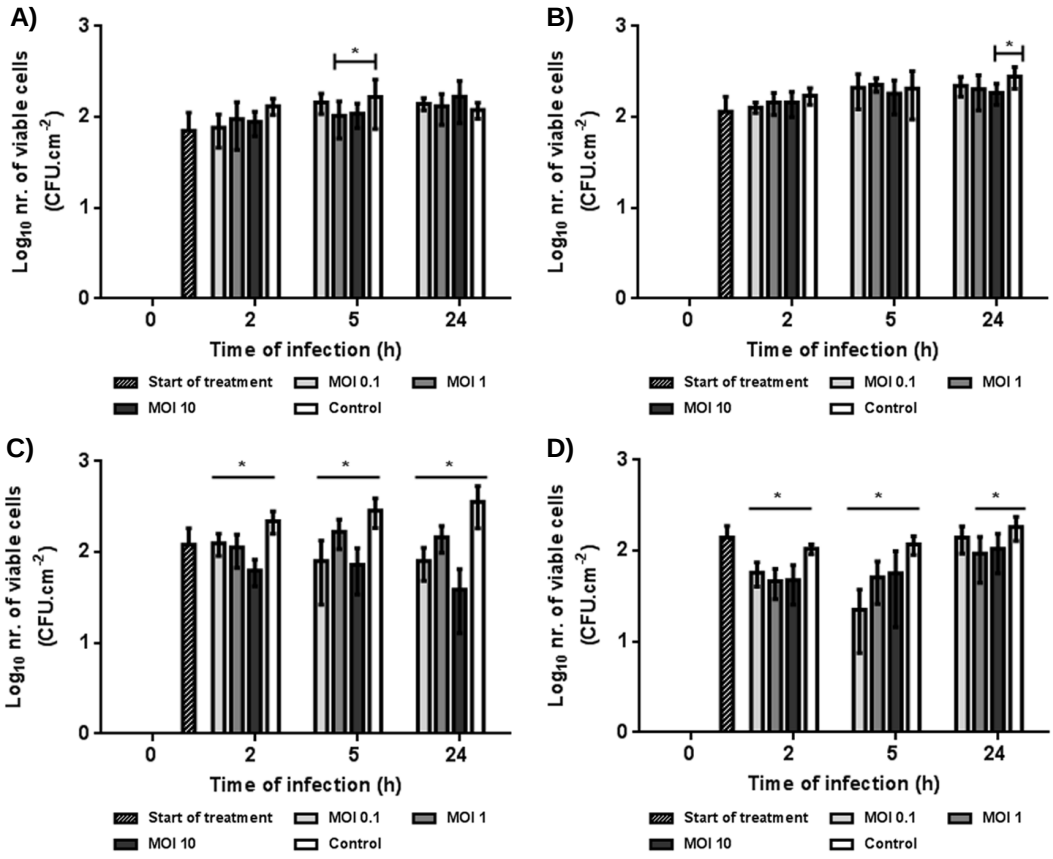

Figure 2.5 - Phage PVP-SE2 control of *S.* Enteritidis S1400 colonizing 24-well polystyrene plates at 4 °C. *S.* Enteritidis colonization during A) 4 h, B) 24 h, C) 48 and D) 72 h and phage treatment during 5, 24 and 24 h. Asterisks (*) indicate significant difference ($p < 0.05$) between PVP-SE2-treated and control samples.

SEM was used to assess biofilm formation at 22 °C on polystyrene prior and after treatment with phage (Figure 2.6). After 24 h, biofilms were mainly a layer of individual cells dispersed on the surface (Figures 2.6 E and F), while after 48 h the cells entirely covered the surface of the coupon (Figures 2.6 G and H). Phage infection resulted in damaged cells, and a high amount of cell debris along with a few intact cells (Figure 2.7).

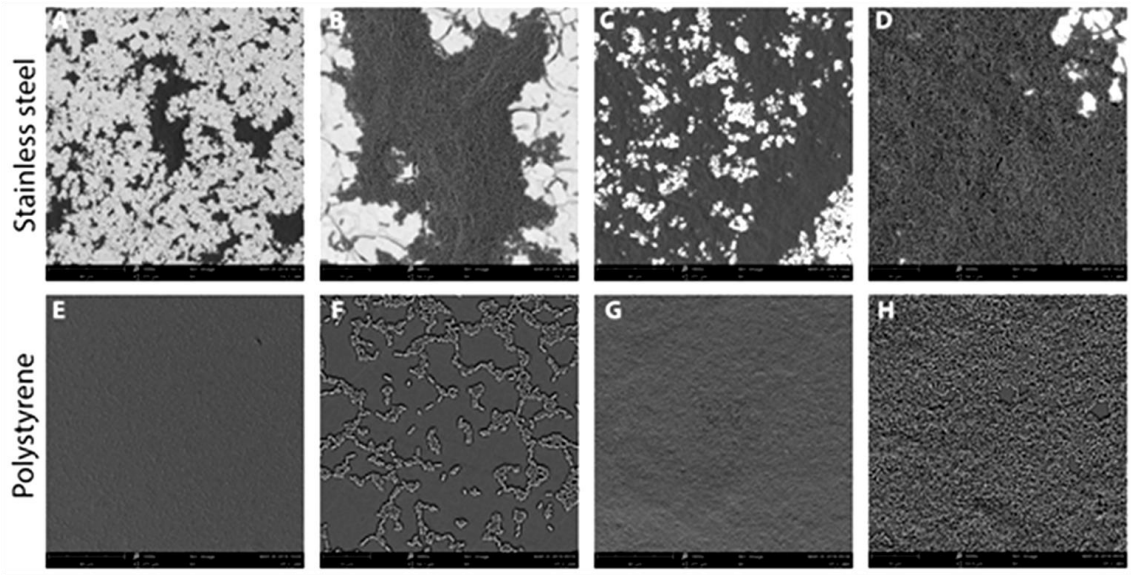

Figure 2.6 - SEM micrographs of *S.* Enteritidis colonization before and after phage application to biofilms formed on stainless steel (A-D) and polystyrene (E-H) at 22 °C, for 24 h (A, B, E and F) and 48 h (C, D, G and H).

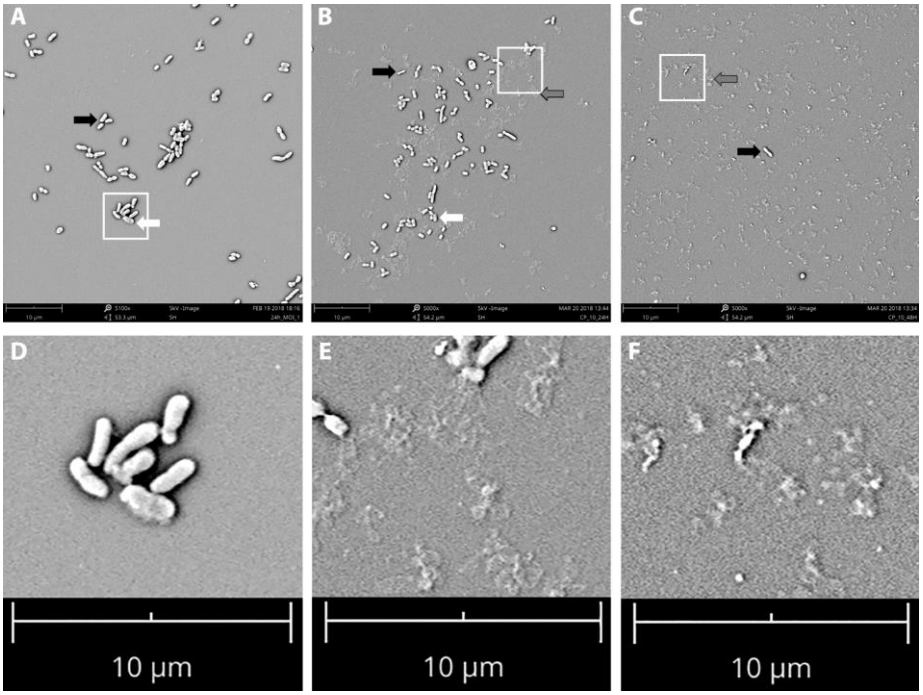

Figure 2.7 - SEM micrographs (A, B and C) and their enlargements (D, E and F, respectively) after phage application to biofilms formed on polystyrene at 22 °C, showing intact cells (black arrows), damaged cells (white arrows), and cells debris (grey arrows). Magnified areas are indicated by white squares.

Stainless steel coupons were artificially contaminated with *S.* Enteritidis S1400 and held for 24 and 48 h before being challenged with phage PVP-SE2 (Figure 2.8). At 22 °C, phage treatment applied to 24 h biofilms caused reductions of up to 1.9 log CFU.cm^{-2} for all MOIs and periods of treatment (Figure 2.8 A). Unlike the case with polystyrene, the main observation at 22 °C was that

PVP-SE2 was more efficient at reducing the number of viable cells in younger (24 h) than in older biofilms (48 h), where only 1.4 log CFU.cm^{-2} was observed (Figure 2.8 B). At 4 °C, the treatment of 24 h contaminated surfaces did not have a pronounced effect on reducing *Salmonella* numbers, despite the numbers being statistically different compared to the control (Figure 2.8 C). At this temperature, phages applied to 48 h contaminated surfaces only slightly limited the growth of cells when a MOI of 0.1 was used (Figure 2.8 D).

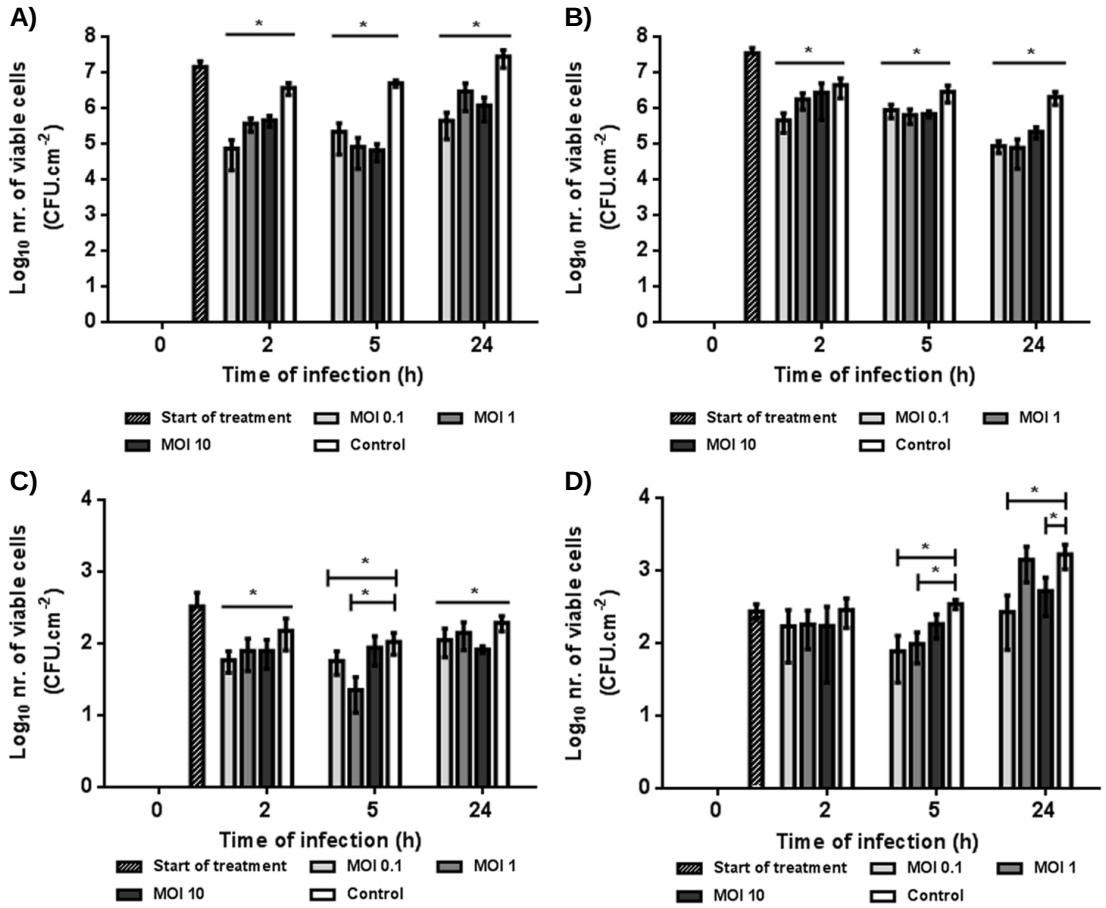

Figure 2.8 - Phage PVP-SE2 control of *S.* Enteritidis S1400 colonizing stainless steel coupons at 22 °C (A and B) and 4 °C (C and D). *S.* Enteritidis colonization during (A, C) 24 h, (B, D) 48 h and phage treatment for 2, 5 and 24 h. Asterisks (*) indicate significant difference ($p < 0.05$) between PVP-SE2-treated and control samples.

SEM images (Figure 2.6) of biofilms on stainless steel showed that these biofilms were structurally different from those formed on polystyrene, with microcolonies observed on 24 h biofilms (Figures 2.6 A and B), and a dense biofilm after 48 h (Figures 2.6 C and D). The same cell damages and debris observed in Figure 2.7 (polystyrene) were also observed on stainless steel coupons (data not shown).

In this work, the effect of phage control was further tested as well as *Salmonella* colonization

inhibition on phage pretreated poultry skins as a potential strategy that could be used before industrial packaging of poultry meats. However, before these experiments, it was important to ensure that all skin surfaces were both *Salmonella*-free and free from other species that could be present in the skin, since these could affect the results obtained by changing the adhesion kinetics of the bacteria, and biofilm formation, due to competition from other microorganisms [41,42]. For instance, the presence of *Salmonella* or even other bacteria could affect the MOI constants used and affect the adsorption of PVP-SE2. Thus, a range of disinfection approaches were tested (Table 2.2), and the easiest, fastest and most efficient method to decontaminate the skin samples, when compared to the other tested methods (e.g. ultrasonic bath, lactic acid at 2% ($v.v^{-1}$)), was adopted as the disinfection procedure.

Table 2.2 - Disinfection of *S.* Enteritidis S1400 contaminated skin samples by application of different treatments and conditions

Treatment	T (°C)	Time (min)	Cell reduction (Log_{10} $CFU.cm^{-2}$ (±SD))
Ultrasonic bath*	**22**	**15**	2.29 (0.56)
Ultrasonic bath + acetic acid (2% ($v.v^{-1}$))*	**4 / 22**	**45 / 15**	LOD
Acetic acid (2% ($v.v^{-1}$))*	**22**	**0.5**	1.55 (0.35)
	4	**45**	LOD
Lactic acid (2% ($v.v^{-1}$))*	**22**	**0.5**	1.63 (0.09)
	22	**2**	LOD
Sodium hypochlorite (2% ($v.v^{-1}$))*	**22**	**0.5**	1.73 (0.12)
Hydrogen peroxide (2% ($v.v^{-1}$))*	**22**	**0.5**	1.53 (0.27)
Ethanol (70% ($v.v^{-1}$))	**22**	**0.5**	2.40 (0.61)
Ethanol (96% ($v.v^{-1}$))	**22**	**0.5**	LOD

* Based on Loretz et al (2010) [43]; LOD – the value obtained was below the limit of detection; SD - standard deviation of three independent experiments using 4 skins.

The treatment consisted in applying ethanol 96% ($v.v^{-1}$) for 30 s at room temperature. For the phage control experiments on poultry skins, the tested MOIs were of 10 (for comparison purposes with the other two types of surfaces), and a higher one (MOI 100) (Figure 2.9 A and B). Furthermore, besides this approach, phage pretreatment of skin surfaces to inhibit *Salmonella* colonization was also assessed (Figure 2.9 C). For this latter experiment, skin samples were

pretreated with PVP-SE2 at concentrations of 10^6, 10^7 and 10^8 PFU.mL^{-1} before *in vitro* contaminating the skin samples with *S.* Enteritidis S1400. Experiments were only carried out at 4 °C since the European Food Safety Authority (EFSA) and the United States Department of Agriculture (USDA) safety recommendations for poultry meat handling do not recommend any type of handling at temperatures above refrigerated temperatures before cooking [44,45]. In the phage control strategy, *in vitro* contamination of skins was allowed to proceed during 4 and 24 h. The treatment showed that PVP-SE2 was always able to cause minor but significant reduction of viable cells and maintained viable *Salmonella* numbers at steady and lower levels than in the control samples. Maximum reductions were obtained with a MOI of 100 (Figures 2.9 A and B). This suggests that phage PVP-SE2 can be added to poultry meats to inhibit any further growth of *Salmonella*. In the prevention strategy, phages were used to pretreat skin samples, treated using phage concentrations of 10^4, 10^5 and 10^6 PFU.mL^{-1}, which were post-contaminated with *S.* Enteritidis at 4 °C (Figure 2.9 C). The highest phage concentration provided the highest inhibition for *S.* Enteritidis to colonize. Phage PVP-SE2 at 10^6 PFU.mL^{-1} after 5, 24 and 48 h reduced the levels of *Salmonella* by 1.4, 1.1 and 1.2 log CFU.cm^{-2}, respectively.

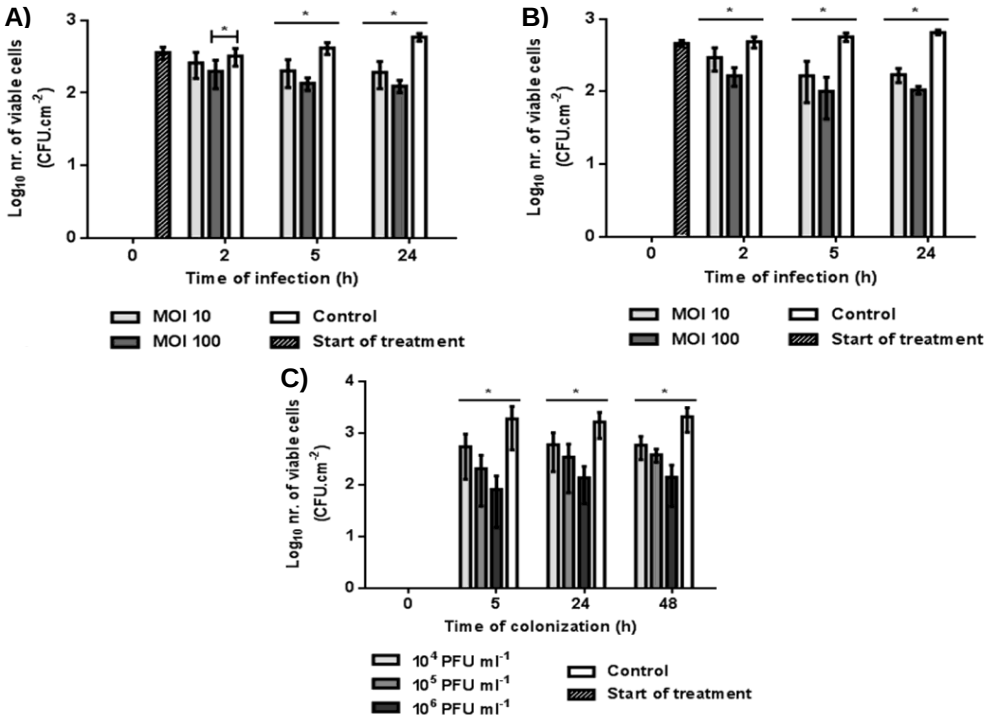

Figure 2.9 - Phage PVP-SE2 control (A and B) and inhibition (C) of *S.* Enteritidis S1400 colonizing poultry skin samples at 4 °C. *S.* Enteritidis colonization during A) 4 and B) 24 h and phage treatment during 2, 5 and 24 h. C) Phage pretreatment of skin samples was done with phage concentrations of 10^4, 10^5 and 10^6 PFU.mL^{-1}. *S.* Enteritidis colonization during 5, 24 and 48 h. Asterisks (*) indicate significant difference ($p < 0.05$) between PVP-SE2-treated and control samples.

These results suggest that phage pretreatment of skins, even using low phage concentrations, can decrease the colonization by *S.* Enteritidis. Furthermore, it is once again important to refer that PVP-SE2 does not lose viability at refrigerated and frozen temperatures as assessed in this work (Figure 2.3). Thus, pretreatment of skins limits growth of *Salmonella* once it is taken from refrigerated or frozen temperatures.

2.3.4 Susceptibility of resistant colonies

The susceptibility of several colonies from the polystyrene surfaces that survived the phage treatment were tested against the stock PVP-SE2 solution, phages φ68 and φ135 (*Siphoviridae),* and PVP-SE1 (*Myoviridae*), respectively (Table 2.3). While the majority of cells remained susceptible to PVP-SE2, several colonies selected from the experiments performed at 22 °C were no longer susceptible to the other tested phages. At 4 °C, surviving cells remained mostly susceptible to three phages (PVP-SE2, φ68, and PVP-SE1), although a percentage of these cells had acquired resistance towards phage φ135.

Table 2.3 - Susceptibility analysis of bacterial colonies that survived infection at 4 °C in all surfaces and at 22 °C in polystyrene and stainless steel to phages PVP-SE2, PVP-SE1, φ68 and φ135

Surface	T (°C)	MOI or phage concentration (Log_{10} PFU.mL^{-1})	Phage resistance (%)			
			PVP-SE2	φ68	PVP-SE1	φ135
Polystyrene	22	0.1	8.3	25.0	25.0	25.0
		10	0.0	8.3	33.3	0.0
	4	0.1	0.0	0.0	0.0	16.7
		10	25.0	0.0	0.0	33.3
Poultry Control	4	10	8.3	0.0	0.0	0.0
		100	25.0	8.33	0.0	0.0
Poultry pretreatment	4	3	0.0	0.0	0.0	0.0
		5	0.0	0.0	0.0	0.0
Stainless steel	22	0.1	100.0	100.0	0.0	33.3
		10	100.0	100.0	100.0	100.0
	4	0.1	0.0	0.0	0.0	0.0
		10	0.0	0.0	0.0	0.0

Surviving colonies from assays on stainless steel at 4 °C were susceptible to the phages tested. However, the surviving colonies from experiments at 22 °C were in general resistant to all tested phages. The survival of colonies from both the control and the pretreatment experiments on poultry skins were susceptible to the phages tested, which is in accordance to the results presented above at 4 °C, when stainless steel and polystyrene were used. This suggests that there is no or very limited emergence of resistant phage phenotypes at low temperatures.

To assess possible gene deletions occurring in *S.* Enteritidis, all phages were plated on LT2 mutant strains, a panel of well-characterized *S.* Typhimurium strains (Figure 2.10). According to Table 2.3 and the results related to ability of phages to form plaques on these strains (Figure 2.10), it was hypothesized that the most probable mutation occurring in the majority of the surviving isolates was a deletion of the complete outer core region until the first or second heptose (hep) (Rd1 and Rd2 mutants) in the inner core region.

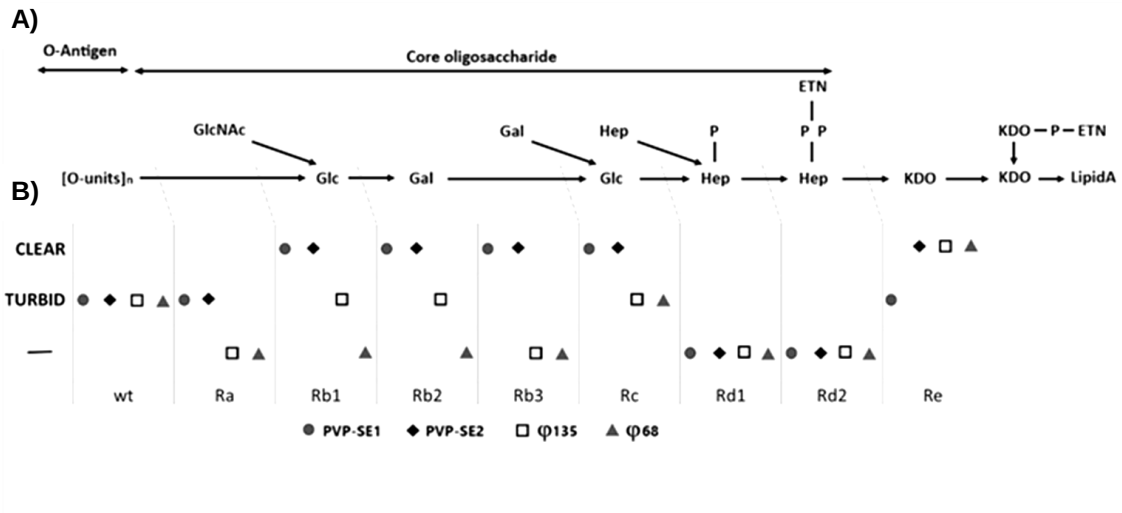

Figure 2.10 - Plaque characteristic of phages PVP-SE1, PVP-SE2, φ68 and φ135 in *S.* Typhimurium LT2 mutants: A) mutations in the LPS chain, B) phage plaque turbidity characteristics when plated in the different LT2 mutants.

2.4 Discussion

The term foodborne disease, or more commonly food poisoning, is used to denote gastrointestinal complications that occur following recent consumption of a particular contaminated food or drink. *Salmonella* is one of the most commonly associated microorganisms with this type of foodborne diseases [3], and its ability to form biofilms on different food working surfaces increases the risk of cross-contamination of food products, particularly of poultry products [6], and the occurrence of food-outbreaks [46]. A closer look to the surface colonization results obtained in this work shows that *Salmonella* can either: i) adhere to the different surfaces and not increase in number or ii) can adhere and form biofilms. Cell adhesion is mostly observed at refrigerated temperatures and after surface incubation at room temperature for 1 h. This timepoint (1 h), at room temperature, was chosen to mimic a processing surface that is not immediately disinfected and where, in a few hours, a significant increase in *Salmonella* numbers was observed (Figure 2.4). This leads to the need of developing new strategies to control this microorganism if present either in the food product itself or on food processing surfaces. The use of phages as substitutes to other antimicrobials appears to be a good alternative.

In this work, the *Salmonella* phage PVP-SE2, previously identified as a good candidate for phage biocontrol of *Salmonella* in poultry meat products [22], was characterized and the genomic analysis revealed that the phage does not encode any genes associated with lysogeny or toxin proteins (Table 2.1). In theory, all virulent phages are able of carrying out generalized transduction, and this would also include phage PVP-SE2. However, this is a rare event, since only a minority of new particles (1 in 10^4) contains bacterial DNA [47], and thus it is not considered a disadvantage of phage therapy.

The potential of this phage to control and inhibit surface colonization by *S.* Enteritidis S1400 was investigated at refrigerated (4 °C) and room temperature (22 °C). The focus on these two temperatures is related to the presence of *Salmonella* in the slaughter and processing areas (room temperature), as well as at lower temperatures (≈ 4 °C), where the products are stored. To test the ability of phage PVP-SE2 to control *S.* Enteritidis, three surfaces were used: polystyrene and stainless steel, since they are commonly used in food processing plants [12], and also poultry skins.

The treatment with phage PVP-SE2 of adhered and biofilm cells grown on both polystyrene and stainless steel was shown to be more effective at 22 °C than at refrigerated temperatures. This result was expected due to the closer optimal growth conditions in which *Salmonella* maintains

a quite active metabolism when compared to 4 °C. It is generally accepted that cell growth and temperature conditions have a major effect on phage replication. For instance, the replication of coliphage FRNA at lower than optimal cell growth temperature conditions is slower and can even cease because of the lower expression of F pili and adsorption inhibition [48,49]. Similar results have also been reported for phages of *Listeria* [50] and *Pseudomonas fluorescens* [51], where incubation at refrigeration temperatures resulted in an increase of the latent period, a reduction of the phage burst size and overall lower killing efficacy.

Increasing the incubation period of *Salmonella* at 22 °C in polystyrene and stainless steel led to approximately similar viable cell counts at the tested biofilm formation periods (approximately 7 log CFU.cm^{-2} after 24 h and closer to 8 log CFU.cm^{-2} after 48 h) (Figures 2.4 and 2.7). Phage treatment of *Salmonella* was highly influenced by the type of surface where bacteria were attached to. Greater reductions were always observed for cells that were attached to polystyrene (3 to 5 log CFU.cm^{-2}) rather than to stainless steel (1 up to 2 log CFU.cm^{-2}). In contrast to these results, it has been reported that biofilms grown on stainless steel were more susceptible to sanitizers compared to those on Teflon surfaces [52,53]. According to these authors, polymers are more prone to chemical and mechanical damage and therefore provide increased shelter for bacteria. In the present study, the differences in phage efficacy might be explained by the different biofilm structures formed on both surfaces. Polystyrene is a hydrophobic smooth surface and therefore cells have more difficulty in attaching, forming thin and small clusters of cells spread on the surface (Figure 2.6 E-H). Adhesion to stainless steel is more favourable due to its roughness and consequently cells form thick layers covering all the surface, leading to a denser structure, which is more difficult to penetrate by phages (Figure 2.6 A-D).

In the experiments performed, there was never a straight correlation between the MOI applied and the cell lysis caused. For instance, in the experiments with polystyrene, the best cell lysis results were obtained with a MOI of 0.1, although it might be expected that the use of an MOI of 1.0 or higher would lead to higher viable cell reductions. For stainless steel, the results for the highest lysis efficiencies were far more inconsistent. This may be due to the roughness of the stainless steel coupons, since it potentiates the retention of the biofilm to the stainless steel and also protects it from shear forces [54,55]. Furthermore, deposition/adhesion of phages occurs to varied abiotic surfaces, such as stainless steel [56], and has been shown to increase, for instance for F-specific RNA phages, with the increase in the degree of hydrophobicity and/or roughness [57]. This non-specific binding may explain the lower effectiveness of phage on stainless steel

where, hypothetically, the phages deposit in a higher amount and consequently not all phages are free to complete infection cycles. Previous work suggests that higher phage doses lead to reduced lysing efficacy due to the mechanism of lysis inhibition, which happens when cell density reaches concentrations of 4×10^7 CFU.mL^{-1} [58]. This observation could explain the results obtained with polystyrene. However, this phenomenon should not be surface dependent, as observed in this experiment. Overall, these results suggest that there is not a universal phage MOI strategy for biofilm control, as it is dependent on the substrata chosen for the experiments, the 3D biofilm architecture, and the level of protection that the extracellular polymeric matrix confers.

In general, it was observed that 2 h of phage application was not enough to reduce substantially the number of viable cells, indicating that for, a rapid surface sanitation, stronger antimicrobials that act immediately are needed. Nevertheless, taking into account our results, phage PVP-SE2 seems to be a very good control agent of *S.* Enteritidis of 24 and 48-h old biofilms at 22 °C. Therefore, for a better antimicrobial effect desirable for short periods, phages could be mixed with other agents for a higher and possibly synergistic action against foodborne pathogens. For instance, phages added together with chlorine, a disinfectant commonly used in the food industry, acted synergistically in the control and removal of *Pseudomonas aeruginosa* biofilms [59]. It has been previously demonstrated that the combination of the phage preparation Listex™ P100 with the chemical compounds potassium lactate and sodium diacetate resulted in an improvement of their action against bacteria present on the surface of ready-to-eat roast beef and cooked turkey, when compared with each agent alone [60]. Also, it has been showed that the combined or sequential application of the phage preparation SalmoFresh™ with lauric arginate or cetylpyridinum chloride was beneficial in reducing *Salmonella* on chicken meat and chicken skin [61].

If the specific action of phage PVP-SE2 is compared with other phages, obviously tested using a different host, some conclusions can be drawn. For instance, in one study, *S.* Enteritidis biofilms grown for four days (≈ 10^6 CFU.mL^{-1}) at 25 °C on stainless steel coupons were challenged with a mixture of five phages at a MOI of 10 for 60 min [62]. In this case, reductions lower than 0.4 log CFU were obtained. In another study, a group of *S. enterica* strains was grown on stainless steel coupons and a pool of phages was applied for a period of eight days at room temperature [63]. Although after phage treatment for seven days *S. enterica* biofilms suffered a high inhibition, after treatment for one day the number of viable cells dropped less than 1 log CFU. Both these results present similar or lower reduction values than those obtained with PVP-SE2.

The ability of PVP-SE2 as a control agent of *Salmonella* in artificially contaminated chicken skin samples was tested at 4 °C with MOIs of 10 and 100. The higher titer was more efficient with an increase of the number of *S.* Enteritidis cells being killed if the treatment period was increased. Similar and higher reductions, at 4 °C, to those obtained with PVP-SE2 have been reported for *S.* Enteritidis on poultry skins [19,64].

The use of PVP-SE2 to prevent contamination of poultry meat showed that the PVP-SE2 phage previously added to the chicken skin samples can decrease significantly the number of viable cells compared to the control samples. Higher phage concentrations used in the pretreatment of skins resulted in greater reductions in bacterial numbers for all time periods of skin colonization assessed (1.4, 1.1 and 1.2 log $CFU.cm^{-2}$ reductions at 5, 24 and 48 h, respectively). This result is a good indication that PVP-SE2 phage can be used as an agent to prevent contamination of poultry meat at refrigerated temperatures.

Even though the results at 4 °C from the stainless steel and polystyrene experiments provided only a slight antimicrobial effect, if the samples are taken from refrigerated temperatures to room temperatures (e.g. periods from store to home) there is an evident advantage of phages to limit the growth of *Salmonella* present in foods. Also, strategically, phage survival at -18 °C was tested. The reason for this is that poultry meat is considered fresh when stored at 4 °C up to three days, otherwise it must be stored at -18 °C [65]. The results at this temperature showed that phage PVP-SE2 maintained its viability on the surface of chicken skins for ten days when kept either under fresh or frozen conditions. Previous studies have shown that tailed phages can remain viable at refrigerated temperatures even for 10-12 years [66]. However, most phages tend not to remain stable at -20 °C and therefore lose viability, which is not the case of phage PVP-SE2. For instance, several *E. coli* phages were submitted to storage at freezing temperatures and were shown to be stable only for one day [67]. After this, the authors observed an accentuated reduction of phage titers (4.0-6.3 logs $PFU.mL^{-1}$). This loss in titer is known to be due to the formation of ice crystals [68,69]. Although tailed phages tend to maintain viability at 4 °C, some phages are highly sensitive, such as phage Stx2, from *E. coli*, that was shown to drastically reduce in viability just after one day [70].

Phage hosts have developed several resistance mechanisms to survive these viruses [71]. In terms of resistance of *S.* Enteritidis to phages, the main mechanism that this bacterium adopts is to lose the core O-polysaccharide [72]. In this work, the susceptibility of cells from the different experiments that had survived phage treatment was tested and four different phages were chosen

(Table 2.3). Three of these phages (PVP-SE2, φ68 and φ135) had been previously shown to be highly similar in genome size, that varied between 32 and 38 kb [22]. As expected, higher numbers of resistant colonies emerged at 22 °C than at 4 °C, with percentages varying between 0 – 33.3% in cells recovered from biofilms formed on polystyrene, and between 0-100% in cells from stainless steel surfaces, respectively. Since biofilms formed on stainless steel were thicker when compared to those formed on polystyrene, cells will be subjected to more stress, and the existence of cellular metabolites and oxygen reactive species surrounding biofilm cells may induce mutations at a higher rate due to the diffusional limitations [73]. At 4 °C, most of the surviving cells recovered from polystyrene and stainless steel surfaces, as well as from poultry skins (control and pretreatment experiments), were susceptible to all four phages. Furthermore, to assess the LPS chain mutations that led to negative results (no phage plaques formed), the four phages were plated on LT2 mutant strains which have mutations in different regions of the LPS chain (Figure 2.10). All phages were infective towards the smooth wild type *S.* Typhimurium strain LT2 and the Re mutant strains. None of the tested phages produced plaques in LT2 mutants Rd1 and Rd2, which suggests that these surviving isolates are devoid of the necessary oligosaccharide component for phage adsorption. However, more surviving colonies should be assessed and their LPS characteristics analysed by sodium dodecyl sulfate (SDS) polyacrylamide gel electrophoresis to confirm the suspected deletions.

In conclusion, it has been demonstrated the ability of phage PVP-SE2 to act as a control agent of *S.* Enteritidis biofilm and adhered cells on different surfaces, such as polystyrene, stainless steel, and poultry skin, at different temperatures (4 and 22 °C). Furthermore, this phage showed promising results when used for the prevention of contamination of poultry skin at 4 °C. Taking all this information into account and the fact that PVP-SE2 genome does not contain genes that encode for bacterial toxins nor lysogeny related genes, it can be concluded that phage PVP-SE2 is a good candidate for safe use in the control/prevention of *S.* Enteritidis contamination of food related surfaces.

References

1. WHO. **WHO estimates of the global burden of diseases - Foodborne disease burden epidemiology reference group 2007-2015.** WHO, editor. Geneva: *WHO*. 2015. 1-268 p.

2. European Food Safety Authority. **The European Union summary report on trends and sources of zoonoses, zoonotic agents and food-borne outbreaks in 2015.** *EFSA J.* 2016;14(12). doi: 10.2903/j.efsa.2016.4634.

3. CDC. ***Salmonella* - Information for Healthcare Professionals and Laboratories.** 2018 [accessed: 2018 Mar 9]. Available from: http://www.cdc.gov/*Salmonella*/general/technical.html

4. Finstad S, O'Bryan CA, Marcy JA, Crandall PG, Ricke SC. ***Salmonella* and broiler processing in the United States: Relationship to foodborne salmonellosis.** *Food Res Int.* 2012;45(2):789–94. doi: 10.1016/j.foodres.2011.03.057.

5. WHO. ***Salmonella* (non-thypoidal).** 2018 [accessed 2018 Jan 29]. Available from:http://www.who.int/ mediacentre/factsheets/fs139/en/

6. Grant A, Hashem F, Parveen S. ***Salmonella* and *Campylobacter*: Antimicrobial resistance and bacteriophage control in poultry.** *Food Microbiol.* 2016;53:104–9. doi: 10.1016/j.fm.2015.09.008.

7. DuPont HL. **The growing threat of foodborne bacterial enteropathogens of animal origin.** *Clin Infect Dis.* 2007;45(10):1353–61. doi: 10.1086/522662.

8. Mead GC, Lammerding AM, Cox NM, Doyle P, Humbert F, Kulikovskiy A et al. **Scientific and technical factors affecting the setting of *Salmonella* criteria for raw poultry: a global perspective.** *J Food Prot.* 2010;73(8):1–22. doi: 10.4315/0362-028X-73.8.1566.

9. CDC. ***Salmonella* - Reports of Selected *Salmonella* Outbreak Investigations.** 2018 [accessed: 2018 Feb 12]. Available from: https://www.cdc.gov/*Salmonella*/outbreaks.html

10. Helke KL, McCrackin MA, Galloway AM, Poole AZ, Salgado CD, Marriott BP. **Effects of antimicrobial use in agricultural animals on drug-resistant foodborne salmonellosis in humans: A systematic literature review.** *Crit Rev Food Sci Nutr.* 2017;53(3):472–88. doi: 10.1080/10408398.2016.1230088.

11. Joseph B, Otta SK, Karunasagar I, Karunasagar I. **Biofilm formation by *Salmonella* spp. on food contact surfaces and their sensitivity to sanitizers.** *Int J Food Microbiol*. 2001;64(3):367–72. doi: 10.1016/S0168-1605(00)00466-9.

12. Steenackers H, Hermans K, Vanderleyden J, De Keersmaecker SCJ. ***Salmonella* biofilms: An overview on occurrence, structure, regulation and eradication.** *Food Res Int.* 2012;45(2):502–31. doi: 10.1016/j.foodres.2011.01.038.

13. Gutiérrez D, Rodríguez-Rubio L, Martínez B, Rodríguez A, García P. **Bacteriophages as weapons against bacterial biofilms in the food industry.** *Front Microbiol.* 2016;7(JUN):1–15.

14. Clark JR, March JB. **Bacteriophages and biotechnology: vaccines, gene therapy and antibacterials.** *Trends Biotechnol.* 2006;24(5):212–8. doi: 10.1016/j.tibtech.2006.03.003.

15. Ashelford KE, Day MJ, Fry JC. **Elevated abundance of bacteriophage infecting bacteria in soil.** *Appl Environ Microbiol.* 2003;69(1):285–9. doi: 10.1128/AEM.69.1.285-289.2003.

16. Hanlon GW. **Bacteriophages: an appraisal of their role in the treatment of bacterial infections.** *Int J Antimicrob Agents.* 2007;30:118–28. doi: 10.1016/j.ijantimicag.2007.04.006.

17. Atterbury RJ, Connerton PL, Dodd CER, Rees CED, Connerton IF. **Application of host-specific bacteriophages to the surface of chicken skin leads to a reduction in recovery of *Campylobacter jejuni*.** *Appl Environ Microbiol*. 2003;69(10):6302–6. doi: 10.1128/AEM.69.10.6302-

6306.2003.

18. Carlton RM, Noordman WH, Biswas B, De Meester ED, Loessner MJ. **Bacteriophage P100 for control of *Listeria monocytogenes* in foods: Genome sequence, bioinformatic analyses, oral toxicity study, and application.** *Regul Toxicol Pharmacol*. 2005;43(3):301–12. doi: 10.1016/j.yrtph.2005.08.005.

19. Goode D, Allen VM, Barrow PA. **Reduction of experimental *Salmonella* and *Campylobacter* contamination of chicken skin by application of lytic bacteriophages.** *Appl Environ Microbiol*. 2003;69(8):5032–6. doi: 10.1128/AEM.69.8.5032-5036.2003.

20. Higgins JP, Higgins SE, Guenther KL, Huff W, Donoghue AM, Donoghue DJ et al. **Use of a specific bacteriophage treatment to reduce *Salmonella* in poultry products.** *Poult Sci*. 2005;84(7):1141–5. doi: 10.1093/ps/84.7.1141.

21. FDA, Department of health and human services. **Food additives permitted for direct addition to food for human consumption; bacteriophage preparation.** Vol. 71. Forth Worth (TX): Federal register; 2006. p. 47729–32.

22. Sillankorva S, Pleteneva E, Shaburova O, Santos S, Carvalho C, Azeredo J et al. ***Salmonella* Enteritidis bacteriophage candidates for phage therapy of poultry.** *J Appl Microbiol*. 2010;108(4):1175–86. doi: 10.1111/j.1365-2672.2009.04549.x.

23. Sillankorva S, Neubauer P, Azeredo J. ***Pseudomonas fluorescens* biofilms subjected to phage phiIBB-PF7A.** *BMC Biotechnol*. 2008;8(79):1–12. doi: 10.1186/1472-6750-8-79.

24. Adams M. **Bacteriophages.** New York: Interscience Publishers, Inc.; 1959. 624 p.

25. Melo LDR, Sillankorva S, Ackermann H-W, Kropinski AM, Azeredo J, Cerca N. **Isolation and characterization of a new *Staphylococcus epidermidis* broad-spectrum bacteriophage.** *J Gen Virol*. 2014;95(Pt 2):506–15. doi: 10.1099/vir.0.060590-0.

26. Ackermann H-W. **Basic phage electron microscopy.** In: Clokie MRJ, Kropinski AM, editors. *Methods in Molecular Biology*. Humana Press Inc.; 2009. p. 113–26.

27. Sillankorva S, Neubauer P, Azeredo J. **Isolation and characterization of a T7-like lytic phage for *Pseudomonas fluorescens*.** *BMC Biotechnol*. 2008;8(80):1–11. doi: 10.1186/1472-6750-8-80.

28. Aziz RK, Bartels D, Best AA, DeJongh M, Disz T, Edwards RA et al. **The RAST Server: rapid annotations using subsystems technology.** *BMC Genomics*. 2008;9(75):1–15. doi: 10.1186/1471-2164-9-75.

29. Altschul SF, Madden TL, Schäffer AA, Zhang J, Zhang Z, Miller W et al. **Gapped BLAST and PSI-BLAST: a new generation of protein database search programs.** *Nucleic Acids Res*. 1997;25(17):3389–402.

30. Altschul SF, Gish W, Miller W, Myers EW, Lipman DJ. **Basic local alignment search tool.** *J Mol Biol.* 1990;215(3):403–10.

31. Finn RD, Bateman A, Clements J, Coggill P, Eberhardt RY, Eddy SR et al. **Pfam: The protein families database.** *Nucleic Acids Res*. 2014;42(Database issue):D222–30. doi: 10.1093/nar/gkt1223.

32. Finn RD, Attwood TK, Babbitt PC, Bateman A, Bork P, Bridge AJ et al. **InterPro in 2017-beyond protein family and domain annotations.** *Nucleic Acids Res*. 2017;45(D1):D190–9. doi: 10.1093/nar/gkw1107.

33. Wilkins M, Gasteiger E, Bairoch A, Sanchez J, Williams K, Appel R et al. **Protein Identification and Analysis Tools in the ExPASy Server.** In: Link AJ, editor. *2-D Proteome Analysis Protocols Methods in Molecular Biology*. Humana Press; 1999. p. 531–52.

34. Käll L, Sonnhammer ELL. **Reliability of transmembrane predictions in whole-genome data.**

FEBS Lett. 2002;532(3):415–8. doi: 10.1016/S0014-5793(02)03730-4.

35. Käll L, Krogh A, Sonnhammer ELL. **A combined transmembrane topology and signal peptide prediction method.** *J Mol Biol*. 2004;338(5):1027–36. doi: 10.1016/j.jmb.2004.03.016.

36. Schattner P, Brooks AN, Lowe TM. **The tRNAscan-SE, snoscan and snoGPS web servers for the detection of tRNAs and snoRNAs.** *Nucleic Acids Res*. 2005;33:W686–9. doi: 10.1093/nar/gki366.

37. Klucar L, Stano M, Hajduk M. **PhiSITE: Database of gene regulation in bacteriophages.** *Nucleic Acids Res*. 2009;38(Database issue):D366–70. doi: 10.1093/nar/gkp911.

38. Naville M, Ghuillot-Gaudeffroy A, Marchais A, Gautheret D. **ARNold: a web tool for the prediction of Rho-independent transcription terminators.** *RNA Biol*. 2011;8(1):11–3. doi: 10.4161/rna.8.1.13346

39. Zuker M. **Mfold web server for nucleic acid folding and hybridization prediction.** *Nucleic Acids Res*. 2003;31(13):3406–15. doi: 10.1093/nar/gkg595.

40. Moons P, Faster D, Aertsen A. **Lysogenic conversion and phage resistance development in phage exposed *Escherichia coli* biofilms.** *Viruses*. 2013;5(1):150–61. doi: 10.3390/v5010150.

41. Tsuno H, Hidaka T, Nishimura F. **A simple biofilm model of bacterial competition for attached surface.** *Water Res*. 2002;36(4):996–1006. doi: 10.1016/S0043-1354(01)00291-3.

42. Stubbendieck RM, Straight PD. **Multifaceted interfaces of bacterial competition.** *J Bacteriol*. 2016;198(16):2145–55. doi: 10.1128/JB.00275-16.

43. Loretz M, Stephan R, Zweifel C. **Antimicrobial activity of decontamination treatments for poultry carcasses: A literature survey.** *Food Control*. 2010;21(6):791–804. doi: 10.1016/j.foodcont.2009.11.007.

44. EFSA Panel on Biological Hazards (BIOHAZ). **Scientific Opinion on the public health risks related to the maintenance of the cold chain during storage and transport of meat. Part 1 (meat of domestic ungulates).** *EFSA J*. 2014;12(3):1–81. doi: 10.2903/j.efsa.2014.3783.

45. USDA, Food Safety and Inspection Service. **Chicken from farm to table**. 2014 [accessed 2017 Sep 19]. Available from:https://www.fsis.usda.gov/wps/wcm/connect/ad74bb8d-1dab-49c1-b05e-390a74ba7471/Chicken_from_Farm_to_Table.pdf?MO D=AJPERES

46. Shi X, Zhu X. **Biofilm formation and food safety in food industries.** *Trends Food Sci Technol*. 2009;20(9):407–13. doi: 10.1016/j.tifs.2009.01.054.

47. Griffiths AJF, Depaula A, Young P, Miller JH, Suzuki DT, Lewontin RC et al. **An Introduction to Genetic Analysis.** 7th ed. New York: W.H.Freeman & Co Ltd; 2000. 960 p.

48. Woody MA, Cliver DO. **Effects of temperature and host cell growth phase on replication of F-specific RNA coliphage Q beta.** *Appl Environ Microbiol*. 1995;61(4):1520–6.

49. Knolle P, Orskov I. **The identity of the f+ antigen and the cellular receptor for the RNA phage fr.** *Mol Gen Genet.* 1967;99(1):109–14. doi: 10.1007/BF00306463.

50. Tokman JI, Kent DJ, Wiedmann M, Denes T. **Temperature significantly affects the plaquing and adsorption efficiencies of *Listeria* phages.** *Front Microbiol*. 2016;7(631):1–10. doi: 10.3389/fmicb.2016.00631.

51. Sillankorva S, Oliveira R, Vieira MJ, Sutherland I, Azeredo J. ***Pseudomonas fluorescens* infection by bacteriophage ΦS1: The influence of temperature, host growth phase and media.** *FEMS Microbiol Lett*. 2004;241(1):13–20. doi: 10.1016/j.femsle.2004.06.058.

52. Poimenidou SV, Chrysadakou M, Tzakoniati A, Bikouli VC, Nychas GJ, Skandamis PN. **Variability of *Listeria monocytogenes* strains in biofilm formation on stainless steel and polystyrene materials and resistance to peracetic acid and quaternary ammonium compounds.** *Int J Food*

Microbiol. 2016;237:164–71. doi: 10.1016/j.ijfoodmicro.2016.08.029.

53. Pan Y, Breidt FJ, Kathariou S. **Resistance of *Listeria monocytogenes* biofilms to sanitizing agents in a simulated food processing environment.** *Appl Environ Microbiol*. 2006;72(12):7711–7.

54. Taylor R, Maryan C, Verran J. **Retention of oral microorganisms on cobalt-chromium alloy and dental acrylic resin with different surface finishes.** *J Prosthet Dent*. 1998;80(5):592–7. doi: 10.1016/S0022-3913(98)70037-X.

55. Nejadnik MR, van der Mei HC, Busscher HJ, Norde W. **Determination of the shear force at the balance between bacterial attachment and detachment in weak-adherence systems, using a flow displacement chamber.** *Appl Environ Microbiol*. 2008;74(3):916–9. doi: 10.1128/AEM.01557-07.

56. Sillankorva S, Neubauer P, Azeredo J. ***Pseudomonas fluorescens* biofilms subjected to phage phiIBB-PF7A.** *BMC Biotechnol*. 2008;8(79). doi: 10.1186/1472-6750-8-79.

57. Dika C, Chatain-Ly MH, Francius G, Duval JFL, Gantzer C. **Non-DLVO adhesion of F-specific RNA bacteriophages to abiotic surfaces: Importance of surface roughness, hydrophobic and electrostatic interactions.** *Colloids Surfaces A Physicochem Eng Asp*. 2013;435:178–87. doi: 10.1016/j.colsurfa.2013.02.045.

58. Abedon ST. **Selection for lysis inhibition in bacteriophage.** *J Theor Biol*. 1990;146(4):501–11. doi: 10.1016/S0022-5193(05)80375-3.

59. Zhang Y, Hu Z. **Combined treatment of *Pseudomonas aeruginosa* biofilms with bacteriophages and chlorine.** *Biotechnol Bioeng*. 2012;110(1):286–95. doi: 10.1002/bit.24630.

60. Chibeu A, Agius L, Gao A, Sabour PM, Kropinski AM, Balamurugan S. **Efficacy of bacteriophage LISTEX™P100 combined with chemical antimicrobials in reducing *Listeria monocytogenes* in cooked turkey and roast beef.** *Int J Food Microbiol*. 2013;167(2):208–14. 10.1016/j.ijfoodmicro.2013.08.018.

61. Sukumaran AT, Nannapaneni R, Kiess A, Sharma CS. **Reduction of *Salmonella* on chicken meat and chicken skin by combined or sequential application of lytic bacteriophage with chemical antimicrobials.** *Int J Food Microbiol*. 2015;207:8–15. doi: 10.1016/j.ijfoodmicro.2015.04.025.

62. Ferreira AA, Mendonça RCS, Hungaro HM, Carvalho MM, Pereira JAM. **Bacteriophages actions on *Salmonella* Enteritidis biofilm.** In: *Science and Technology Against Microbial Pathogens*. Valladolid, Spain: World Scientific; 2011. p. 135–9. doi: 10.1142/9789814354868_0026.

63. Gong C, Jiang X. **Application of bacteriophages to reduce *Salmonella* attachment and biofilms on hard surfaces.** *Poult Sci*. 2017;96(6):1838–48. doi: 10.3382/ps/pew463.

64. Hagens S. **Salmonelex™ GRAS Notification.** Micreos. Wageningen: Micreos B.V.; 2015. p. 1–45.

65. USDA, Food Safety and Inspection Service. **Basics for Handling Food Safely.** 2015 [accessed 2017 May 29]. Available from: http://www.fsis.usda.gov/wps/portal/fsis/topics/food-safety-education /get-answers/food-safety-fact-sheets/safe-food-handling/basics-for-handling-food-safely/ct_index

66. Ackermann HW, Tremblay D, Moineau S. **Long-Term Bacteriophage Preservation.** *WFCC Newsl*. 2004;38(August 2016):35–40.

67. Litt PK, Jaroni D. **Isolation and Physiomorphological Characterization of *Escherichia coli* O157:H7-Infecting Bacteriophages Recovered from Beef Cattle Operations.** *Int J Microbiol*. 2017;2017:1–12. doi: 10.1155/2017/7013236.

68. Warren J, Hatch M. **Survival of T3 coliphage in varied extracellular environments.** *Appl Microbiol*. 1969;17(2):256–61.

69. Gould E. **Methods for long-term virus preservation.** *Mol Biotechnol*. 1999;13(1):57–66. doi:

10.1385/MB:13:1:57.

70. Rode TM, Axelsson L, Granum PE, Heir E, Holck A, L'Abée-Lund TM. **High stability of Stx2 phage in food and under food-processing conditions.** *Appl Environ Microbiol*. 2011;77(15):5336–41. doi: 10.1128/AEM.00180-11.

71. Labrie SJ, Samson JE, Moineau S. **Bacteriophage resistance mechanisms.** *Nat Rev Microbiol*. 2010;8(5):317–27. doi: 10.1038/nrmicro2315.

72. Santander J, Robeson J. **Phage-resistance of *Salmonella enterica* serovar Enteritidis and pathogenesis in *Caenorhabditis elegans* is mediated by the lipopolysaccharide.** *Electron J Biotechnol*. 2007;10(4):627–32. doi: 10.2225/vol10-issue4-fulltext-14.

73. Pires DP, Dötsch A, Anderson EM, Hao Y, Khursigara CM, Lam JS et al. **A genotypic analysis of five *P. aeruginosa* strains after biofilm infection by phages targeting different cell surface receptors.** *Front Microbiol*. 2017;8(JUN):1–14. doi: 10.3389/fmicb.2017.01229.

Chapter III

Construction and Characterization of *Salmonella* Enteritidis Mutant Phage PVP-SE2ΔOrf_01

This chapter was based on the following paper:

Milho C, Azeredo J, Sillankorva S. Using synthetic biology tools to engineer *Salmonella* phage PVP-SE2: mutation stability and infectivity characterization (submitted).

Abstract

Synthetic biology has been applied countless times for the genetic modification and improvement of bacterial strains for the synthesis of products that do not exist in nature. Phages, the natural predators of bacteria, have been extensively studied to be used in the control of food-related pathogens. However, their approval and application are strongly dependent on the regulatory agencies that still show some concerns, mostly due to a scarcity of strong scientific evidence of efficacy, emergence of phage resistant phenotype, and the high percentage of genes in phage genomes with unknown function, which can encode for virulence factors or toxins. To address these concerns, Bacteriophage Recombineering of Electroporated DNA technique, a synthetic biology tool often used for the genetic modification of phages, was used to assess how gene deletion of an unknown function gene influences phage growth and infection parameters, and to infer if there is a reversion of the phage genome after sequential phage replication cycles. One open reading frame was successfully deleted. Orf_01 was shown to influence the phage growth parameters, but not the phage's infectivity. Genetically manipulated phages defective in Orf_01 remained genetically stable for at least for 10 cycles of replication. The study provides proof-of-concept that this methodology can be used to generate phages with more compact genomes which may carry only genes directly involved in phage replication.

Keywords: Bacteriophage; synthetic biology; gene deletion; BRED

3.1 Introduction

Phages have played a key role in the birth of molecular biology, and the enthusiasm over phage research endures mostly due to their genome diversity and their overall abundance in nature. We live in a sequencing revolution era where the landmark of over 8000 sequenced phage genomes are available in databases [1]. This genomic information keeps continuously providing new insights into the potential uses of phages, and their derived proteins in different clinical, industrial, and environmental settings. The term 'synthetic biology' emerged in 1990s with the perception that engineering could be applied to the study of cellular systems and to easily manipulate them to become more productive [2]. Synthetic biology is an emerging field of research which relies on artificially created DNA to build new biochemical systems or organisms with novel or enhanced characteristics [3,4]. It comprises a selection of approaches and methodologies with a focus on engineering biology and biotechnology. Tools like recombineering [5], MAGE [6], CRISPR/Cas systems [7], and Gibson assembly [8] are linked to the synthetic biology process and are regularly used in the genetic manipulation of microorganisms for introduction or improvement of certain properties. Some of the applications of this growing field of science include speeding up vaccine development, creating medicines and novel biomaterials, developing new biofuels as clean energy substitutes for fossil fuels [9], and it has also been used for engineered phage genomes. Genetic modification of phages, in particular, has been done for multiple purposes such as introduction of genes encoding for fluorescent proteins and phosphatases for bacterial detection [10,11], expression of new molecules for phage protection against harsh environments [12], for enhancement of phage's antibacterial properties [13], and even to improve antibiofilm properties [14].

The use of phages as control agents of the growth of pathogenic bacteria like *Salmonella* in food products of animal and plant origin has shown very promising results [15–18]. However, the application of phages as food safety agents is highly dependent on regulatory agencies willpower, that still show some distrust regarding the use of these viruses, as more than 30% of phage genes have unknown function [19]. To overcome this obstacle, one hypothesis is to eliminate non-essential genes with unknown functions from phage genomes. This can be achieved by using molecular and synthetic biology tools like Bacteriophage Recombineering of Electroporated DNA (BRED) [12,20,21]. Using this technique, sequence insertions or deletions can be obtained using double-stranded DNA sequences with approximately 50 bp of homology upstream and downstream to the region to be modified, which has been done for *Escherichia coli* and *Mycobacterium*

smegmatis phages, as an example [20,22]. The targeting substrates are introduced by electroporation, but the proportion of total cells that take up DNA is very low (≈ 0.1%), although enough for mutant retrieval [20]. Hence, phage DNA and a targeting substrate are co-electroporated into bacterial cells, which recombineering functions were previously induced from a plasmid expressing *exo*, *beta* and *gam* genes, like the pSIM plasmids [23]. These genes encode for λ-Red Exo, Beta and Gam proteins that catalyze homologous recombination, making the process of recombineering more efficient [24]. After electroporation, cells are plated so that phage plaques that derive from individual cells that have been transformed with phage DNA, are obtained. Since a high proportion of cells that take up phage DNA also take up targeting substrates, and as higher levels of recombination are reached, a considerable amount of recovered plaques, around 10%, contains a mixture of recombinant and wild-type phage particles [20]. The ratio of recombinant:wild-type phages varies substantially among primary plaques, but screening, by polymerase chain reaction (PCR), of individual plaques that are formed by re-plating the mixed phage population and recovery of mutant phages are relatively easy and fast [20].

The main objective of this study was to use a synthetic biology tool, BRED, to perform the deletion of a gene with unknown function. This was completed using a sequenced phage genome, phage PVP-SE2, that has been completely annotated and is deposited at National Center for Biotechnology Information (NCBI) site under the accession number MF431252. Another purpose of this study was to understand if the mutation caused was irreversible, and how this impacted the phage growth cycle parameters and its infectivity towards exponentially and stationary phase planktonic cells.

3.2 Materials and methods

3.2.1 Bacteria, phages and plasmids

S. enterica serovar Enteritidis 821 was used to propagate phages PVP-SE2 and PVP-SE2ΔOrf1_01, and *S.* Enteritidis 821:pSIM8 cells were used for the construction of mutant phage PVP-SE2ΔOrf1_01. *S.* Enteritidis 821 was grown at 37 °C and *S.* Enteritidis 821:pSIM8 at 32 °C, in liquid or solid LB medium (LB + 1.5% ($w.v^{-1}$) of agar), supplemented with ampicillin (100 $\mu g.mL^{-1}$), when necessary. The plasmid pSIM8, which belongs to the Court Laboratory of the National Cancer Institute in Frederick, MD, USA (https://redrecombineering.ncifcrf.gov/strains–plasmids.html), expresses λ-Red *exo*, *beta* and *gam* genes, and was used for recombineering purposes. This plasmid contains an ampicillin resistance cassette [23].

3.2.2 Phage propagation and titration

Salmonella phages PVP-SE2 and PVP-SE2ΔOrf_01 were propagated and titred as described in chapter II, section 2.2.2.

3.2.3 Phage DNA extraction

Phage DNAs from PVP-SE2 and PVP-SE2ΔOrf_01 phages were extracted as detailed in chapter II, section 2.2.5.

3.2.4 Selection of ORFs for deletion from PVP-SE2 genome

The PVP-SE2 genome, that has been previously sequenced and characterized [25], was found to contain 60 open reading frames (ORFs), 31 of which encode for proteins that may contain functional domains that have never been described before and that are commonly named as hypothetical proteins (Table 3.1). To turn PVP-SE2 into a phage devoid of genes of unknown and unnecessary functions, the 31 ORFs aforementioned were selected for sequential deletion using the BRED method.

Table 3.1 - List of PVP-SE2 ORFs encoding for proteins of unknown functions

ORF	Start (bp)	End (bp)	Length (bp)	AA*	ORF	Start (bp)	End (bp)	Length (bp)	AA*
1	95	325	231	76	**24**	15109	15300	192	63
2	342	620	279	92	**26**	17759	17929	171	56
3	638	994	357	118	**29**	22664	23029	366	121
4	991	1146	156	51	**30**	23026	23541	516	171
5	1143	1301	159	52	**31**	23538	24038	501	166
6	1298	1483	186	61	**33**	26366	26725	360	119
9	2785	3219	435	144	**36**	27559	28689	1131	376
10	3225	3602	378	125	**37**	28686	28916	231	76
11	3605	3808	204	67	**38**	28884	29030	147	48
12	3871	4035	165	54	**41**	30898	31317	420	139
12A	4230	4337	108	35	**43**	31709	32068	360	119
13	4405	4581	177	58	**44**	32068	32673	606	201
15	5643	5876	234	77	**45**	32676	33185	510	169
18	8486	9010	525	174	**46**	33189	33377	189	62
20	9589	10839	1251	416	**53**	36502	36621	120	39
21	10921	11547	627	208					

AA* - Amino acids

3.2.5 *S.* Enteritidis 821:pSIM8 electrocompetent cells

To prepare *S.* Enteritidis 821:pSIM8 electrocompetent cells, 100 mL of LB containing ampicillin (100 μg.mL^{-1}) were inoculated with 100 μL of a *S.* Enteritidis 821:pSIM8 overnight culture and incubated at 32 °C, 120 rpm, until an OD_{620} ≈ 0.6 was reached. After this, cells were chilled on ice for 20 min, induced at 42 °C, 150 rpm, 15 min, in a water bath, for the expression of λ-Red genes [23], harvested by centrifugation (7,000 × *g*, 10 min) and the supernatant discarded. The pellet was then sequentially washed in 100 mL of ice-cold dH_2O; 50, 25 and 10 mL of ice-cold glycerol (10% (v.v^{-1})), and finally resuspended in 1 mL of ice-cold glycerol (10% (v.v^{-1})). Cells were stored as 100 μL aliquots at - 80 °C for subsequent use.

3.2.6 Construction of PVP-SE2ΔOrf_01 mutant

For the construction of PVP-SE2ΔOrf_01 mutant, BRED approach was used [20,26]. Briefly, to delete the first ORF encoding for a hypothetical protein, Orf_01 (231 bp), a 100 bp dsDNA product, with 50 bp homology upstream and 50 bp downstream of the region to be deleted, was amplified by polymerase chain reaction (PCR) using 100 bp forward and 20 reverse oligonucleotides, Del_orf01_fw and Del_orf01_rv, respectively (Table 3.2). PCR was carried out using Phusion High-Fidelity DNA Polymerase (ThermoFisher Scientific, MA, USA), with the conditions described in Table 3.3. The DNA fragment obtained, named Frag_01, was purified using the DNA Clean and Concentrator™ (Zymo Research, CA, USA) and its size confirmed by running an agarose gel (1% (w.v^{-1})). Purified PVP-SE2 DNA (10 ng) and targeting sequence Frag_01 (100 ng) were mixed with 100 µL of *S.* Enteritidis:pSIM8 λ-Red system-induced electrocompetent cells and placed in a 1 mm gap electroporation cuvette (VWR™, PA, USA). A pulse was applied (25 µF, 200 Ω, 1.8 kV), after which 900 µL of liquid LB medium were added to the mixture. Cells were incubated at 37 °C, 120 rpm, for a 3 min period, and immediately mixed with 3 mL of molten soft-agar (LB + 0.6% (w.v^{-1}) of agar), plated in solid LB medium (1.5% (w.v^{-1}) of agar) and incubated at 37 °C until phage plaques were clearly visible. Primary phage plaques, containing a mixture of wild-type and recombinant phages, were transferred to 20 µL of SM buffer (5.8 g.L^{-1} NaCl, 2 g.L^{-1} $MgSO_4$.7 H_2O, 50 mL 1 M Tris, pH 7.5) and eluted for 2 h at room temperature.

Table 3.2 - List of oligonucleotides/ primers used in this study

Oligonucleotide/primer	Sequence	Tm (° C)	Product size (bp)
Del_orf01_fw	AGGCCTGTGTACAGAAAAGCCCGCAGAAGCGGG CTTGGTGGTAAGCTATTGTTCGCCCTCTCCTCTT TAGCAATGCTCGTCTTTATAAACCCACCATTTA	45	100
Del_orf01_rv	TAAATGGTGGGTTTATAAAG	45	
Conf_del_orf01_fw	GGGCTTGGTGGTAAGCTATT	54.9	595 (successful deletion)
Conf_del_orf01_rv	CCGTGCCGGACTATCTTAAT	54.3	826 (no deletion)

Table 3.3 - PCR conditions used to amplify Frag_01 DNA targeting sequence

	T (°C)	Time	Nr. of cycles
Initial denaturation	98	30 s	1
Denaturation	98	5 s	34
Annealing	48	10 s	
Extension	72	15 s	
Final extension	72	5 min	1
	4	∞	

3.2.7 Screening of PVP-SE2ΔOrf_01 mutants

Detection of mutant phages was done by PCR, using 1 µL of phages eluted from primary phage plaques, KAPA Taq DNA polymerase (Kapa Biosystems, MA, USA) and the pair of primers flanking the region to be deleted, Conf_del_orf01_fw and Conf_del_orf01_rv (Table 3.2), using the conditions described in Table 3.4. The region amplified using these two primers could present two sizes: 595 bp, if Orf_01 deletion was successful, or 826 bp, if no deletion occurred. Primary plaques containing recombinant and wild-type phages were serially diluted and plated with *S.* Enteritidis 821. Lysates and new secondary plaques were screened by PCR as described above, to identify pure mutant phages.

Table 3.4 - PCR conditions used for mutant screening

	T (°C)	Time	Nr. of cycles
Initial denaturation	95	3 min	1
Denaturation	95	30 s	34
Annealing	48.5	30 s	
Extension	72	50 s	
Final extension	72	5 min	1
	4	∞	

3.2.8 Evaluation of PVP-SE2ΔOrf_01 mutant stability

To determine the stability of Orf_01's deletion, lysate from generation 0 of phage PVP-SE2ΔOrf_01 was plated on *S.* Enteritidis 821 lawns at 37 °C. The plate showing a confluent lysis was eluted with SM buffer for 2 h, at 4 °C, 90 rpm, being this lysate considered to be generation

1. This procedure was repeated until generation 10 was reached. After the lysates from each generation were plated, 10 individual plaques from generations 0 to 10 were tested by PCR using the same conditions described in section 3.2.7. Sanger DNA sequencing of the regions flanking Orf_01 was performed with generation 0 and 10 phage DNAs to confirm the presence and maintenance of the mutation DNA sequence.

3.2.9 Phage one-step growth characteristics

The one-step growth curves of phages PVP-SE2 and PVP-SE2Δ_Orf01 were performed as described on chapter II, section 2.2.4.

3.2.10 Evaluation of PVP-SE2ΔOrf_01 infectivity against planktonic cultures

To assess the ability of phage PVP-SE2ΔOrf_01 to infect planktonic cells in the exponential phase, a *S.* Enteritidis 821 liquid culture was grown overnight in LB, at 37 °C, 120 rpm. The next day, cells were diluted 1:100 in fresh liquid LB medium and grown until a final $OD_{620} \approx 0.3$ was obtained. The ability of PVP-SE2ΔOrf_01 to infect planktonic cells in the stationary phase was also determined. In this case, cells from an overnight grown culture of *S.* Enteritidis 821 were harvested by centrifugation (7,000 × *g*, 4 °C, 5 min), and diluted in nutrient depleted LB medium to obtain a final $OD_{620} \approx 0.3$. In both experiments, cells were infected with PVP-SE2ΔOrf_01, or PVP-SE2 for comparison, at a MOI of 0.1, and OD_{620} was read at 0, 1, 2, 3, 4 and 5 h. To the control cultures, SM buffer was added instead of phage.

3.2.11 Statistical analysis

Statistical analysis of the results was performed using GraphPad Prism 6 (GraphPad Software, CA, USA). Mean and standard deviations (SD) were determined for the independent experiments and the results were presented as mean±SD. Results were compared using two-way ANOVA, with Tukey's multiple comparison statistical test. Differences were considered statistically significant if $p < 0.05$ (95% confidence interval).

3.3 Results

3.3.1 Construction of PVP-SE2ΔOrf_01 mutant phage

Phage PVP-SE2 has been described to be a good control candidate of *S.* Enteritidis on both biotic and abiotic surfaces [25]. Although its genome does not express known toxins nor antibiotic resistance, 51% of the ORFs present in PVP-SE2's genome encodes for proteins of unknown function [25]. These ORFs with unknown function, colored in grey in Figure 3.1, were primarily located in the beginning of the phage genome, but were also found in the functional modules related with replication, morphogenesis, and packaging (Figure 3.1).

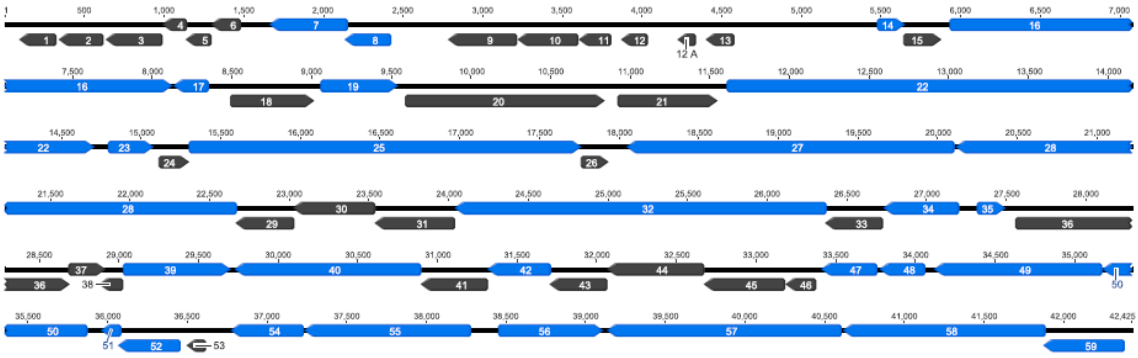

Figure 3.1 - Location of the ORFs with unknown function throughout PVP-SE2 genome. ORFs with unknown function are colored in grey while those with attributed function appear in blue.

This lack of knowledge regarding the proteins expressed by PVP-SE2 is an obstacle when considering the possibility of using this phage as a food safety agent. Hence, the BRED approach was used to eliminate ORFs encoding proteins with unknown function. The chosen ORF to be deleted was Orf_01 (Table 3.1), and, for that, a targeting DNA substrate (Frag_01), with upstream and downstream homology to the region to be deleted, and the wild-type phage DNA were electroporated into *S.* Enteritidis 821:pSIM8 electrocompetent cells that had been previously induced for recombineering functions (Figure 3.2).

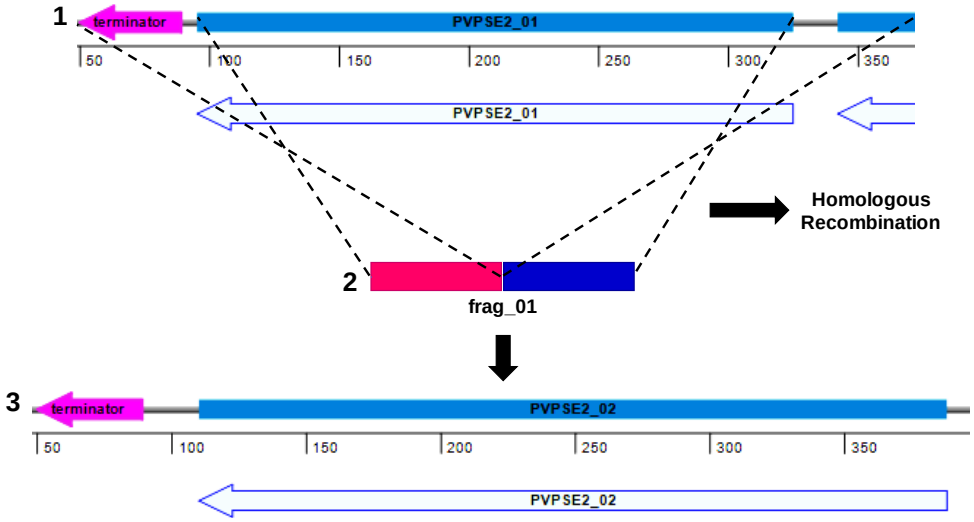

Figure 3.2 - Schematic representation of the deletion process of Orf_01. Wild-type PVP-SE2 phage DNA (1) is co-electroporated with the targeting DNA substrate (2), that contains a 100 bp sequence homologous to the upstream and downstream regions of the sequence to be deleted, Orf_01, into electrocompetent *S.* Enteritidis:pSIM8 cells previously induced for recombination functions. By homologous recombination, the final product is the PVP-SE2 phage genome without Orf_01, PVP-SE2ΔOrf_01.

The size of Frag_01, 100 bp, was confirmed by running an agarose gel (1% (w.v^{-1})) (Figure 3.3). After electroporation, cells were plated in molten soft agar (LB + 0.6% (w.v^{-1}) of agar) and the phage plaques obtained were screened by PCR for the presence of the desired mutation. Figure 3.4 shows that a band corresponding to the amplification of a DNA fragment with 595 bp is present in lanes A and B (red arrow), which indicates that deletion of Orf_01 (231 bp) was successful. These lanes correspond to primary plaques A and B, respectively, containing a mixture of mutant and wild-type PVP-SE2 DNA. The stronger band present in all lanes (826 bp) corresponds to the amplification of the wild-type DNA (blue arrow).

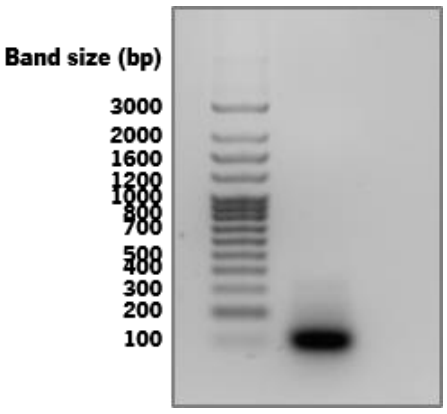

Figure 3.3 - Agarose gel (1% (w.v^{-1})) showing the DNA product Frag_01 (100 bp) amplified by PCR.

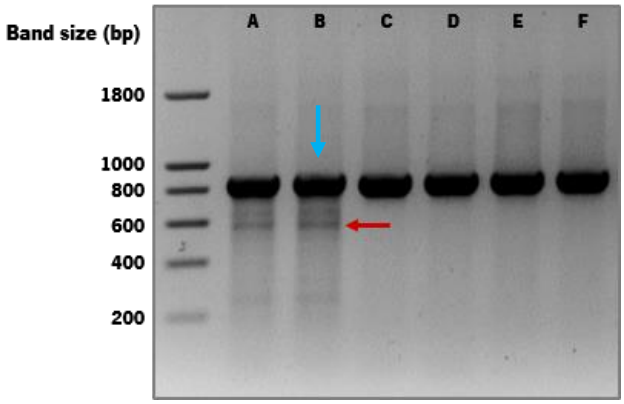

Figure 3.4 - Agarose gel (1% (w.v^{-1})) showing mutant screening by PCR of primary plaques containing a mixture of mutant (red arrow) and wild-type PVP-SE2 (blue arrow) DNAs (A, B), only wild-type DNA (C-E), and a PCR from purified PVP-SE2 genomic DNA as control (F).

Plaque A was chosen for small scale production of the mutant phage, and as shown in Figure 3.5, in lanes B and C, the presence of a unique band of ≈ 595 bp (red arrow) is clear and corresponds to the amplification of PVP-SE2 genomic DNA without Orf_01. These results indicate that plaques B and C contain only pure mutant genomic DNA. Mutant B was chosen for further purification, DNA sequencing and evaluation of Orf_01 deletion stability. All the other lanes show a band of approximately 826 bp (blue arrow), corresponding to the amplification of wild-type DNA.

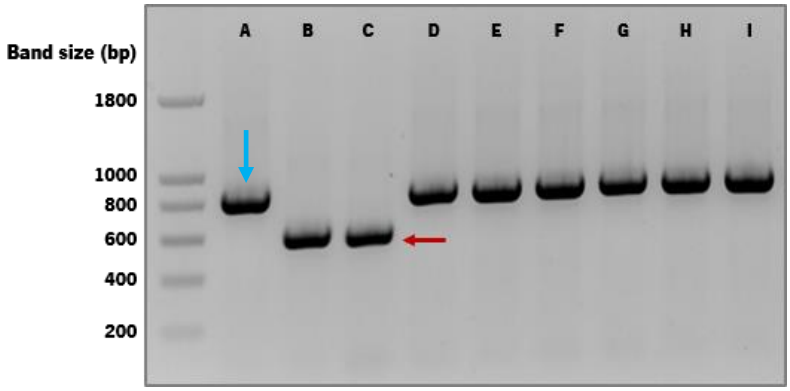

Figure 3.5 - Agarose gel (1% (w.v^{-1})) showing mutant screening by PCR of secondary plaques containing only pure mutant DNA (B and C, red arrow), pure wild-type DNA (A, C-H, blue arrow), and a PCR from purified PVP-SE2 genomic DNA as control (I).

3.3.2 Assessment of Orf_01 deletion stability

To evaluate the stability of Orf_01 deletion, the first lysate obtained from plaque B, considered to be generation 0, was subsequently plated together with *S.* Enteritidis 821 to obtain confluent

lysis. This plate was eluted with SM buffer, successively plated in its host, and the plate showing confluent lysis was eluted in SM buffer to obtain a lysate. Repeated cycles were completed until generation 10. In each generation, 10 isolated plaques were tested by PCR for the presence of the wanted mutation using the pair of primers Conf_del_orf01_fw/ Conf_del_orf01_rv and the same amplification conditions used for mutant screening (Figure 3.6).

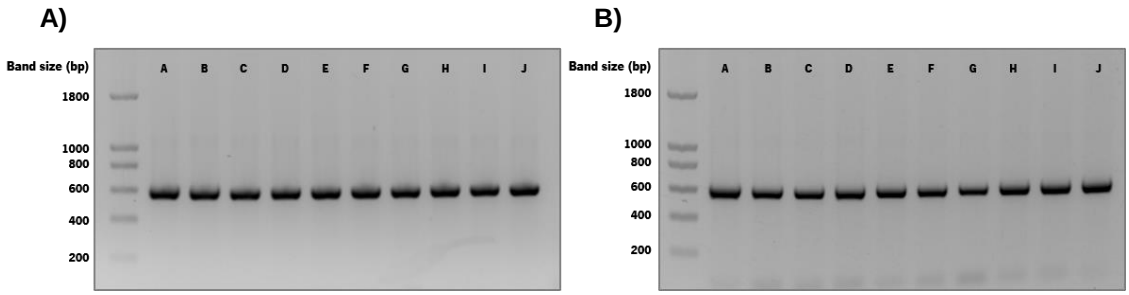

Figure 3.6 - Agarose gel (1% (w.v^{-1})) showing PCR products from DNA present on phage plaques obtained from phage lysate from generation 0 (A) and generation 10 (B).

All plaques tested by PCR, from generation 0 to 10, showed a band with approximately 600 bp, which confirms the deletion of Orf_01 and its stability throughout successive cycles of replication in its host (Figure 3.6). After confirming the stability of Orf_01 deletion, the recombinant phage was named PVP-SE2ΔOrf_01. Sequencing of PVP-SE2ΔOrf_01 DNA from generations 0 and 10 was performed and the presence and stability of the mutation was confirmed (Figure 3.7). The results obtained by sequencing the upstream and downstream regions of the deleted sequence from phage PVP-SE2ΔOrf_01 generations 0 and 10 were aligned with the theoretical PVP-SE2ΔOrf_01 genome. Figure 3.7 shows that the theoretical PVP-SE2ΔOrf_01 genome aligns perfectly with PVP-SE2ΔOrf_01 generation 0 sequence (Figure 3.7 A) and with generation 10 sequence (Figure 3.7 B). These results confirm that the deletion of Orf_01 is stable for, at least, 11 generations.

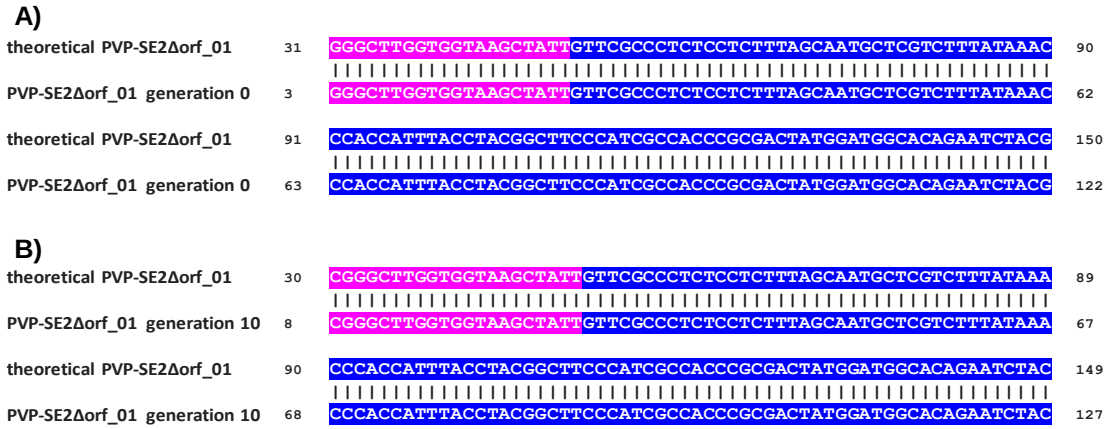

Figure 3.7 - Confirmation of Orf_01's deletion and its stability by sequencing of PVP-SE2ΔOrf_01 DNA from generation 0 (A) and 10 (B) and alignment of the theoretical and the actual mutant phage genome sequence.

3.3.3 Characterization of phage PVP-SE2ΔOrf_01

Phage PVP-SE2ΔOrf_01 was produced and titred as described in chapter II, section 2.2.2, resulting in 2.5×10^{11} PFUs.mL^{-1}, which is close to the titre obtained using the same production parameters for phage PVP-SE2 (1.8×10^{11} PFUs.mL^{-1}). Also, the plaque morphology of both phages was compared, and were indistinguishable from each other, with both presenting clear plaques that are 3 mm in diameter (Figure 3.8).

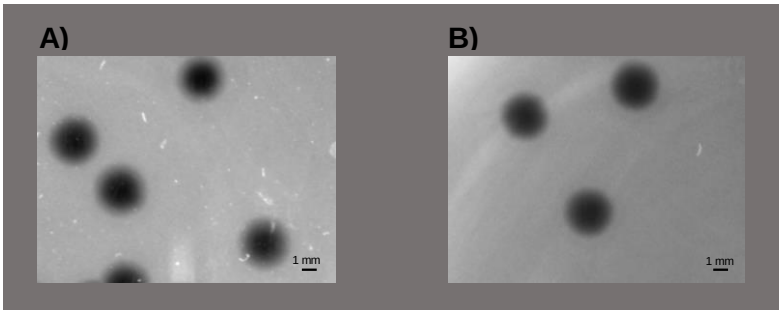

Figure 3.8 - Plaque morphology of phages PVP-SE2 (A) and (B) PVP-SE2ΔOrf_01. Scale bar represents 1 mm.

The one-step growth of mutant phage PVP-SE2ΔOrf_01 was performed and compared to PVP-SE2 (Figure 3.9).

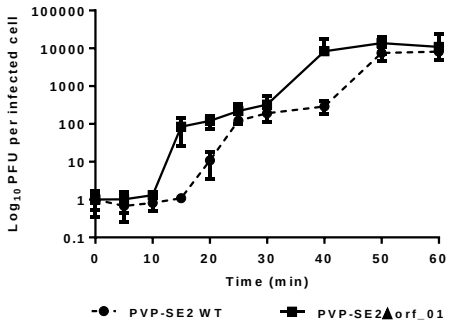

Figure 3.9 - One-step growth curves of phages PVP-SE2 and PVP-SE2ΔOrf_01.

This experiment showed latent and rise periods of 10 min for PVP-SEΔ2Orf_01, and that one phage particle originated roughly 135 progeny phages. The parental phage PVP-SE2 presented a latent period of 15 min and a rise period of 15 min that gave in average 202 progeny phages per infected cell, which is in agreement with our previous results [25]. Overall, one PVP-SE2 phage infected *S.* Enteritidis 821 cell gives rise to twice more progeny than the mutant phage. However, PVP-SE2ΔOrf_01 replicates faster than the wild type phage.

The ability of PVP-SE2ΔOrf_01 to infect planktonic *S.* Enteritidis 821 cells was assessed using exponential and stationary phase cultures, and the infection kinetics of PVP-SE2 and PVP-SE2ΔOrf_01 were compared (Figure 3.10). Figure 3.10 A shows that the ability to reduce the OD_{620} of planktonic *S.* Enteritidis 821 cells in the exponential phase is highly similar between the two phages, reaching a reduction of OD_{620} of approximately 0.18 (Figure 3.10 A). Infection of *S.* Enteritidis 821 planktonic cells in the stationary phase using PVP-SE2ΔOrf_01 led to a poor decrease of planktonic cultures OD_{620} of 0.09. However, 0.09 was also the OD_{620} reduction obtained for the wild-type phage PVP-SE2 (Figure 3.10 B). Even though the cells were used in the stationary phase, for some unknown reason the optical density increased very slightly over the 5-hour experiment (OD_{620} increase of 0.13), which may be due to the incomplete depletion of nutrients in the LB medium used in this experiment.

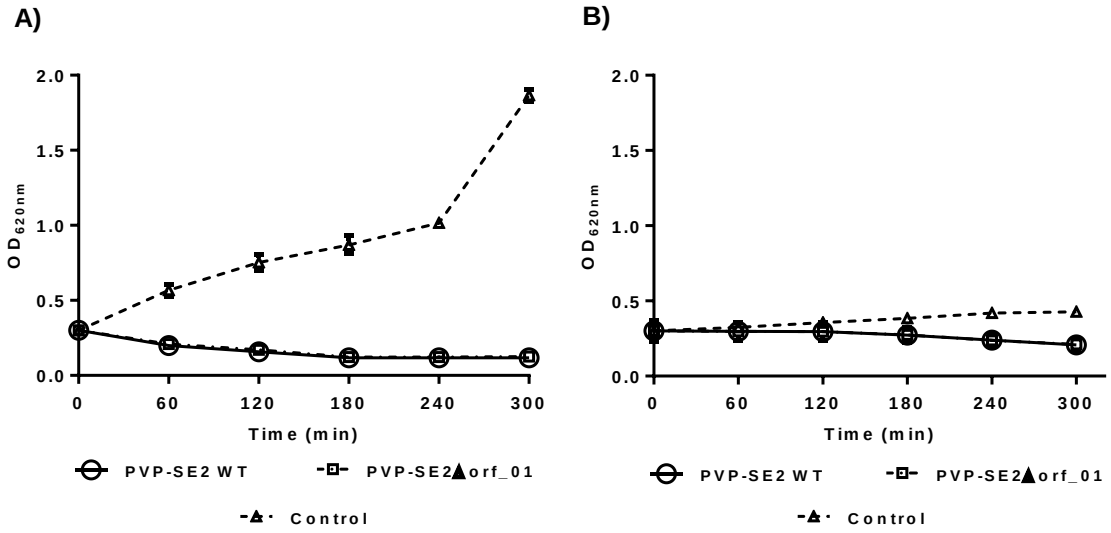

Figure 3.10 - PVP-SE2 and PVP-SE2ΔOrf_01 performances when infecting *S.* Enteritidis 821 cells in the exponential (A) and stationary (B) phases.

3.4 Discussion

BRED, a method developed by Marinelli et al (2008) [20], has been successfully used for the construction of recombinant phages [22,26,27]. The use of this methodology to assess if PVP-SE2 ORFs could be successfully deleted was selected. The genome of PVP-SE2 was sequenced and annotated recently [25], and found to contain 60 ORFs, 31 of which encode for proteins with hypothetical (unknown) functions, and that are in representatively higher numbers in the beginning of the phage genome (See Figure 3.1 and Table 3.1). From these 31 ORFs, the first one in the genome, Orf_01, was chosen to be deleted. After electroporating λ-Red system-induced *S.* Enteritidis:pSIM8 with PVP-SE2 DNA and the targeting sequence DNA, a mixed population of plaques containing either only wild-type phage or both wild-type and mutant phages was obtained. From the 20 phage plaques screened, two showed amplification of two PCR products of 826 (blue arrow) and 595 bp (red arrow), approximately (Figure 3.4, lane A and B), which correspond to amplification of phages PVP-SE2 and PVP-SE2ΔOrf_01 DNAs, respectively. The proportion of plaques containing wild-type and mutant phages is of ≈ 10%, a percentage that has been reported before [20], and which shows that BRED is relatively fast and an easy method to construct recombinant phages. The recombinant phage was further isolated, the mutation confirmed by PCR screening (Figure 3.5), and one plaque (plaque B) was propagated for further characterization of the possible deletion effects. The mutant phage was named PVP-SE2ΔOrf_01. Stability of Orf_01 deletion was checked from generation 0 of PVP-SE2ΔOrf_01 to generation 10, and it was possible to confirm that the deletion was permanent (Figures 3.6). Furthermore, DNA from both phages was sequenced, confirming deletion of Orf_01 and its stability (Figure 3.7).

The production and phage characteristics, using the same conditions, were also characterized. The titre obtained for the small-scale production of the recombinant phage, 2.5×10^{11} PFUs.mL^{-1}, was very similar to PVP-SE2's titre, 1.8×10^{11} PFUs.mL^{-1}, which indicates that PVP-SE2ΔOrf_01 is as easy to produce as the wild-type phage and that Orf_01 is not essential for phage infection and replication. Plaque morphology was not altered by deletion of Orf_01, which indicates that the deleted gene is not involved in the diffusion of the phage particles into the soft-agar (Figure 3.8). Even though the production and plaque morphologies remained unaltered, some phage replication parameters were different in the wild-type and mutant phages (Figure 3.9). The main differences were the shorter latent period of PVP-SE2ΔOrf_01 compared to the wild-type phage. This fastest initiation of the burst period and the overall shorter period of the recombinant

phage (10 min) does not, however, lead to the same production of progeny per infected *Salmonella* as PVP-SE2. The registered burst sizes are of 202 and 135 progeny phages per infected cell for PVP-SE2 and PVP-SE2ΔOrf_01, respectively. The fastest latent and rising periods of PVP-SE2ΔOrf_01 could explain why this phage has a lower burst size than PVP-SE2, since the rate of production of new phage particles is constant but the length of the progeny-producing period is shorter for PVP-SE2ΔOrf_01 [28]. Phages with shorter latent periods are usually naturally selected for higher host densities, since a fastest progeny production indicates a faster infection of new host cells [29]. Hypothetically, the use of PVP-SEΔ2Orf_01 would be an advantage when dealing with high loads of bacterial cells. However, to test this theory, higher densities than the ones used in the experiment should be tested. Despite the difference in burst size, another interesting aspect of PVP-SEΔ2Orf_01 is that the ability to infect *S.* Enteritidis 821 cells in the exponential is similar to that observed using the wild-type phage (Figure 3.10 A). Regarding stationary phase, both phages have poor ability to infect these cells, leading only to an OD_{620} reduction of 0.1 (Figure 3.10 B). This was somewhat expected since stationary phase cells are in an inactive metabolic state and the majority of phages has a preference for metabolically active hosts [30].

Analysing the results obtained, it is safe to say that Orf_01 can be deleted without affecting PVP-SE2 growth, since, in all parameters tested, phages PVP-SE2 and PVP-SE2ΔOrf_01 behaved in an identical manner, except regarding the kinetics of infection (Figure 3.9). This could be explained by the fact that probably Orf_01 is not essential for phage effective replication. These results may be also explained by the existence of cryptic genes duplications or suppressor mutations that can compensate the loss of one gene [31].

In conclusion, it has been proven BRED can be used for gene-engineering phage PVP-SE2 and that the particular deletion of an early hypothetical gene product did not cause noticeable changes in the mutant phage PVP-SE2ΔOrf_01, remaining infective towards the host bacterium. This suggests that Orf_01 is not essential for PVP-SE2 effective replication.

References

1. NCBI. **Genomes Groups - Viruses of Bacteria Database.** 2018 [accessed 2018 Nov 14]. Available from: https://www.ncbi.nlm.nih.gov/genomes/GenomesGroup.cgi?taxid=10239&host=bacteria

2. Cameron DE, Bashor CJ, Collins JJ. **A brief history of synthetic biology.** *Nat Rev Microbiol.* 2014;12(5):381–90. doi: 10.1038/nrmicro3239.

3. Gibson DG, Glass JI, Lartigue C, Noskov VN, Chuang R-Y, Algire MA et al. **Creation of a Bacterial Cell Controlled by a Chemically Synthesized Genome.** *Science.* 2010 Jul 2;329(5987):52–6. doi: doi/10.1126/science.1190719.

4. Gibson DG, Smith HO, Hutchison CA, Venter JC, Merryman C. **Chemical synthesis of the mouse mitochondrial genome.** *Nat Methods.* 2010 Nov 10;7(11):901–3. doi: 10.1038/nmeth.1515.

5. Kong W, Kapuganti VS, Lu T. **A gene network engineering platform for lactic acid bacteria.** *Nucleic Acids Res.* 2016 Feb 29;44(4):e37. doi: 10.1093/nar/gkv1093.

6. Gallagher RR, Li Z, Lewis AO, Isaacs FJ. **Rapid editing and evolution of bacterial genomes using libraries of synthetic DNA.** *Nat Protoc.* 2014;9(10):2301–16. doi: doi: 10.1038/nprot.2014.082.

7. Qi LS, Larson MH, Gilbert L, Doudna J, Weissman JS, Arkin AP et al. **Repurposing CRISPR as an RNA-guided platform for sequence-specific control of gene expression.** *Cell.* 2013;152(5):1173–83. doi: 10.1016/j.cell.2013.02.022.

8. Gibson DG, Young L, Chuang R-Y, Venter JC, Hutchison CA, Smith HO. **Enzymatic assembly of DNA molecules up to several hundred kilobases.** *Nat Methods.* 2009 May 12;6(5):343–5. doi: 10.1038/nmeth.1318.

9. Presidential Commission for the Study of Bioethical Issues. **New Directions. The Ethics of Synthetic Biology and Emerging Technologies. Executive Summary and Recommendations.** 2012 Jan;16(1):1–192.

10. Tanji Y, Furukawa C, Na S-H, Hijikata T, Miyanaga K, Unno H. ***Escherichia coli* detection by GFP-labeled lysozyme-inactivated T4 bacteriophage.** *J Biotechnol.* 2004 Oct 19;114(1–2):11–20. doi: 10.1016/j.jbiotec.2004.05.011.

11. Alcaine S, Pacitto D, Sela D, Nugen S. **Phage & phosphatase: a novel phage-based probe for rapid, multi-platform detection of bacteria.** *Analyst.* 2015;140(22):7629–36. doi: 10.1039/C5AN01181G.

12. Nobrega FL, Costa AR, Santos JF, Siliakus MF, Van Lent JWM, Kengen SWM et al. **Genetically manipulated phages with improved pH resistance for oral administration in veterinary medicine.** *Sci Rep.* 2016;6(November):1–12. doi: 10.1038/srep39235.

13. Lu TK, Collins JJ. **Engineered bacteriophage targeting gene networks as adjuvants for antibiotic therapy.** *Proc Natl Acad Sci U S A.* 2009 Mar 24;106(12):4629–34. doi: 10.1073/pnas.0800442106.

14. Lu TK, Collins JJ. **Dispersing biofilms with engineered enzymatic bacteriophage.** *Proc Natl Acad Sci U S A.* 2007 Jul 3;104(27):11197–202. doi: 10.1073/pnas.0704624104.

15. Zinno P, Devirgiliis C, Ercolini D, Ongeng D, Mauriello G. **Bacteriophage P22 to challenge *Salmonella* in foods.** *Int J Food Microbiol.* 2014 Sep;191:69–74. doi: 10.1016/j.ijfoodmicro.2014.08.037.

16. Huang C, Shi J, Ma W, Li Z, Wang J, Li J et al. **Isolation, characterization, and application of a novel specific *Salmonella* bacteriophage in different food matrices.** *Food Res Int.* 2018;111(May):631–41. doi: 10.1016/j.foodres.2018.05.071.

17. Xu D, Jiang Y, Wang L, Yao L, Li F, Zhai Y et l. **Biocontrol of *Salmonella* Typhimurium in Raw Salmon Fillets and Scallop Adductors by Using Bacteriophage SLMP1.** *J Food Prot.* 2018;81(8):1304–12. doi: 10.4315/0362-028X.JFP-17-525.

18. Huang C, Virk SM, Shi J, Zhou Y, Willias SP, Morsy MK et al. **Isolation, characterization, and application of Bacteriophage LPSE1 against *Salmonella enterica* in Ready to Eat (RTE) Foods.** *Front Microbiol.* 2018;9(MAY):1–11. doi: 10.3389/fmicb.2018.01046.

19. Hatfull GF, Hendrix RW. **Bacteriophages and their genomes.** *Curr Opin Virol.* 2011;1(4):298–303. doi: 10.1016/j.coviro.2011.06.009.

20. Marinelli LJ, Piuri M, Swigoňová Z, Balachandran A, Oldfield LM, van Kessel JC et al. **BRED: A simple and powerful tool for constructing mutant and recombinant bacteriophage genomes.** *PLoS One.* 2008;3(12):3957–75. doi: 10.1371/journal.pone.0003957.

21. Rita Costa A, Milho C, Azeredo J, Pires DP. **Synthetic Biology to Engineer Bacteriophage Genomes.** In: Sillankorva S, Azeredo J, editors. *Bacteriophage Therapy*. New York, NY, USA: Humana Press; 2018. p. 285–300.

22. Fehér T, Karcagi I, Blattner FR, Pósfai G. **Bacteriophage recombineering in the lytic state using the lambda red recombinases.** *Microb Biotechnol.* 2012 Jul;5(4):466–76. 10.1111/j.1751-7915.2011.00292.x.

23. Datta S, Costantino N, Court DL. **A set of recombineering plasmids for gram-negative bacteria.** *Gene.* 2006;379(1–2):109–15. doi: 10.1016/j.gene.2006.04.018.

24. Murphy KC. **Use of bacteriophage λ recombination functions to promote gene replacement in *Escherichia coli*.** *J Bacteriol.* 1998;180(8):2063–71.

25. Milho C, Silva MD, Melo L, Santos S, Azeredo J, Sillankorva S. **Control of *Salmonella* Enteritidis on food contact surfaces with bacteriophage PVP-SE2.** *Biofouling.* 2018;30:1–16. doi: 10.1080/08927014.2018.1501475.

26. da Silva JL, Piuri M, Broussard G, Marinelli LJ, Bastos GM, Hirata RDC et al. **Application of BRED technology to construct recombinant D29 reporter phage expressing EGFP.** *FEMS Microbiol Lett.* 2013;344(2):166–72. doi: 10.1111/1574-6968.12171.

27. Catalão MJ, Milho C, Gil F, Moniz-Pereira J, Pimentel M. **A Second Endolysin Gene Is Fully Embedded In-Frame with the lysA Gene of Mycobacteriophage Ms6.** *PLoS One.* 2011 Jun 9;6(6):e20515. doi: 10.1371/journal.pone.0020515.

28. Abedon ST. **Selection for bacteriophage latent period length by bacterial density: A theoretical examination.** *Microb Ecol.* 1989;18(2):79–88. doi: 10.1007/BF02030117.

29. Abedon ST, Herschler TD, Stopar D. **Bacteriophage latent-period evolution as a response to resource availability.** *Appl Environ Microbiol.* 2001;67(0099-2240):4233–41. doi: 10.1128/AEM.67.9.4233-4241.2001.

30. Birch EW, Ruggero NA, Covert MW. **Determining Host Metabolic Limitations on Viral Replication via Integrated Modeling and Experimental Perturbation.** *PLoS Comput Biol.* 2012;8(10). doi: 10.1371/journal.pcbi.1002746.

31. Heineman RH, Bull JJ, Molineux IJ. **Layers of evolvability in a bacteriophage life history trait.** *Mol Biol Evol.* 2009;26(6):1289–98. doi: 10.1093/molbev/msp037.

Chapter IV

Interspecies Interactions of *Escherichia coli* and *Salmonella* Enteritidis in Dual-species Biofilms and their Control by Phages

This chapter was based on the following paper:

Milho C, Silva MD, Alves D, Oliveira H, Sousa C, Azeredo J, Sillankorva S. Interspecies interactions of *Escherichia coli* and *Salmonella* Enteritidis in dual-species biofilms and their control by phages (submitted)

Abstract

Escherichia coli and *Salmonella* Enteritidis are foodborne pathogens forming challenging biofilms that contribute to their virulence, antimicrobial resistance and survival on food contact surfaces. Interspecies interactions occur in dual-species biofilms promoting different outcomes to each species. Here we describe the interactions between two *E. coli* (EC 434 and EC 515) and two *S.* Enteritidis (SE EX2 and SE 269) strains, as well as the use of phages to control these biofilms. Mono- and dual-species 48 h-old biofilms were formed *in vitro,* and the kinetics of biofilm formation were characterized, showing that these strains form biofilms with higher numbers of viable cells in mono-species than in dual-species biofilms. Confocal microscopy visualization showed that the spatial organization of strains in dual-species biofilms resembles their spatial organization when forming mono-species biofilms. Differences in the EPS matrix composition from single and mixed biofilms were assessed by Fourier-transform infrared spectroscopy. This analysis showed that the EPS spectra of dual-species biofilms can either be a mixture of both species EPS, or that the EPS of one strain predominates. Mono- and dual-species biofilms infected with *S.* Enteritidis and *E. coli* phages φ135 and DaICa, respectively, showed that phage application to single species biofilms leads to higher viable cell reductions than when a phage cocktail was used to control mixed biofilms. Furthermore, the efficacy of phages was shown to be highly dependent on the phage characteristics, the bacterial growth parameters, and also bacterial spatial distribution in biofilms. A combination of different methodologies such as analysing bacterial and phage growth parameters, viable cell counting, CLSM imaging and FTIR-ATR analysis of the EPS matrix, provided new knowledge regarding species-species and phage-host interactions in biofilms.

Keywords: *E. coli*, *S.* Enteritidis, dual-species biofilms, EPS matrix.

4.1 Introduction

The presence of pathogenic and spoilage bacteria in food products is a known worldwide problem that not only leads to food spoilage but is also linked to foodborne outbreaks due to consumption of contaminated food products. In food industries, product contamination can occur at different food processing stages via direct and indirect cross-contamination [1]. Direct contamination of foods may be due to exposure to pathogens present in the soil, contaminated irrigation waters, and animals in the growing area [2]. Cross-contamination of the food products may occur as a result of moisture drops and aerosols that are formed, which indirectly contaminate working surfaces and products, contaminated washing waters, and improper handling of the product by the workers, for instance, due to poor hand sanitations [3]. *Escherichia coli* and *Salmonella* are two major foodborne pathogens frequently isolated from varied surfaces, particularly from those that are difficult to access [4], soil [5,6], product washing waters [7], and food products [8]. According to the Centers for Disease Control and Prevention (CDC), these two species are responsible for millions of illnesses, 2,000 and 23,000 hospitalizations, and 60 and 450 deaths every year in the US alone, respectively [9].

Both *E. coli* and *Salmonella* have been found attached in the form of biofilms to varied surfaces where they secrete extracellular polymeric substances (EPS) that maintain cells together forming complex 3D structures [10]. Biofilm cells can tolerate higher levels of antimicrobial agents than their planktonic counterparts, which makes them extremely challenging to remove [10]. Although both species can form single-species biofilms, *E. coli* and *Salmonella* are often found coexisting in multispecies communities that can be attached to food processing surfaces or even food products [11]. The interactions observed in dual-species biofilms are characterized as being positive, negative or neutral for each species [12]. As it has been shown, biofilms formed by *E. coli* and *Salmonella* can display an enhanced resistance to a quaternary ammonium chloride-based sanitizer used named Vanquish, a one-step concentrated cleaner, broad-spectrum disinfectant/virucide, sanitizer, with application on hard, non-porous surface (Total Solutions, WI, USA). Resistance was due to the production of EPS by *Salmonella*, which conferred protection to both species [4]. The interaction between these two species has also been studied in biofilms formed on HEp-2 cells [13]. In this case, *Salmonella* biofilm outgrew and displaced a pre-formed *E. coli* biofilm. In another study, it was found that a strain of *Salmonella*, unable to form biofilms, could use curli proteins cross-seeded by *E. coli*, which led to enhanced adherence of the dual-species biofilm [14].

Phages, the natural predators of bacteria, have been extensively used in the control of single-species biofilms commonly present in the food industry [15–20]. However, evidences of their application in mixed bacterial populations is scarce. In a previous work, a cocktail containing two phages, φIBB-SL58B and φIBB-PF7A, was used to successfully control *Staphylococcus lentus* and *Pseudomonas fluorescens*, respectively, in dual-species biofilms [21]. Furthermore, it was shown that phage φIBB-PF7A alone was able not only to decrease *P. fluorescens* population, but also to promote the release of *S. lentus* from the mixed biofilm. Dual-species biofilms comprised by *Staphylococcus aureus* and *Staphylococcus epidermidis* were challenged by phages phiIPLA-RODI and phiIPLA-C1C in cocktail, which led to a significant reduction in the number of attached cells [22]. Taking this information into account, it is clear that phages can be used in the control of mixed bacterial communities, although this subject has not been properly addressed.

In this work, mono- and dual-species biofilms of *E. coli* and *S.* Enteritidis strains were studied to assess the influence these two species have on each other. Moreover, phages vB_EcoM_DalCa (DalCa) and φ135, specific for *E. coli* and *S.* Enteritidis, respectively, were characterized and used for the control of mono- and dual-species biofilms formed by these two bacteria species.

4.2 Materials and Methods

4.2.1 Bacterial strains and phages

E. coli CECT 434 (EC 434) and CECT 515 (EC 515), from the Spanish Type Culture Collection, and *Salmonella* Enteritidis EX2 (SE EX2) and 269 (SE 269) [23] were used in this study. EC 434 and SE EX2, and EC 515 and SE 269 were determined to be, by a previously described method [26], strong and weak biofilm producers, respectively. All strains were grown at 37 °C in liquid or in solid LB medium (LB + 1.5% ($w.v^{-1}$) of agar). The *Salmonella* phage used was phage φ135, that has already been partially characterized [23]. The *E. coli* phage DaICa was isolated from raw sewage as previously described [24].

4.2.2 *E. coli* and *S.* Enteritidis electrocompetent cells

To prepare electrocompetent cells from both strains of *E. coli* and *S.* Enteritidis, 100 mL of LB were inoculated with 100 µL of an overnight culture and incubated at 37 °C, 200 rpm, until an $OD_{620} \approx 0.6$ was reached. After this, cells were chilled on ice for 20 min, harvested by centrifugation (7,000 × *g*, 10 min) and the supernatant was discarded. The pellet was then sequentially washed in 100 mL of ice-cold dH_2O; 50, 25 and 10 mL of ice-cold glycerol (10% ($v.v^{-1}$)), and finally resuspended in 1 mL of ice-cold glycerol (10% ($v.v^{-1}$)). Cells were stored as 100 µL aliquots at -80 °C for subsequent use.

4.2.3 Construction of sfGFP and mCherry strains

To distinguish *Salmonella* and *E. coli* strains, in microscopy imaging, *S.* Enteritidis strains were transformed with plasmid sfGFP-pBAD (available at addgene.com, plasmid #54519), that encodes for the superfolder green fluorescent protein (sfGFP), and *E. coli strains* with plasmid pNUT086, which encodes for the mCherry fluorophore and that was kindly provided by professor Knut Drescher, from Max Planck Institute for Terrestrial Microbiology, Germany. Electrocompetent *S.* Enteritidis or *E. coli* cells (100 µL) were mixed with sfGFP-pBAD and pNUT086, respectively, and placed in a 1 mm gap electroporation cuvette (VWR™, PA, USA). A pulse was applied (25 µF, 200 Ω, 1.8 kV), after which 900 µL of liquid LB medium were added to the mixture. Cells were incubated at 37 °C, 120 rpm, for 1 h, and plated on solid LB supplemented with ampicillin (100

μg.mL^{-1}), for *S.* Enteritidis cells, or supplemented with kanamycin (50 μg.mL^{-1}), for *E. coli* cells. From this point forward, all experiments were performed with these constructed strains.

4.2.4 Characterization of the growth parameters of *E. coli* and *S.* Enteritidis strains

Specific growth rates and doubling times of all strains were determined according to previously described methods [25]. Overnight cultures were used to inoculate 10 mL of LB medium and the Erlenmeyer flasks incubated at 120 rpm (ES-20, Biosan, 10 mm orbit) at 37 °C. The optical density (OD_{620}) of the samples was measured at different timepoints. Two independent experiments were performed in duplicate.

4.2.5 Biofilm formation

Mono- and dual-species biofilms of *E. coli* and *S.* Enteritidis were formed based on the microtiter plate test previously described [26], with some modifications. Briefly, an overnight culture was grown in liquid LB supplemented with kanamycin (50 mg.mL^{-1}) or ampicillin (100 mg.mL^{-1}), at 37 °C, under agitation (120 rpm, ES-20, Biosan, 10 mm orbit) being then adjusted to a final concentration of 1×10^{7} CFU.mL^{-1}. For dual-species biofilms, each bacterium was adjusted to the same final concentration. Afterwards, 200 μL.well^{-1} of the bacterial suspension were transferred to 96-well flat-bottom polystyrene microtiter plates (Sarstedt, Inc., Germany) that were incubated at 37 °C for 48 h on a horizontal shaker (120 rpm, ES-20, Biosan, 10 mm orbit) under aerobic conditions. After 48 h, biofilms were washed twice with sterile saline solution (NaCl 0.9% (w.v^{-1})) and detached by ultrasonic bath (Sonicor SC-52, Sonicor Instruments, UK) operating at 50 kHz, during 6 min [27]. Bacterial suspensions were collected, thoroughly vortexed to disrupt possible cell aggregates and serially diluted. Serial 10-fold dilutions were performed and plated into solid LB supplemented with kanamycin (50 mg.mL^{-1}) or ampicillin (100 mg.mL^{-1}), which were incubated overnight at 37 °C under aerobic conditions. The number of viable biofilm cells was expressed as CFU per cm^{-2}.

4.2.6 Determination of the Competitive Index (CI) and the Relative Increase Ratio (RIR)

In dual-species biofilms, the Competitive Index (CI) was established as the EC 434/SE EX2 or EC 515/SE 269 ratio within the output sample divided by the corresponding ratio in the inoculum (input): CI = (EC 434/SE EX2 or EC 515/SE 269) output /(EC 434/SE EX2 or EC 515/SE 269) input, where output and input are the counts of viable cells [Log_{10}(CFU.cm^{-2})] obtained at defined timepoints or the inoculum (t = 0), respectively [12]. For statistical purposes, CI values were first subjected to a Log_{10} transformation for normal distribution, and then interpreted as follows: a CI value equal to 0 indicates equal competition of the two species; a positive CI value indicates a competitive advantage for the species on the numerator; a negative CI value indicates a competitive advantage for the species on the denominator. The Relative Increase Ration (RIR) was calculated based on the counts of viable cells [Log_{10}(CFU.cm^{-2})] obtained from mono-species biofilms of each strain [12].

4.2.7 Confocal Scanning Laser Microscopy

For microscopy imaging, single- and dual-species biofilms were formed on polystyrene coupons (Nunc™Thermanox™, Thermo Scientific™, MA, USA) placed on 24-well polystyrene microtiter plates (Sarstedt Inc, Germany). Biofilm formation was performed as previously described but with a bacterial suspension volume adjusted to 1 mL.$well^{-1}$ instead of 200 µL.$well^{-1}$. Expression of mCherry fluorophore and sfGFP was induced for 5 h by adding 1 mM IPTG and 0.2% (v.v^{-1}) of L-arabinose [28,29], respectively, after 43 h of biofilms formation. Confocal z-stack images of biofilms were acquired on a Confocal Scanning Laser Microscope Olympus BX61, Model FluoView 1000 (Olympus®, Tokyo, Japan) equipped with 405-635 nm laser lines. Images were obtained with FV10-Ver4.1.1.5 program (Olympus®, Tokyo, Japan).

4.2.8 Extraction of EPS from biofilms

For EPS extraction, *E. coli* and *S.* Enteritidis mono and dual-species biofilms were grown using the colony biofilm procedure previously described [30] with some modifications. A black polycarbonate sterile membrane filter (Whatman®, Maidstone, UK) (47 mm diameter, 0.2 µm pore size) was placed on a solid LB plate with the shiny side of the membrane facing up. Each membrane was inoculated with 50 µL of EC 434, EC 515, SE EX2, SE 269, or alternatively with

dual-species mixtures of EC 434 + SE EX2 or EC 515 + SE 269, with each strain being diluted from overnight culture to a final concentration of ≈ 1×10^8 CFU.mL^{-1}. Biofilms were allowed to form for 48 h at 37 °C without agitation, and membranes were transferred to fresh solid LB plates every 24 h. For each strain or combination of strains, ten membranes were used. Extraction of EPS from biofilms was performed as previously described [31]. Briefly, *E. coli* and *S.* Enteritidis mono- and dual-species biofilms grown on ten polycarbonate membranes were scrapped and resuspended in 2 mL tubes with sterile 1.5 M NaCl by vortexing. Then, the suspensions were centrifuged at 5000 × *g* for 10 min at 25 °C, and the resulting supernatants were transferred to new 2 mL tubes. Six replicas of each extraction were performed.

4.2.9 FTIR analysis of EPS

After extracting the EPS from the different biofilms, the samples were lyophilized and analyzed by Fourier Transform Infrared-Attenuated Total Reflectance (FTIR-ATR) spectroscopy. Samples were directly transferred to the ATR crystal and a pressure of 150 N.cm^{-2} was applied. Infrared spectra were acquired using a PerkinElmer Spectrum BX FTIR System spectrophotometer (PerkinElmer®, Waltham, MA, USA) with a PIKE Technologies Gladi ATR accessory (PIKE Technologies, Inc., Madison, WI, USA) from 4000 to 600 cm^{-1} with a resolution of 4 cm^{-1} and 32 scans co-additions. For each sample, three instrumental replicates (obtained in the same day) and two biological replicates (obtained in two different days from two independent bacterial growths) were obtained, corresponding to a total of six spectra for each extracted EPS. Between each EPS measurement, the background was acquired. Spectra corresponding to the instrumental replicates were averaged prior to the analysis.

4.2.10 Phage propagation and titration

SE EX2 and EC 434 were used for the production and titration of phages φ135 and DalCa, respectively. These procedures are described in chapter II, section 2.2.2.

4.2.11 TEM analysis of phages

Transmission electron microscopy (TEM) observation of phage particles was performed as described in chapter II, section 2.2.3.

4.2.12 Phage DNA extraction

Phage DNA was extracted according to chapter II, section 2.2.5.

4.2.13 Genome sequencing and annotation

Genome sequencing was performed on an Illumina HiSeq platform (STAB VIDA, Portugal). DNA library preparations were prepared using the Illumina Nextera XT library preparation kit to generate 250 bp paired-end sequencing reads. After processing, reads were trimmed to remove adapters, contaminations, or low-quality sequences. Contigs were assembled with a relatively homogenous coverage with the CLC genomics Workbench version 7 (CLC Bio, Aarhus, Denmark), using the *de novo* assembly algorithm and manual inspection. Phage genomes were autoannotated using MyRAST [32] and the presence of non-annotated coding sequences (CDSs), along with genes in which the initiation codon was miscalled, were checked manually using Geneious 9.1.4 (Biomatters, Newark, NJ, USA) and potential frameshifts were checked with BLASTX [33]. The functions of translated open-reading frames were searched by BLASTP programs [34] (E-value $\leq 10^{-5}$) and HHPRED server [35], consulted between June and July 2018. Protein parameters (isoelectric point and molecular weight) were determined using Sequence Manipulation Suite: Protein Isoelectric Point and Sequence Manipulation Suite: Protein Molecular Weight [36]. The presence of transmembrane domains was checked using TMHMM [37] and Phobius [38], and membrane proteins were annotated when both tools were in concordance. The search of tRNA encoding genes was performed using tRNAscan-SE [39]. Putative promoters were searched using PhiSITE [40], and putative regions were manually verified. ARNold [41] was used to predict rho-independent terminators and the energy was calculated using Mfold [42]. Whole-genome comparisons were performed using EasyFig [43] and OrthoVenn [44]. The complete genome sequence of phages *E. coli* phage DalCa and *S.* Enteritidis phage φ135 were submitted to GenBank under the accession numbers MH992509 and MH992510, respectively.

4.2.14 Phage one-step growth characteristics

The one-step growth curves of phages DalCa and φ135 on the two tested *E. coli* and *S.* Enteritidis strains were performed as described on chapter II, section 2.2.4.

4.2.15 Biofilm treatment with phages

Biofilms were allowed to form on 96-well microtiter plates (Sarstedt, Inc., Germany) for 24 h as previously described, washed once with saline solution and exposed to 100 μL of LB and 100 μL of phage solution in order to have a multiplicity of infection (MOI) of 1. Single-species biofilms of *S.* Enteritidis were exposed to φ135, single-species biofilms of *E. coli* were exposed to DalCa, and dual-species biofilms were exposed to a phage cocktail comprising both phages. Microtiter plates were incubated at 37 °C, in the same conditions at which the biofilms were formed, but for different periods of time: 4, 8 and 24 h. Control experiments were performed by exposing the 24 h-old biofilms to 100 μL of LB and 100 μL of SM buffer (5.8 $g.L^{-1}$ NaCl, 2 $g.L^{-1}$ $MgSO_4.7\ H_2O$, 50 mL 1 M Tris, pH 7.5) without phages. The number of viable biofilm cells ($CFU.cm^{-2}$) was determined before and after phage infections, as previously described, but serial dilutions were performed in saline solution (NaCl 0.9% ($w.v^{-1}$)) containing 2 mM of FAS to destroy all non-infecting phages [45].

4.2.16 Statistical analysis

Statistical analysis of the results was performed using GraphPad Prism 6 (GraphPad Software, La Jolla, CA, USA). Mean and standard deviations (SD) were determined for the independent experiments and the results were presented as mean±SD. Differences of mono- versus dual-species biofilm formation were assessed using two-way ANOVA followed by Tukey's multiple comparison statistical test. CI and RIR were compared using unpaired Student's *t*-test, which significant differences are indicative of a probable competition between the species [12]. Differences were considered statistically significant if $p < 0.05$ (95% confidence interval).

Two principal component analysis (PCA) models [46] were developed including EPS spectra from the two *E. coli* and two *S.* Enteritidis strains, in mono- and dual-species biofilms. Prior modelling, spectra were pre-processed with standard normal variate (SNV) followed by the application of a Savitzky-Golay filter (15 smoothing points, 2nd order polynomial and 1st derivative) [47,48] and mean centred. All data analyses were performed in Matlab version 7.9 (Mathworks, Natick, MA, USA) and the PLS Toolbox version 5.5.1 for Matlab (Eigenvector Research, Manson, WA, USA).

4.3 Results

4.3.1 Characterization of *E. coli* and *S.* Enteritidis strains growth parameters

The constructed *E. coli* and *S.* Enteritidis strains carrying sfGFP- and mCherry-expression plasmids were characterized to determine their specific growth rates and doubling times (Table 4.1). Only these strains were used in all following experiments and, therefore, the characteristics of their parental strains were not determined.

Table 4.1 - *E. coli* and *S.* Enteritidis strains specific growth rate (μ_{max}) and doubling time (t_d)

Strains	$\mu_{max} \pm$ SD (h^{-1})	$t_d \pm$ SD (min)
EC 434	0.763 ± 0.03*	54.67 ± 2.44
EC 515	0.902 ± 0.094*†	46.36 ± 4.83 †
SE EX2	0.791 ± 0.038*	52.67 ± 2.45**
SE 269	0.668 ± 0.073*†	99.33 ± 12.50**†

Asterisks (*) indicate significant differences between strains (* $p < 0.05$; ** $p < 0.01$) and daggers (†) indicate significant differences between species ($p < 0.01$).

There were minor differences in EC 434 and EC 515 growth, resulting in fairly similar μ_{max} values (Table 4.1). Nevertheless, these were statistically different ($p < 0.05$). The same was observed for SE EX2 and SE 269 that resulted in statistically significant differences ($p < 0.05$). Since biofilm formation studies were completed with two sets of combinations: the strong (EC 434 and SE EX2) and the weak biofilm formers (EC 515 and SE 269), statistical analysis of μ_{max} was also performed for these combinations. According to the results, only the μ_{max} between EC 515 and SE 269 was statistically significant ($p < 0.01$). The doubling times (t_d) varied more in the two tested *Salmonella* strains ($p < 0.001$) and were not significantly different between the *E. coli* used herein. This parameter was also only statistically different ($p < 0.01$) for the combination of weak biofilm producer strains.

4.3.2 Characterization of mono- and dual-species biofilms

Interactions stablished in multispecies biofilms may be of: i) synergism, when all species benefit from the relationship; ii) antagonism, when one of the species takes advantage from the others; or iii) neutral, which results in no benefit or detriment to the species [49]. *E. coli* and *Salmonella*, pathogens that are often responsible for foodborne outbreaks, have been previously found to form mixed biofilms in food working surfaces [4,50]. To study possible interactions between these two species when forming biofilms, two strains of *S.* Enteritidis, EX2 and 269, and two of *E. coli*, 434 and 515, were chosen, and single and dual-species biofilms were formed for 48 h. The two *E. coli* belong to different serotypes: EC 434 belongs to the serotype O6 (Biotype 1), while EC 515 belongs to the serovar O1:K1(L1):H7. The results show that, overall, all strains are present in higher numbers when in mono-culture biofilms (Figure 4.1). For instance, EC 434 and SE EX2 reached 7.5×10^7 and 1.73×10^8 CFU.cm^{-2} in mono-species biofilms, respectively, but when grown together both strains showed values of growth of approximately 2.5×10^6 CFU.cm^{-2} (Figure 4.1 A). EC 515 and SE 269 strains, in mono-culture biofilms reached, after 48 h of growth, 2.3×10^8 and 1.28×10^7 CFU.cm^{-2}, respectively, and showed 1 log less viable cells when forming dual-species biofilms (Figure 4.1 B).

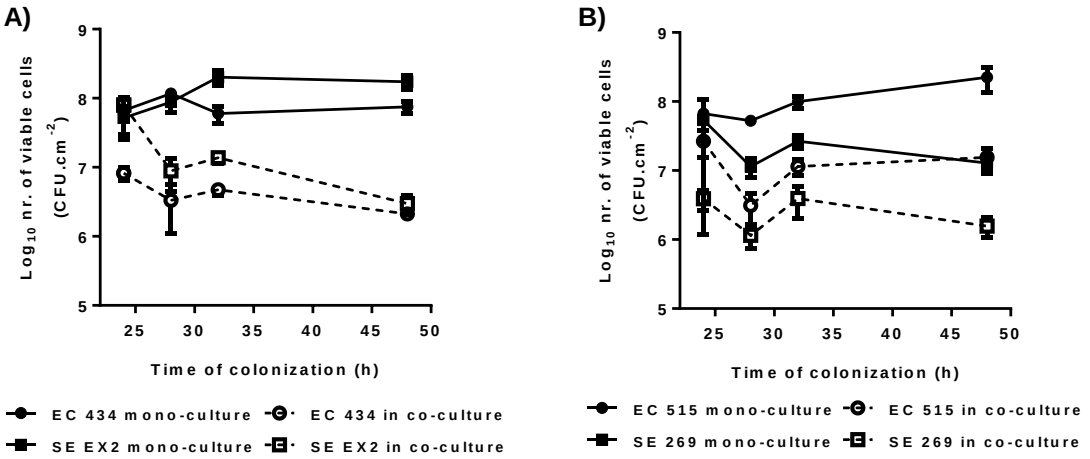

Figure 4.1 - Biofilm formation kinetics of A) EC 434 and SE EX2, and B) EC 515 and SE 269, alone and in co-culture. Comparison values of single versus dual-species biofilms are all statistical significant ($p < 0.05$), except for EC 515 mono- versus EC 515 + SE 269 dual-species biofilm, at 24 h of growth, and SE 269 mono- versus SE 269 + EC 515 dual-species biofilm, at 24 h of growth.

To better understand the differences between the *E. coli* and *S.* Enteritidis strains biofilm forming abilities in single- and dual-species biofilms, RIR and CI indexes were calculated (Figure

4.2). While in CI the growth curves of the two species in mixed biofilms are compared, RIR compares the growth curves of both species in single-species biofilms. Figure 4.2 A shows a negative CI throughout all timepoints However, only at 24 and 28 h of biofilm growth CI and RIR are statistically different ($p < 0.05$), indicating a competitive advantage of SE EX2 over EC 434 at these timepoints, when grown together. On the other hand, a positive CI is observed at 24 and 28 h of growth for EC 515 + SE 269 dual-species biofilms, which indicates a competitive advantage for EC 515 at these timepoints (Figure 4.2 B).

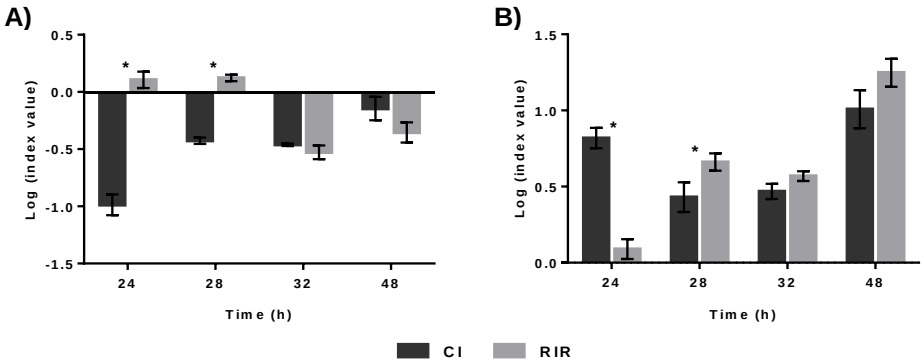

Figure 4.2 - Relative Increase Ratio (RIR) and Competitive Index (CI) obtained for A) EC 434 alone and when combined with SE EX2, and B) for EC 515 alone and when combined with SE 269, respectively. Asterisks (*) indicate significant difference ($p < 0.05$) between CI and RIR.

To characterize the bacterial distribution within the 48-h mono- and dual-species biofilms formed by *E. coli* strains, expressing mCherry fluorophore, and/ or *S.* Enteritidis, expressing sfGFP, images were taken by CLSM (Figures 4.3 and 4.4). Regarding the EC 434 mono-species biofilm, its spatial distribution appeared to be heterogeneous, with bacteria being more accumulated in some areas than others and reaching a thickness of approximately 4 μm (Figure 4.3 A, I and II). On the other hand, the SE EX2 mono-species biofilm looked more evenly spread throughout the polystyrene coupon, showing a thickness of ≈ 13 μm (Figure 4.3 A, III and IV). The difference in thickness between the two biofilms is in agreement with the number of viable cells obtained for each biofilm at 48 h, 7.50×10^7 CFU.cm^{-2} for EC 434, and 1.73×10^8 CFU.cm^{-2} for SE EX2 (Figure 4.1 A), since a thicker biofilm may indicate the presence of a higher number of bacterial cells when comparing different bacteria with similar sizes, which is the case [51,52]. When analysing by CLSM a dual-species biofilm formed by EC 434 and SE EX2, the two strains seemed to grow on the same areas on the coupon, suggesting that they influence each other's spatial distribution (Figure 4.3 B I-III). The thickness of the dual-species biofilm reached approximately 11 μm (Figure 4.3 B, IV), which suggests that less bacterial cells were present in it when compared to the SE EX2 mono-

species biofilm (13 µm), which could contribute to a thicker biofilm. This result is in accordance to the number of bacterial counts obtained for each strain in the dual-species biofilm, 2.12×10^6 CFU.cm^{-2} and 2.98×10^5 CFU.cm^{-2} for EC 434 and SE EX2, respectively, values that are substantially lower than the ones obtained for each strain when forming mono-species biofilm (Figure 4.1 A).

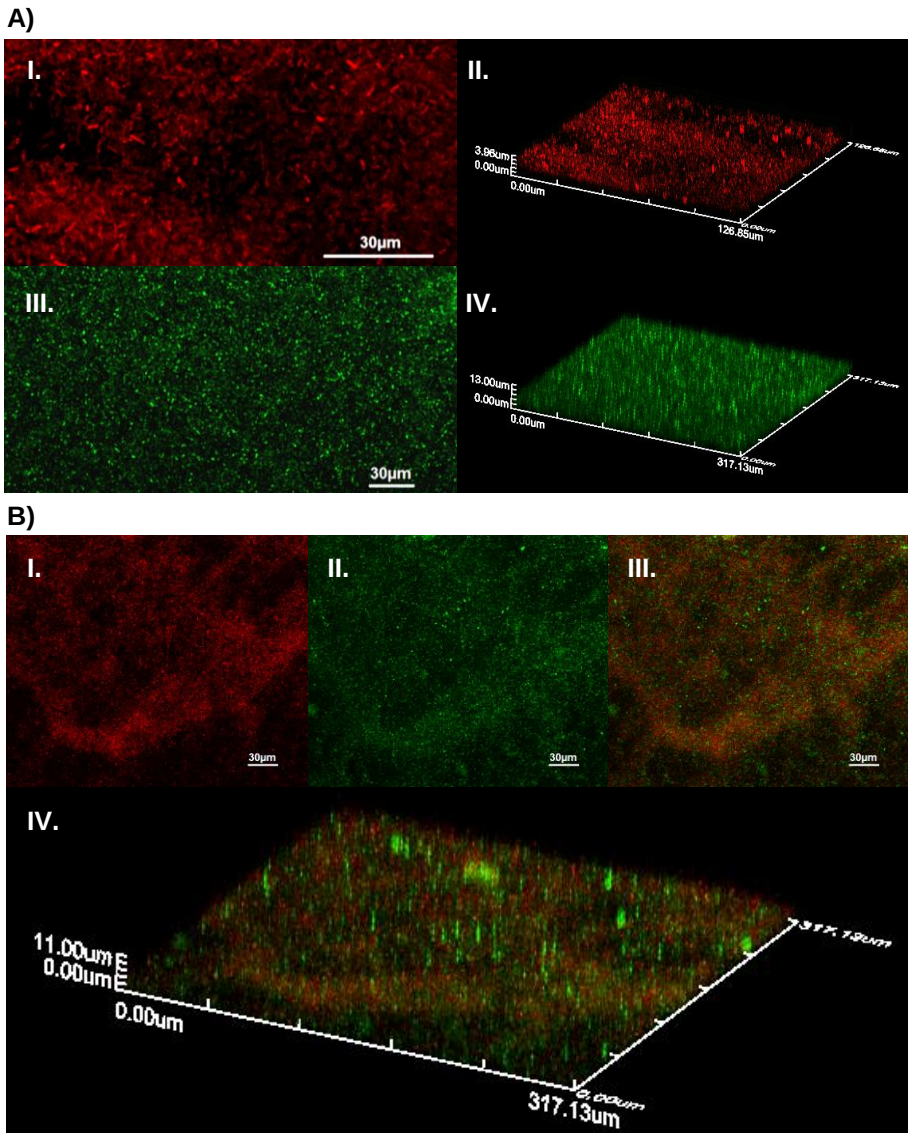

Figure 4.3 - CLSM images showing spatial organization of A) EC 434 (I – 2D, II – 3D) and SE EX2 (III – 2D, IV – 3D) mono-species biofilms, and B) EC 434 + SE EX2 dual-species biofilm (I – EC 434 colored in red; II – SE EX2 colored in green; III – superposition of both colors, 2D; IV – biofilm 3D spatial distribution).

The same spatial characterization was performed for 48-h EC 515 and SE 269 mono- and dual-species biofilms (Figure 4.4). In the case of EC 515, a more clustered biofilm was observed, and its thickness reached 11 µm in some areas of the coupon (Figure 4.4 A, I and II), which is much higher when compared to the thickness of EC 434 biofilm, 4 µm (Figure 4.3 A, I and II),

even though these bacteria belong to the same species. With respect to SE 269, this strain formed a biofilm with a reticulate appearance, although it was equally dispersed through the coupon (Figure 4.4 A, III and IV). This biofilm reached a thickness of approximately 24 µm, which, once again, is very different from the thickness of SE EX2 (13 µm). When looking at the images obtained for the EC 515 + SE 269 dual-species biofilms, it is clear that both strains maintained their mono-species biofilm spatial arrangement (Figure 4.4 B, I-III). Still, the thickness of mixed biofilm only reached ≈ 15 µm (Figure 4.4 B - IV).

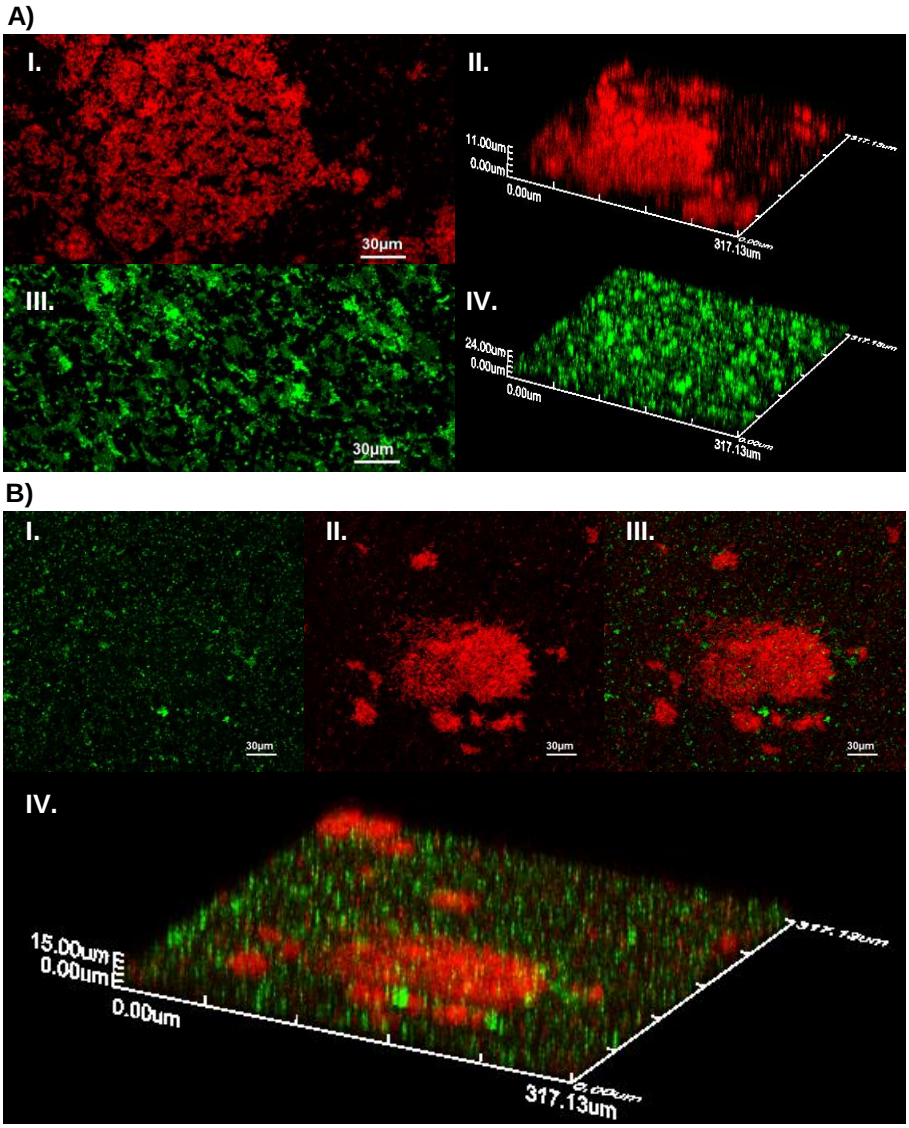

Figure 4.4 - CLSM images showing spatial organization of A) EC 515 (I – 2D, II – 3D) and SE 269 (III – 2D, IV – 3D) mono-species biofilms, and B) EC 515 + SE 269 dual-species biofilm (I – SE 269 colored in green; II – EC 515 colored in red; III – superposition of both colors, 2D; IV – biofilm 3D spatial distribution).

EPS spectra obtained by FTIR-ATR spectroscopy of *E. coli* and *S.* Enteritidis mono- and dual-species biofilms are represented in Figure 4.5. Globally, the spectra presented a very similar and

typical shape containing the absorption bands of lipids (3000-2800 cm^{-1}), proteins/amides I and II (1700-1500 cm^{-1}), a mixed region of phospholipids and nucleic acids (1500-1185 cm^{-1}), polysaccharides (1185-900 cm^{-1}), and the fingerprint region (900-600 cm^{-1}) [53,54]. Regarding the EC 434 + SE EX2 mixed biofilm, it seems the EPS spectrum is similar to EC 434 or to SE EX2 spectra, depending on the considered spectral region (Figure 4.5 A). This finding points to the absence of a predominant species EPS in the dual-species biofilm. In fact, the PCA model revealed an undefined clusterization with all spectra being quite disperse in the whole scores map (Figure 4.6 A). Concerning the EC 515 + SE 269 mixed biofilms, it seems that the EPS spectrum is more similar to the one of EC 515. Indeed, their infrared spectra are almost totally superimposable, being quite different from SE 269 spectrum (Figure 4.5 B). The corresponding scores map of the PCA model also reflects this similarity, showing two defined clusters, one containing the EPS spectra from *S.* Enteritidis biofilms and the other containing the EPS spectra from both *E. coli* and the dual-species biofilms (Figure 4.6 B).

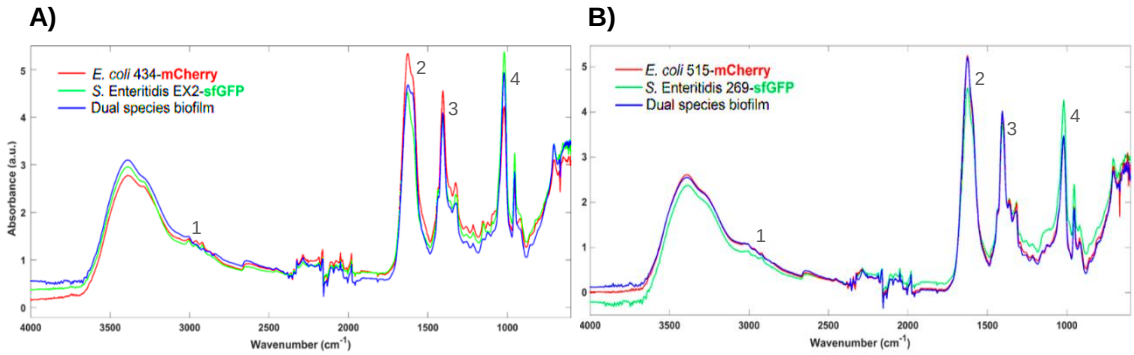

Figure 4.5 - Mean infrared spectra, processed with standard normal variate, of the EPS extracted from single and dual-species biofilms of A) EC 434 + SE EX2 and B) EC 515 + SE 269. Peaks: 1 – lipids, 2 - proteins/amides I and II, 3 - phospholipids and nucleic acids, 4 – polysaccharides.

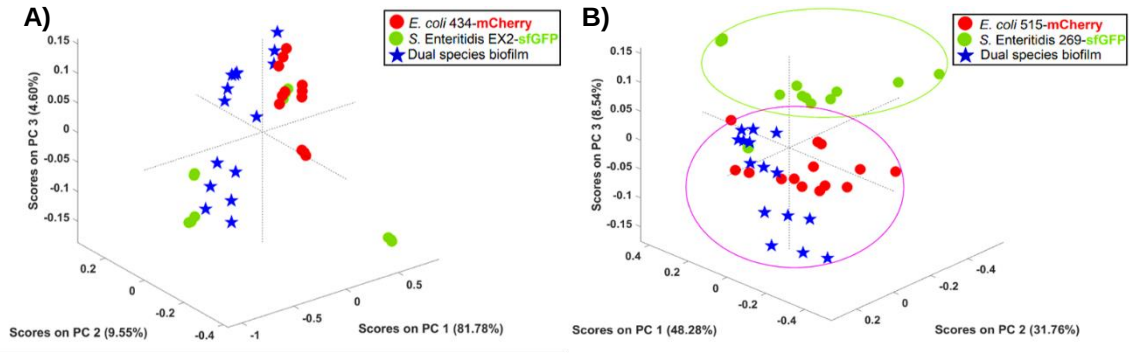

Figure 4.6 - Scores map of the PCA model of the EPSs infrared spectra extracted from single and dual-species biofilms of EC 434 + SE EX2 (A) and EC 515 + SE 269 (B) strains. The PCA model was built considering the spectral regions from 3600-2800 cm^{-1} and 1700-900 cm^{-1}.

4.3.3 Phage characterization

The phages used in this study were visualized by TEM and belong to two different families of the *Caudovirales* order. *E. coli* phage DalCa is a myovirus, having a long contractile tail (Figure 4.7 A), while the *S.* Enteritidis phage φ135 is a siphovirus with a long non-contractile tail (Figure 4.7 B).

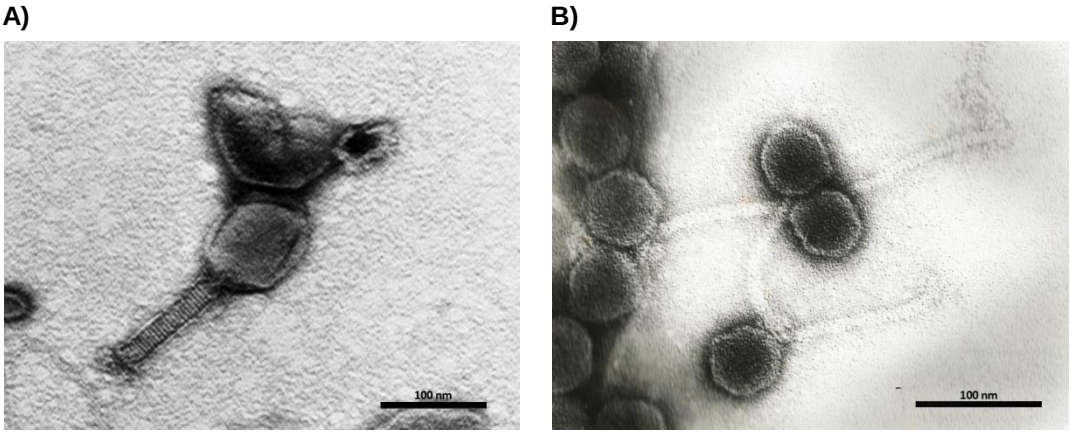

Figure 4.7 - TEM micrographs of *E. coli* phage DalCa (A) and *S.* Enteritidis phage φ135 (B). Scale bar is 100 nm.

Genomic analysis of DalCa revealed a genome of 166,040 bp in length assembled with a mean coverage value of 54×. DalCa encodes 268 putative CDSs, of which 130 have known function, regulated with 4 bacterial promoters and 34 rho-independent terminators. Whole-genome comparison showed *Escherichia* phage YUEEL01 (KY290975) as the closest homolog, with which it shares 94.1% of nucleotide identity and 256 genes (Figure 4.8 A). Regarding φ135, the genome of this phage was *de novo* assembled into a single contig of 43,142 bp in length and with an

average coverage of 1574×. φ135 genome is predicted to encode 59 CDSs, 28 of which with a predicted function. Furthermore, φ135 is also predicted to have 7 bacterial promoters and 22 rho-independent terminators. Most proteins have high homology (>90% amino acid identity) to *S.* Enteritidis phage PVP-SE2 (MF431252) proteome. Genomic comparisons show that φ135 is collinear with vB_SenS_PVP-SE2 phage, sharing 91% nucleotide identity and 53 genes (Figure 4.8 B).

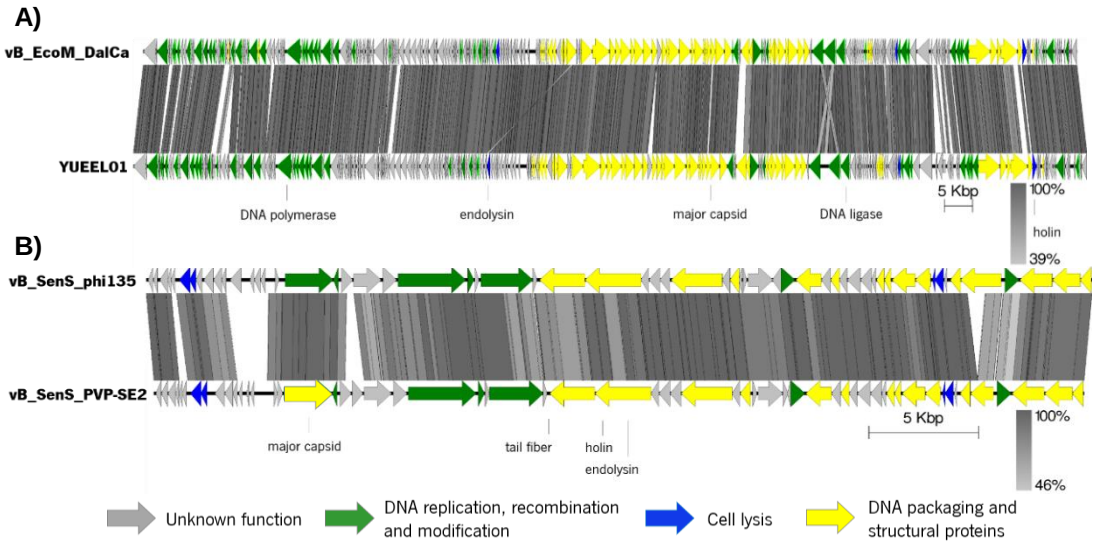

Figure 4.8 - Linear map of phages A) DalCa and B) φ135 genome sequences. The arrows point the direction of transcription, represent the predicted ORFs and are coloured (yellow, green, blue, and gray) according to their predicted functions. Major transcriptional units are represented. Phage DalCa was compared to *E. coli* phage YUEEL01 and φ135 to *S.* Enteritidis phage vB_SenS_PVP-SE2 using Easyfig.

To characterize the infectious potential of phages DalCa and φ135 on *E. coli* and *S.* Enteritidis, one-step growth curves were performed (Figure 4.9). DalCa revealed a latent period of approximately 20 and 15 min on EC 434 and EC 515, respectively. However, these strains present differences in burst size, producing only 5.3 PFU per infected cell, on EC 434, and 38.9 PFU per infected cell, on EC 515 (Figure 4.9 A). Regarding φ135, this phage had a latent period of approximately 25 min on SE 269, and 30 min on SE EX2. The burst size of φ135 was of 110.9 and 162.9 particles per infected cell on SE 269 and SE EX2, respectively (Figure 4.9 B).

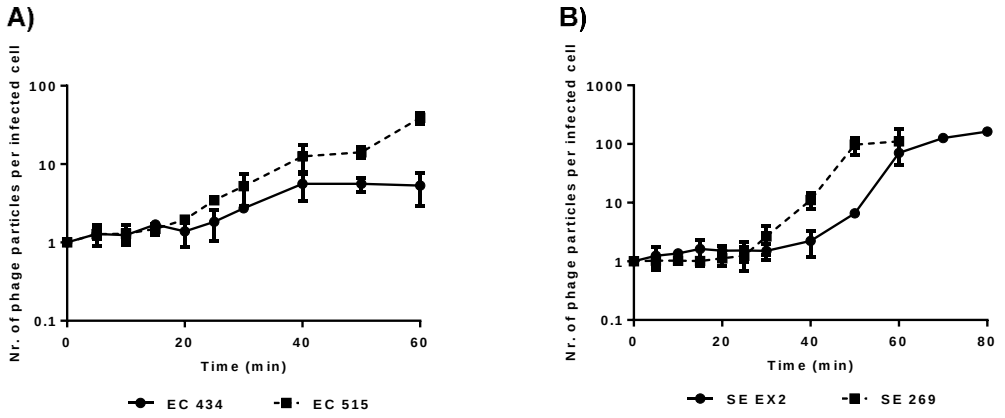

Figure 4.9 - One-step growth curves of phage DalCa in EC 434 and EC 515 (A), and phage φ135 in SE EX2 and SE 269 (B), at room temperature.

4.3.4 Phage treatment of mono- and dual-species *E. coli* and *S.* Enteritidis biofilms

Phages have been regarded as an alternative for the control of biofilms for quite some time (extensively reviewed in [55–57]) and so 24 h mono-species biofilms formed by EC 434 and EC 515, and SE EX2 and SE 269 were treated with DalCa and φ135 phages, respectively, for 4, 8 and 24 h (Figure 4.10). The results obtained show that DalCa produced the highest reduction in the number of viable cells at 4 h of treatment for both EC 434 (1.33 log) and EC 515 (1.29 log) biofilms (Figure 4.10 A). When SE EX2 and SE 269 biofilms were treated with φ135, the greatest reduction of bacterial loads, for SE EX2 biofilm, was obtained at 8 h of treatment (1.02 log), and for SE 269 at 4 h (1.63 log) (Figure 4.10 B).

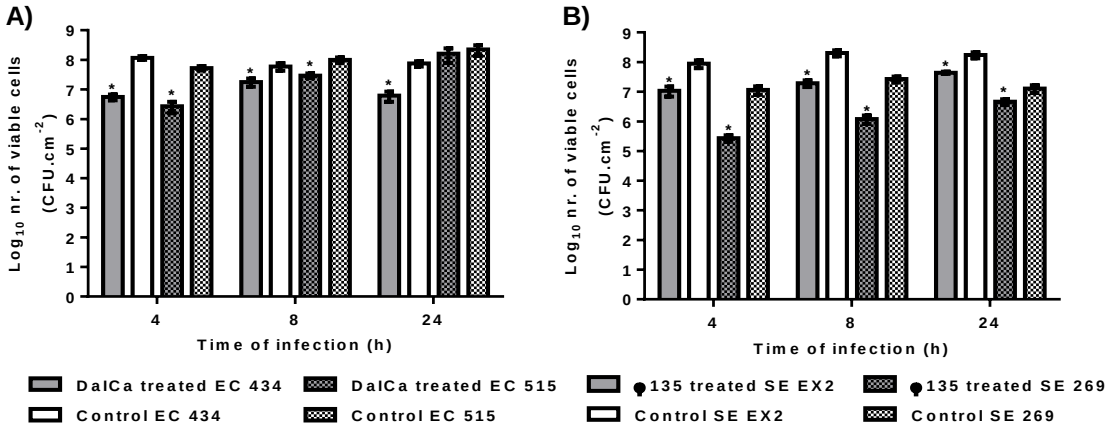

Figure 4.10 - *E. coli* (A) and *S.* Enteritidis (B) mono-species biofilms formed for 24 h in 96-well plates at 37 °C treated with phages DalCa and φ135, respectively, for 4, 8 and 24 h. Asterisks (*) indicate significant difference ($p < 0.05$) between phage-treated and control samples.

Since *E. coli* and *S.* Enteritidis are the most common pathogens found contaminating food facilities and food products [58], mixed biofilms of these two species were formed for 24 h and treated for 4, 8 and 24 h with a phage cocktail, comprised by *E. coli* phage DaICa and *S.* Enteritidis phage φ135 (Figure 4.11). For the mixed biofilm formed by EC 434 and SE EX2, the maximum decrease of bacterial loads was observed at 8 h of cocktail application, with EC 434 being reduced by 1.15 log and SE EX2 by 0.88 log (Figure 4.11 A). Regarding the EC 515 + SE 269 dual-species biofilm, the greatest reduction in the number of viable cells was achieved at 4 h of treatment for EC 515 (1.07 log) and at 8 h for SE 269 (2.42 log) (Figure 4.11 B).

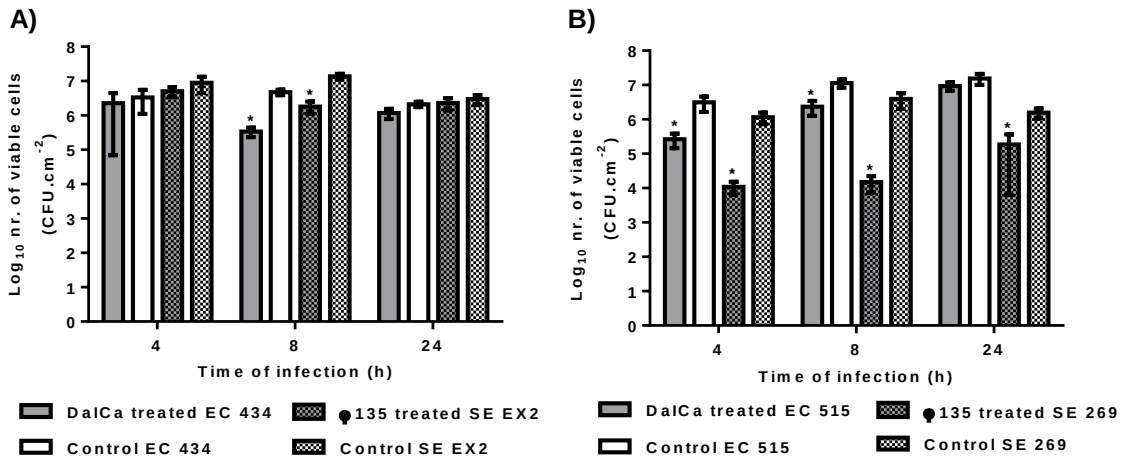

Figure 4.11 - EC 434 + SE EX2 (A) and EC 515 + SE 269 (B) dual-species biofilms formed for 24 h in 96-well plates at 37 °C treated with phages DaICa and φ135 for 4, 8 and 24 h. Asterisks (*) indicate significant difference ($p < 0.05$) between phage-treated and control samples.

4.4 Discussion

E. coli and *Salmonella* are pathogenic bacteria that represent an important public health concern [59,60]. Both pathogens have been responsible for numerous outbreaks, being often found contaminating meat [61,62] and vegetables [63,64], as well as food processing surfaces, that can ultimately lead to the contamination of food products [65]. *E. coli* and *Salmonella*'s ability to form biofilms makes these bacteria less susceptible to commonly used disinfectants, physical removal and other elimination processes [66,67]. Taking this knowledge into account, the objective of this work was to assess the efficacy of two phages, DaICa, specific for *E. coli*, and φ135, specific for *S.* Enteritidis, when used alone or in a cocktail, for the control of mono- and dual-species biofilms, respectively. Furthermore, focus was also given to structural and compositional characteristics of *E. coli* and *S.* Enteritidis mono- and dual-species biofilms to understand if the effectiveness of phages can be dependent on interspecies interactions between these two pathogens, when forming biofilms together.

Before assessing biofilm control with phages, it was necessary to evaluate the biofilm formation ability of the strains involved. The information available of these strains shows that the two *E. coli* tested herein belong to different serotypes, O6 (EC 515) and O1:K1:H7 (EC 434). Mono-species biofilm formation by different *E. coli* serotypes has been reported by other authors who showed that biofilm formation is serotype-dependent [69]. Biofilm variability is also influenced by the levels of curli expression, and presence or absence of other virulence factors, such as Shiga toxins 1 and 2 (*stx1* and *stx2*), intimin (*eaeA*), enterohemolysin A (*hlyA*), fimbriae, and autotransporters (e.g. EhaB and EspP) [68–70]. For instance, in a study using 39 different Shiga toxin-producing *E. coli* isolates, that belonged to the seropathotypes A, B, and C [69], results showed that seropathotype A, that includes the serotypes responsible for the highest incidence of foodborne outbreaks (serotypes O157:H7 and O157:NM), had greater ability to form biofilms than isolates from B (e.g. O26:H11, O45:H2, and O103:H2) and C (O157:H26) seropathotypes. According to our results, there are significant disparities between the biofilm forming ability by the *E. coli* serotypes O1 and O6, which resulted in 1.5 log differences in viable cell counts, with EC 515 having greater cell numbers (2.25×10^8 CFU.cm^{-2}) compared to EC 434 (0.75×10^8 CFU.cm^{-2}) (Figure 4.1). Both SE EX2 and SE 269 isolates belong to *S.* Enteritidis serovar, and have, so far, unknown genotypes. Phage typing (PT), multilocus sequence typing (MLST) or pulse-field gel electrophoresis (PFGE) have been used to discriminate the lineage of *Salmonella* isolates. Phage

typing of *S.* Enteritidis is usually done with the typing systems of the Laboratory of Enteric Pathogens (Health Protection Agency, London, UK), while *S.* Typhimurium phage typing is commonly performed using the Felix/Callow (England) and the Lilleengen (Sweden) typing systems. The information resulting from these analyses, or from other typing schemes, could have provided useful information to make assumptions regarding the biofilm formation ability according to the *Salmonella* strains genotypic characteristics. Nonetheless, some conclusions can be drawn based merely on the CFU.cm^{-2} determinations, which showed that isolates SE EX2 and SE 269, when in mono-species biofilms, formed fairly different biofilms with higher bacterial counts for the SE EX2 strain. The difference in biofilm ability between these two strains was of 1.6 log, with SE EX2 reaching 1.73×10^{8} CFU.cm^{-2} and SE 269 showing 0.13×10^{8} CFU.cm^{-2} (Figure 4.1).

The strain combinations for dual-species biofilm formation were EC 434 + SE EX2 and EC 515 + SE 269, as the first strain combination harbours the strong *E. coli* and *S.* Enteritidis biofilm formers, while the latter combination is composed by the weak biofilm producers. The competitive ability of strains in mixed biofilms has been linked to the relative density of each bacterium added to form biofilms [71]. However, in this work, the number of cells added for biofilm formation was the same, and, therefore, this factor cannot be used to explain the higher/lower surface coverage by the different *E. coli* and *S.* Enteritidis strains. EC 434 and SE EX2 formed biofilms with higher numbers of viable cells alone than in mixed species biofilms (Figure 4.1 A), and the same was perceived for EC 515 and SE 269 (Figure 4.1 B), showing an antagonistic effect from both strains towards each other. This phenomenon has already been described for *E. coli* O157:H7 strain USDA 5 added together with *Salmonella* strain 457-88 for biofilm formation studies in 96-well plates [72]. One hypothesis to the presence of a lower number of bacterial cells in mixed biofilms could be species competition for adherence to the polystyrene surface, leaving a smaller area available for adhesion and consequent biofilm formation by the less competitive species involved. However, the number of viable cells per area analysed (CFU.cm^{-2}) in both mixed biofilms tested, EC 434 + SE EX2 (5.1×10^{6} CFU.cm^{-2}) and EC 515 + SE 269 (1.7×10^{7} CFU.cm^{-2}) (Figure 4.1 A), was far less than the number of viable cells per area, for example, obtained for the mono-species EC 515 biofilms (2.25×10^{8} CFU.cm^{-2}). Hence, surface area availability for dual-species biofilm formation was shown to be an irrelevant factor for the low cell numbers reported herein. Mixed biofilm populations can have dominance of one species over the other. For instance, biofilms formed by *Staphylococcus aureus* and *E. coli* showed dominance of the latter species [73], and this was, according to the authors, due to the shorter generation time of *E. coli* compared to *S. aureus.* Other

authors have also shown that bacteria having faster growth rates will control the environment and favour their growth over other strains that have slower growth characteristics [74,75]. Furthermore, it has been shown that dominance by one bacterium usually results in its long-term prevalence in the same surface area. In the work described in this chapter, both bacterial species used belong to the *Enterobacteriacea* family. In the bacterial growth characterization experiments, significant differences of μ_{max} were detected for both *E. coli* (EC 434 and EC 515) and *S.* Enteritidis (SE EX2 and SE 269) used (Table 4.1). Statistical analysis of t_d values between the two strains used, for *S.* Enteritidis and *E. coli*, showed differences only between strains SE EX2 and SE 269 ($p < 0.01$). In terms of μ_{max} and t_d values between the two sets of species used for mixed biofilm formation, only the EC 515 + SE 269 combination was significantly different ($p < 0.01$). This may explain the higher numbers of EC 515 cells (1.55×10^7 CFU.cm^{-2}) present in the mixed biofilms compared to SE 269 cell numbers (1.57×10^6 CFU.cm^{-2}) (Figure 4.1 B). The explanation for this is due to the slightly faster growth rate of EC 515 that will consequently lead to a larger surface area covered. CLSM analysis of mixed species biofilms showed that EC 515 formed preferentially 3D structures where cells remained closely gathered, while SE 269 was found more scattered in the polystyrene surface (Figure 4.4 B). The same spatial distribution was already seen in mono-species biofilms of SE 269 and EC 515. It was expected that, since SE 269 single-species biofilms presented a thickness of 24 µm, similar values would be reached in the mixed biofilms. However, both SE 269 and EC 515 had a decrease of viable cells by 1 log each, compared to the cell counts obtained in mono-species biofilms, which can explain the lower height of the mixed biofilm (15 µm) (Figure 4.4 B). On the other hand, EC 434 and SE EX2 strains showed non-statistically differences in μ_{max} and t_d values ($p > 0.05$) (Table 4.1), legitimating a similar number of viable cells of both strains present in the mixed biofilms, 2.12×10^6 and 2.98×10^6 CFU.cm^{-2} for EC 434 and SE EX2, respectively (Figure 4.1 A). Biofilms of these two species analysed by CLSM showed thinner biofilms (11 µm), with both species equally distributed in the same areas of the coupons (Figure 4.3 B). This evenly distribution was also observed when these strains formed mono-species biofilms (Figure 4.3 A).

FTIR-ATR spectroscopy coupled with chemometrics has been used as a reliable and alternative method to accurately discriminate bacteria at different taxonomic levels, including *E. coli* clones [76], and *Salmonella* serogroups and serotypes [77]. FTIR-ATR spectroscopy has also been used in biofilm contexts, for instance, to monitor biofilm *in situ*, in real-time, and under fully hydrated conditions [78]. Work performed with *P. fluorescens*, a known food spoilage bacterium, studied

early stages of biofilm formation by FTIR-ATR spectroscopy, and also planktonic cultures at different growth phases [78]. FTIR has also been used to analyze the composition of the EPS matrix of exponential and stationary phase cultures. For instance, FTIR spectra of two *Rhodotermus marinus* were quite similar, nonetheless, they could be distinguished based on few spectral differences: one isolate showed stronger absorption at 910 cm^{-1} (β-glycosidic bond); and only one of the isolates exhibited a peak at 818 cm^{-1} [79]. In another work, FTIR-ATR spectroscopy application to assess EPS matrix from two biofilms at different phases of formation, mid-development and mature phases, showed that spectra had differences in shape and intensity, with mature biofilms presenting substantially higher protein and carbohydrate peaks, and a low level of lipids that were, nonetheless, higher than those observed for biofilms in mid-development phase [78]. In the present work, FTIR-ATR was used to compare EPS composition of mono- and dual-species biofilms (Figure 4.5). The EPS matrix consists of proteins, eDNA, and polysaccharides, among other components. However, the polysaccharide component of the matrix offers diverse benefits to the cells in biofilms, sustaining surface and cell-to-cell adhesions, providing protection, and allowing cell growth in 3D structures [80]. The FTIR-ATR spectroscopy analysis showed few spectral differences among the samples (Figure 4.5). The absorption band of lipids (3000-2800 cm^{-1}), in all EPS samples analyzed, was much lower than the absorption bands of proteins or carbohydrates. Also, it seems that the ratio between proteins/carbohydrates was higher for the weaker biofilm producers (EC 515 and SE 269) (Figure 4.5 B). Previous studies have reported a competitive advantage of EPS producer strains in mixed biofilm populations, and also reported that the secretion of more EPS helps progeny cell movement up and out of the focal cell layer, providing better oxygen conditions to their descendants [81]. Taking into account the EPS spectral peaks analysed by FTIR-ATR spectroscopy, the mixed biofilms of EC 434 and SE EX2 resembled more with the EPS spectra obtained with EC 434 in terms of proteins/amides I and II, and the phospholipids and nucleic acids absorption peaks, and with the polysaccharide absorption band of SE EX2 (Figure 4.5 A). So, in this set of strains, none seemed to be better EPS producer than the other. FTIR-ATR spectroscopy is a semi-quantitative method and therefore direct conclusions cannot be drawn. However, if we take into account only the polysaccharide absorption peak (peak 4), that clearly resembles to the one obtained by SE EX2 in mono-species biofilms, we can, in theory, make an assumption that SE EX2 secretes more polysaccharides than EC 434, which confers this strain a competitive advantage for surface adhesion and predominance in the mixed consortia (Figure 4.5 A). If this assumption is valid, this explains the higher levels of SE EX2 cells in the surface compared to EC 434 (see Figure

4.1 A and negative CI index in Figure 4.2 A). The other set of strains analysed comprising the weaker biofilm producers (EC 515 + SE 269) showed that the FTIR-ATR spectra superimposed the spectrum of EC 515 when grown in single-species biofilms (Figure 4.5 B), assuming an EPS matrix predominance of EC 515 in these dual-species biofilms. Interestingly, these results are in agreement with the CI index obtained (positive CI index in Figure 4.2 B), which demonstrated that, indeed, EC 515 should be the predominant strain in the polystyrene surfaces. Therefore, in the case of these two strains, the surface colonization was both growth- (Table 4.1) and polysaccharide-dependent. Overall, these experiments showed that dominance by one specific bacterium in mixed biofilms can either be both polysaccharide- and growth rate-dependent, as observed in EC 515 + SE 269 biofilms, or can be polysaccharide-dependent, as shown for EC 434 + SE EX2 biofilms. However, this latter observation needs to be further validated, since only the FTIR-ATR absorbance peak between 1185 and 900 cm^{-1} was taken into consideration.

The use of phages as antibiofilm agents showed that short treatment periods with DaICa and φ135 were more effective towards both mono- and dual-species biofilms (Figures 4.10 and 4.11). Single-species biofilms of *E. coli* treated with DaICa resulted in an equivalent antibiofilm effect in both strains (Figure 4.10). This is possibly due to a combination of three different factors: the latent period of DaIca in the tested strains, the burst size reached per infected bacterium, and also the strain growth parameters (μ_{max} and t_d). DaIca has a burst size of merely 5.4 PFU per infected EC 434 cell, but a faster latent period. However, EC 434 strain showed a lower growth rate and consequently higher doubling time which could result in less new cells to be infected by the phage. DaIca in EC 515 has an ability to produce around 7.3 times more progeny phage particles per infected cell, compared to EC 434. However, the phage latent period is longer. Together with a faster doubling time, EC 515 reaches similar reductions (see Figures 4.9 A and 4.10 A, and also Table 4.1). In terms of *Salmonella* phage treatment experiments with φ135, the antibiofilm outcome was better in mono-species SE 269 biofilms, compared to SE EX2. This is greatly due to a higher burst size in the first strain (162.9 PFU per infected SE 269 compared to 110.9 PFU per infected SE EX2). Also, the growth rate of SE 269 was lower and therefore the non-infected biofilm cells proliferated at a slower rate than the SE EX2 non-infected cells, consequently resulting in a smaller number of descendent cells present at the sampling timepoints assessed (Figures 4.9 B and 4.10 B, and also Table 4.1).

Phage application to dual-species biofilms was also investigated herein (Figure 4.11). In terms of antibiofilm effect using the phage cocktail comprising DaIca and φ135 phages, their action on

EC 434 + SE EX2 biofilms resulted in similar log reductions for both species (Figure 4.11 A). Both strains have non-statistically different μ_{max} and, therefore, in theory, the phage producing a higher burst size should reduce more biofilm cells. This was not, however, the situation observed after phage treatment of biofilms of these two strains. Taking into consideration that EC 434 and SE EX2 biofilms presented fairly similar viable cell numbers throughout the phage treatment experiments and being φ135 able to produce 30.7 times more new phage particles per infected SE EX2 cell compared to Dalca on EC 434, this indeed should have resulted in greater SE EX2 reductions. CLSM analysis shows that these strains are scattered throughout the coupon surface, and this can hinder phages from reaching their hosts (Figure 4.3 B). FTIR-ATR analysis of EPS matrix showed that the spectral peaks of these strains were more similar, in some parts, to SE EX2, while, in other parts, was more related to EC 434 (Figure 4.5 A). However, the polysaccharide absorption peak (peak 4) resembled more the SE EX2 polysaccharide peak, as already describe above. If the assumption made before that SE EX2 secretes more polysaccharides, these can be masking the phage receptors present in the host cell surfaces. This hypothesis could explain why a higher phage burst did not result in an enhanced antibiofilm activity. Nevertheless, further experiments need to be performed to understand this behaviour. The methods that could possibly give us further clues contemplate time-lapse microscopy imaging [82], flow cytometry [83] or even spinning disk confocal microscopy [84].

The application of phages to the other set of strains (EC 515 and SE 269) resulted in higher reduction of SE 269 biofilm cells than of EC 515 (Figure 4.11 B). This result is a reflection of φ135 having a better burst size than Dalca, and also due to the slower growth rate of SE 269 (Figure 4.10 B and Table 4.1). Furthermore, CLSM shows that SE 269 is more dispersed on the surfaces while EC 515 preferentially forms 3D clusters, which can impair phage diffusion to reach cells that are in deeper biofilm layers (Figure 4.4 B). According to FTIR-ATR analysis, the EC 515 + SE 269 EPS spectrum obtained was remarkably similar to the spectrum of EC 515 EPS. These results can indicate that, even though EC 515's EPS predominates in the dual-species biofilm samples, it is possibly confined only to the clustered areas, and therefore does not constitute an obstacle for phage φ135 to reach SE 269 cells.

In conclusion, this work gives new insights into the many factors influencing dual-species biofilm development. Moreover, it sheds light into the interaction of single and cocktail phages for the control of mono- and dual-species biofilms. A better understanding of species-species and phage-host interactions was reached through analysis of bacterial and phage growth parameters,

viable cell determination, before and after phage treatment, CLSM imaging of the biofilm structures, and also EPS matrix analyses by FTIR-ATR spectroscopy. Even though some of the strains showed to be more competitive regarding their surface attachment, reaching higher viable cell numbers than the other species involved, this did not have a direct influence on the action of phages. Infectivity of the phage was more associated with its growth characteristics, in particular the latent period durations and the burst size, and also due to the difficulty of phages to infect one particular strain, EC 515, which formed 3D biofilms structures rather than having cells uniformly dispersed over the surface, possibly impairing phage diffusion. Furthermore, the EPS matrix of one species can constitute a problem to the other one, and the phage killing ability the latter species, by possibly covering the phage receptors necessary for the adsorption step to take place.

References

1. DuPont HL. **The growing threat of foodborne bacterial enteropathogens of animal origin.** *Clin Infect Dis.* 2007;45(10):1353–61. doi: 10.1086/522662.

2. Pachepsky Y, Shelton DR, McLain JET, Patel J, Mandrell RE. **Irrigation Waters as a Source of Pathogenic Microorganisms in Produce. A Review.** In: *Advances in Agronomy*. 1st ed. Elsevier Inc.; 2011. p. 73–138.

3. Greig JD, Ravel A. **Analysis of foodborne outbreak data reported internationally for source attribution.** *Int J Food Microbiol*. 2009;130(2):77–87. doi: 10.1016/j.ijfoodmicro.2008.12.031.

4. Wang R, Kalychayanand N, Schmidt JW, Harhay DM. **Mixed Biofilm Formation by Shiga Toxin-Producing *Escherichia coli* and *Salmonella enterica* Serovar Typhimurium Enhanced Bacterial Resistance to Sanitization due to Extracellular Polymeric Substances.** *J Food Prot.* 2013;77(5):805–13. doi: 10.4315/0362-028X.JFP-13-077.

5. Islam M, Morgan J, Doyle MP, Phatak SC, Millner P, Jiang X. **Fate of *Salmonella enterica* Serovar Typhimurium on Carrots and Radishes Grown in Fields Treated with Contaminated Manure Composts or Irrigation Water.** *Appl Environ Microbiol.* 2004;70(4):2497–502. doi: 10.1128/AEM.70.4.2497-2502.2004.

6. Islam M, Morgan J, Doyle MP, Phatak SC, Millner P, Jiang X. **Persistence of *Salmonella enterica* Serovar Typhimurium on Lettuce and Parsley and in Soils on Which They Were Grown in Fields Treated with Contaminated Manure Composts or Irrigation Water.** *Foodborne Pathog Dis.* 2004;1(1):27–35. doi: 10.1089/153531404772914437.

7. Jensen DA, Friedrich LM, Harris LJ, Danyluk MD, Schaffner DW. **Cross contamination of *Escherichia coli* O157:H7 between lettuce and wash water during home-scale washing.** *Food Microbiol*. 2015 Apr;46:428–33. doi: 10.1016/j.fm.2014.08.025.

8. Teplitski M, Barak JD, Schneider KR. **Human enteric pathogens in produce: un-answered ecological questions with direct implications for food safety.** *Curr Opin Biotechnol.* 2009;20(2):166–71. doi: 10.1016/j.copbio.2009.03.002.

9. Scallan E, Hoekstra RM, Angulo FJ, Tauxe R V., Widdowson M-A, Roy SL et al. **Foodborne Illness Acquired in the United States—Major Pathogens.** *Emerg Infect Dis*. 2011 Jan;17(1):7–15. doi: 10.3201/eid1701.091101p1.

10. Garrett TR, Bhakoo M, Zhang Z. **Bacterial adhesion and biofilms on surfaces.** *Prog Nat Sci.* 2008 Sep;18(9):1049–56. doi: 10.1016/j.pnsc.2008.04.001.

11. Giaouris E, Heir E, Hébraud M, Chorianopoulos N, Langsrud S, Møretrø T et al. **Attachment and biofilm formation by foodborne bacteria in meat processing environments: Causes, implications, role of bacterial interactions and control by alternative novel methods.** *Meat Sci.* 2014;97(3):289–309. doi: 10.1016/j.meatsci.2013.05.023.

12. Macho AP, Zumaquero A, Ortiz-Martín I, Beuzón CR. **Competitive index in mixed infections: a sensitive and accurate assay for the genetic analysis of *Pseudomonas syringae* plant interactions.** *Mol Plant Pathol.* 2007 Jul;8(4):437–50. doi: 10.1111/j.1364-3703.2007.00404.x.

13. Esteves CLC, Jones BD, Clegg S. **Biofilm Formation by *Salmonella enterica* Serovar Typhimurium and *Escherichia coli* on Epithelial Cells following Mixed Inoculations.** *Society.* 2005;73(8):5198–203. doi: 10.1128/IAI.73.8.5198-5203.2005.

14. Zhou Y, Smith D, Leong BJ, Brännström K, Almqvist F, Chapman MR. **Promiscuous Cross-seeding between Bacterial Amyloids Promotes Interspecies Biofilms.** *J Biol Chem.* 2012 Oct 12;287(42):35092–103. doi:10.1074/jbc.M112.383737.

15. Sillankorva S, Neubauer P, Azeredo J. ***Pseudomonas fluorescens*** **biofilms subjected to phage phiIBB-PF7A.** *BMC Biotechnol.* 2008;8(79). doi: 10.1186/1472-6750-8-79.

16. Garcia KC, Corrêa IM, Pereira LQ, Silva TM, Mioni M, Izidoro AC et al. **Bacteriophage use to control** ***Salmonella*** **biofilm on surfaces present in chicken slaughterhouses.** *Poult Sci.* 2017;1–7. doi: 10.3382/ps/pex124.

17. Gong C, Jiang X. **Application of bacteriophages to reduce** ***Salmonella*** **attachment and biofilms on hard surfaces.** *Poult Sci.* 2017;96(6):1838–48. doi: 10.3382/ps/pew463.

18. Sasikala D, Srinivasan P. **Characterization of potential lytic bacteriophage against** ***Vibrio alginolyticus*** **and its therapeutic implications on biofilm dispersal.** *Microb Pathog.* 2016;101:24–35. doi: 10.1016/j.micpath.2016.10.017.

19. Arachchi GJ, Cridge AG, Dias-Wanigasekera BM, Cruz CD, McIntyre L, Liu R et al. **Effectiveness of phages in the decontamination of** ***Listeria monocytogenes*** **adhered to clean stainless steel, stainless steel coated with fish protein, and as a biofilm.** *J Ind Microbiol Biotechnol.* 2013;40(10):1105–16. doi: 10.1007/s10295-013-1313-3.

20. Sharma M, Ryu JH, Beuchat LR. **Inactivation of** ***Escherichia coli*** **O157:H7 in biofilm on stainless steel by treatment with an alkaline cleaner and a bacteriophage.** *J Appl Microbiol.* 2005;99(3):449–59. doi: 10.1111/j.1365-2672.2005.02659.x.

21. Sillankorva S, Neubauer P, Azeredo J. **Phage control of dual species biofilms of** ***Pseudomonas fluorescens*** **and** ***Staphylococcus lentus*****.** *Biofouling.* 2010;26(5):567–75. doi: 10.1080/08927014.2010.494251.

22. Gutiérrez D, Vandenheuvel D, Martínez B, Rodríguez A, Lavigne R, García P. **Two Phages, phiIPLA-RODI and phiIPLA-C1C, Lyse Mono- and Dual-Species Staphylococcal Biofilm.** *Appl Environ Microbiol.* 2015;81(10):3336–48. doi: 10.1128/AEM.03560-14.

23. Sillankorva S, Pleteneva E, Shaburova O, Santos S, Carvalho C, Azeredo J et al. ***Salmonella*** **Enteritidis bacteriophage candidates for phage therapy of poultry.** *J Appl Microbiol.* 2010;108(4):1175–86. doi: 10.1111/j.1365-2672.2009.04549.x.

24. Sillankorva S, Neubauer P, Azeredo J. **Isolation and characterization of a T7-like lytic phage for** ***Pseudomonas fluorescens*****.** *BMC Biotechnol.* 2008 Jan;8(80):1–11. 10.1186/1472-6750-8-80.

25. Hall BG, Acar H, Nandipati A, Barlow M. **Growth Rates Made Easy.** *Mol Biol Evol.* 2014 Jan 1;31(1):232–8. doi: 10.1093/molbev/mst187.

26. Stepanović S, Vuković D, Dakić I, Savić B, Švabić-Vlahović M. **A modified microtiter-plate test for quantification of staphylococcal biofilm formation.** *J Microbiol Methods.* 2000;40(2):175–9.

27. Milho C, Silva MD, Melo L, Santos S, Azeredo J, Sillankorva S. **Control of** ***Salmonella*** **Enteritidis on food contact surfaces with bacteriophage PVP-SE2.** *Biofouling.* 2018;30:1–16. doi: 10.1080/08927014.2018.1501475.

28. Pédelacq JD, Cabantous S, Tran T, Terwilliger TC, Waldo GS. **Engineering and characterization of a superfolder green fluorescent protein.** *Nat Biotechnol.* 2006;24(1):79–88. doi: 10.1038/nbt1172.

29. Amarasinghe JJ, D'Hondt RE, Waters CM, Mantis NJ. **Exposure of** ***Salmonella enterica*** **serovar Typhimurium to a protective monoclonal IgA triggers exopolysaccharide production via a diguanylate cyclase-dependent pathway.** *Infect Immun.* 2013;81(3):653–64. doi: 10.1128/IAI.00813.

30. Merritt JH, Kadouri DE, O'Toole GA. **Growing and Analyzing Static Biofilms.** *Curr Protoc Microbiol.* 2005;1–29. doi: 10.1002/9780471729259.mc01b01s00.

31. Chiba A, Sugimoto S, Sato F, Hori S, Mizunoe Y. **A refined technique for extraction of extracellular matrices from bacterial biofilms and its applicability.** *Microb Biotechnol.* 2015

May;8(3):392–403. doi:10.1111/1751-7915.12155.

32. Aziz RK, Bartels D, Best A, DeJongh M, Disz T, Edwards R et al. **The RAST Server: rapid annotations using subsystems technology.** *BMC Genomics.* 2008;9(75):1–15. doi: 10.1186/1471-2164-9-75.

33. Altschul SF, Madden TL, Schäffer AA, Zhang J, Zhang Z, Miller W et al. **Gapped BLAST and PSI-BLAST: a new generation of protein database search programs.** *Nucleic Acids Res.* 1997;25(17):3389–402. doi: 10.1093/nar/25.17.3389.

34. Altschul SF, Gish W, Miller W, Myers EW, Lipman DJ. **Basic local alignment search tool.** *J Mol Biol.* 1990;215(3):403–10. doi: 10.1016/S0022-2836(05)80360-2.

35. Soding J, Biegert A, Lupas AN. **The HHpred interactive server for protein homology detection and structure prediction.** *Nucleic Acids Res.* 2005 Jul 1;33(Web Server):W244–8. doi: 10.1093/nar/gki408.

36. Stothard P. **The Sequence Manipulation Suite: JavaScript Programs for Analyzing and Formatting Protein and DNA Sequences.** *Biotechniques.* 2000 Jun;28(6):1102–4. doi: 10.2144/00286ir01.

37. Käll L, Sonnhammer ELL. **Reliability of transmembrane predictions in whole-genome data.** *FEBS Lett.* 2002;532(3):415–8. doi: 10.1016/S0014-5793(02)03730-4.

38. Käll L, Krogh A, Sonnhammer ELL. **A combined transmembrane topology and signal peptide prediction method.** *J Mol Biol.* 2004;338(5):1027–36. doi: 10.1016/j.jmb.2004.03.016.

39. Schattner P, Brooks AN, Lowe TM. **The tRNAscan-SE, snoscan and snoGPS web servers for the detection of tRNAs and snoRNAs.** *Nucleic Acids Res.* 2005;33:W686–9. doi: 10.1093/nar/gki366.

40. Klucar L, Stano M, Hajduk M. **PhiSITE: Database of gene regulation in bacteriophages.** *Nucleic Acids Res.* 2009;38(Database issue):D366–70. doi: 10.1093/nar/gkp911.

41. Naville M, Ghuillot-Gaudeffroy A, Marchais A, Gautheret D. **ARNold: a web tool for the prediction of Rho-independent transcription terminators.** *RNA Biol.* 2011;8(1):11–3. doi: 10.4161/rna.8.1.13346.

42. Zuker M. **Mfold web server for nucleic acid folding and hybridization prediction.** *Nucleic Acids Res.* 2003;31(13):3406–15. doi: 10.1093/nar/gkg595.

43. Sullivan MJ, Petty NK, Beatson SA. **Easyfig: A genome comparison visualizer.** *Bioinformatics.* 2011;27(7):1009–10. doi: 10.1093/bioinformatics/btr039.

44. Wang Y, Coleman-Derr D, Chen G, Gu YQ. **OrthoVenn: a web server for genome wide comparison and annotation of orthologous clusters across multiple species.** *Nucleic Acids Res.* 2015 Jul 1;43(W1):W78–84. doi: 10.1093/nar/gkv487.

45. McNerney R, Wilson SM, Sidhu AM, Harley VS, Al Suwaidi Z, Nye PM et al. **Inactivation of mycobacteriophage D29 using ferrous ammonium sulphate as a tool for the detection of viable *Mycobacterium smegmatis* and *M. tuberculosis*.** *Res Microbiol.* 1998;149(7):487–95. doi: 10.1016/S0923-2508(98)80003-X.

46. Jolliffe IT. **Principal Component Analysis**. 1st ed. New York, NY: Springer New York; 1986. 271 p. (Springer Series in Statistics).

47. Naes T, Isaksson T, Fearn T, Davies T. **A user Friendly guide to Multivariate Calibration and Classification.** 1st ed. Chichester, UK: NIR Publications; 2002. 344 p.

48. Savitzky A, Golay MJE. **Smoothing and Differentiation of Data by Simplified Least Squares Procedures.** *Anal Chem.* 1964 Jul;36(8):1627–39. doi: 10.1021/ac60214a047.

49. Giaouris E, Heir E, Desvaux M, Hébraud M, Møretrø T, Langsrud S et al. **Intra- and inter-species interactions within biofilms of important foodborne bacterial pathogens.** *Front Microbiol.*

2015;6(JUL):1–26. doi: 10.3389/fmicb.2015.00841.

50. Almeida C, Azevedo NF, Santos S, Keevil CW, Vieira MJ. **Discriminating multi-species populations in biofilms with peptide nucleic acid fluorescence *in situ* hybridization (PNA FISH).** *PLoS One.* 2011;6(3). doi: 10.1371/journal.pone.0014786.

51. Smit J, Kamio Y, Nikaido H. **Outer membrane of *Salmonella* Typhimurium: chemical analysis and freeze fracture studies with lipopolysaccharide mutants.** *J Bacteriol.* 1975;124(2):942–58.

52. Grossman N, Ron EA, Woldringh CL. **Changes in cell dimensions during amino acid starvation of *Escherichia coli*.** *J Bacteriol.* 1982;152(1):35–41.

53. Naumann D, Helm D, Labischinski H. **Microbiological characterizations by FT-IR spectroscopy.** *Nature.* 1991 May 2;351(6321):81–2. doi: 10.1038/351081a0.

54. Maquelin K, Kirschner C, Choo-Smith L-P, van den Braak N, Endtz HP, Naumann D et al. **Identification of medically relevant microorganisms by vibrational spectroscopy.** J *Microbiol Methods.* 2002 Nov;51(3):255–71. doi: 10.1016/S0167-7012(02)00127-6.

55. Escobedo S, Guti D, Portilla S, Mart B, Garc P, Rodr A. **Bacteriophages in the Dairy Environment: From Enemies to Allies.** *Antibiotics.* 2017 Nov 8;6(4):27. doi: 10.3390/antibiotics6040027.

56. Pires D, Melo L, Vilas Boas D, Sillankorva S, Azeredo J. **Phage therapy as an alternative or complementary strategy to prevent and control biofilm-related infections.** *Curr Opin Microbiol.* 2017 Oct;39:48–56. doi: 10.1016/j.mib.2017.09.004.

57. Coughlan LM, Cotter PD, Hill C, Alvarez-Ordóñez A. **New weapons to fight old enemies: Novel strategies for the (bio)control of bacterial biofilms in the food industry.** *Front Microbiol.* 2016;7(OCT):1–21. doi: 10.3389/fmicb.2016.01641.

58. Jensen D, Friedrich L, Harris L, Danyluk M, Schaffner D. **Quantifying Transfer Rates of *Salmonella* and *Escherichia coli* O157:H7 between Fresh-Cut Produce and Common Kitchen Surfaces.** J *Food Prot.* 2013 Sep;76(9):1530–8. doi: 10.4315/0362-028X.JFP-13-098.

59. CDC. ***E. coli* - outbreaks.** 2018 [accessed 2018 Nov 13]. Available from: https://www.cdc.gov/ecoli/outbreaks.html

60. CDC. ***Salmonella* - outbreaks.** 2018 [accessed 2018 Nov 13]. Available from: https://www.cdc.gov/*Salmonella*/outbreaks.html

61. CDC. **Outbreak of *E. coli* Infections Linked to Ground Beef**. 2018 [accessed 2018 Nov 13]. Available from: https://www.cdc.gov/ecoli/2018/o26-09-18/index.html

62. CDC. **Outbreak of *Salmonella* Infections Linked to Ground Beef**. 2018 [accessed 2018 Nov 13]. Available from: https://www.cdc.gov/*Salmonella*/newport-10-18/index.html

63. CDC. **Multistate Outbreak of *E. coli* O157:H7 Infections Linked to Romaine Lettuce (Final Update)**. 2018 [accessed 2018 Nov 13]. Available from: https://www.cdc.gov/ecoli/2018/o157h7-04-18/index.html

64. CDC. **Multistate Outbreak of *Salmonella* Poona Infections Linked to Imported Cucumbers (Final Update)**. 2015 [accessed 2018 Nov 13]. Available from: https://www.cdc.gov/*Salmonella*/poona-09-15/index.html

65. Chmielewski RAN, Frank JF. **Biofilm Formation and Control in Food Processing Facilities.** *Compr Rev Food Sci Food Saf.* 2003 Jan;2(1):22–32. doi: 10.1111/j.1541-4337.2003.tb00012.x.

66. Steenackers H, Hermans K, Vanderleyden J, De Keersmaecker SCJ. ***Salmonella* biofilms: An overview on occurrence, structure, regulation and eradication.** *Food Res Int.* 2012;45(2):502–31. doi: 10.1016/j.foodres.2011.01.038.

67. Galié S, García-Gutiérrez C, Miguélez EM, Villar CJ, Lombó F. **Biofilms in the food industry: Health**

aspects and control methods. *Front Microbiol.* 2018;9(MAY):1–18. doi: 10.3389/fmicb.2018.00898.

68. Uhlich GA, Chen C-Y, Cottrell BJ, Nguyen L-H. **Growth media and temperature effects on biofilm formation by serotype O157:H7 and non-O157 Shiga toxin-producing *Escherichia coli*.** *FEMS Microbiol Lett.* 2014 May;354(2):133–41. doi: 10.1111/1574-6968.12439.

69. Vogeleer P, Tremblay YDN, Jubelin G, Jacques M, Harel J. **Biofilm-Forming Abilities of Shiga Toxin-Producing *Escherichia coli* Isolates Associated with Human Infections.** Elkins CA, editor. *Appl Environ Microbiol.* 2016 Mar 1;82(5):1448–58. doi: 10.1128/AEM.02983-15.

70. Wang R, Kalchayanand N, Bono JL, Schmidt JW, Bosilevac JM. **Dual-Serotype Biofilm Formation by Shiga Toxin-Producing *Escherichia coli* O157:H7 and O26:H11 Strains.** *Appl Environ Microbiol.* 2012 Sep 1;78(17):6341–4. doi: 10.1128/AEM.01137-12.

71. Oliveira NM, Martinez-Garcia E, Xavier J, Durham WM, Kolter R, Kim W et al. **Biofilm Formation As a Response to Ecological Competition.** *PLOS Biol.* 2015 Jul 9;13(7):e1002191. doi: 10.1371/journal.pbio.1002191.

72. Chen D, Zhao T, Doyle MP. **Single- and mixed-species biofilm formation by *Escherichia coli* O157:H7 and *Salmonella*, and their sensitivity to levulinic acid plus sodium dodecyl sulfate.** *Food Control.* 2015 Nov;57:48–53. doi: 10.1016/j.foodcont.2015.04.006.

73. Pompermayer DMC, Gaylarde CC. **The influence of temperature on the adhesion of mixed cultures of *Staphylococcus aureus* and *Escherichia coli* to polypropylene.** *Food Microbiol.* 2000 Aug;17(4):361–5. doi: 10.1006/fmic.1999.0291.

74. West SA, Griffin AS, Gardner A, Diggle SP. **Social evolution theory for microorganisms.** *Nat Rev Microbiol.* 2006 Aug 1;4(8):597–607. doi: 10.1038/nrmicro1461.

75. Nadell CD, Xavier JB, Foster KR. **The sociobiology of biofilms.** *FEMS Microbiol Rev.* 2009 Jan;33(1):206–24. doi: 10.1111/j.1574-6976.2008.00150.x.

76. Sousa C, Novais Â, Magalhães A, Lopes J, Peixe L. **Diverse high-risk B2 and D *Escherichia coli* clones depicted by Fourier Transform Infrared Spectroscopy.** *Sci Rep.* 2013 Dec 20;3(1):3278. doi: 10.1038/srep03278.

77. Campos J, Sousa C, Mourão J, Lopes J, Antunes P, Peixe L. **Discrimination of non-typhoid *Salmonella* serogroups and serotypes by Fourier Transform Infrared Spectroscopy: A comprehensive analysis.** *Int J Food Microbiol.* 2018 Nov;285(March):34–41. doi: 10.1016/j.ijfoodmicro.2018.07.005.

78. Quilès F, Humbert F, Delille A. **Analysis of changes in attenuated total reflection FTIR fingerprints of *Pseudomonas fluorescens* from planktonic state to nascent biofilm state**. *Spectrochim Acta Part A Mol Biomol Spectrosc.* 2010 Feb;75(2):610–6. doi: 10.1016/j.saa.2009.11.026.

79. Sardari RRR, Kulcinskaja E, Ron EYC, Björnsdóttir S, Friðjónsson ÓH, Hreggviðsson GÓ et al. **Evaluation of the production of exopolysaccharides by two strains of the thermophilic bacterium *Rhodothermus marinus*.** *Carbohydr Polym.* 2017 Jan;156:1–8. doi: 10.1016/j.carbpol.2016.08.062.

80. Limoli DH, Jones CJ, Wozniak DJ. **Bacterial Extracellular Polysaccharides in Biofilm Formation and Function.** *Microbiol Spectr.* 2015 Jun 25;3(3):223–47. doi: 10.1128/9781555817466.chap11.

81. Kovács Á. **Impact of spatial distribution on the development of mutualism in microbes.** *Front Microbiol.* 2014 Nov 24;5(NOV):1–5. doi: 10.3389/fmicb.2014.00649/abstract.

82. Rani SA, Pitts B, Stewart PS. **Rapid Diffusion of Fluorescent Tracers into *Staphylococcus epidermidis* Biofilms Visualized by Time Lapse Microscopy.** *Antimicrob Agents Chemother.* 2005 Feb 1;49(2):728–32. doi: 10.1128/AAC.49.2.728-732.2005.

83. Oliveira A, Ribeiro HG, Silva AC, Silva MD, Sousa JC, Rodrigues CF, Melo LDR et al. **Synergistic**

Antimicrobial Interaction between Honey and Phage against *Escherichia coli* Biofilms. *Front Microbiol.* 2017 Dec 8;8(DEC):1–18. doi: 10.13140/RG.2.2.13176.96003.

84. Vidakovic L, Singh PK, Hartmann R, Nadell CD, Drescher K. **Dynamic biofilm architecture confers individual and collective mechanisms of viral protection.** *Nat Microbiol.* 2018 Jan 30;3(1):26–31. doi: 10.1038/s41564-017-0050-1.

Chapter V

Final Remarks and Future Perspectives

5.1 Final remarks

Food-related outbreaks, especially the ones caused by *Salmonella*, are still very common, in a global scale. *Salmonella* outbreaks are not only responsible for hundreds of human illnesses and even several deaths each year, but also lead to great economical losses for the food industry. *Salmonella* control in food working facilities and food products is essential for a substantial reduction of these outbreaks, and consequent illnesses and deaths, to be achieved. One of the most important characteristics of this pathogen to be so difficult to eliminate is its ability to form biofilms. While in the biofilm state, *Salmonella* cells become more resistant to chemical and physical removal procedures, which indicates that alternative control methods must be developed and applied so the elimination of *Salmonella* biofilms becomes more efficient.

The use of phages to control sessile *Salmonella* cells both in the biofilm state and as a monolayer of attached cells has revealed to be very promising, leading to very good reduction levels of *Salmonella* cell numbers. However, the potential emergence of phage-resistant bacteria, phage's narrow host ranges, and the difficulty of some phage to reach deeper layers of the biofilm structure, has impelled researchers to find ways to overcome these disadvantages. Here enters the application of synthetic biology tools to genetically engineer phage genomes in order to improve phage's natural properties. Some advances have been reached in this field, with the generation of phages with broader host ranges or with added anti-biofilm abilities, which shows that a greater effort to develop phage genome engineering approaches should be invested. Furthermore, as *Salmonella* can appear associated in biofilms with other pathogenic bacteria, like *E. coli*, the interactions species-species should be investigated more deeply in order to understand how these relationships may affect the phage action when applied as a biocontrol agent of mixed biofilms.

In this work, the *Salmonella* Enteritidis phage PVP-SE2 was thoroughly characterized regarding its genome, infectivity ability, and anti-biofilm capacity. It was shown, by sequencing and annotating its genome, that PVP-SE2 does not encode known antibiotic-resistance nor toxins, which makes this phage probably safe to be used as a biocontrol agent. Thus, phage PVP-SE2 was applied to *S.* Enteritidis adhered cells and biofilms, at different temperatures (4 °C and 22 °C), present on different food processing surfaces, such as polystyrene and stainless steel, and also contaminating poultry skin, since poultry is a main vehicle for *Salmonella* dissemination. Results showed that PVP-SE2 phage efficiently reduced 24- and 48-h old biofilms on both working surfaces, leading to 2 to 5 log CFU.cm^{-2} bacterial cell reductions, with better results being obtained at room temperature. This phage was also able to successfully reduce *S.* Enteritidis levels on poultry skins. Taking these

results together, this work showed that PVP-SE2 is a potential candidate to be a *Salmonella* control agent on food products and food contacting surfaces.

Although it was shown that PVP-SE2 performs really well on reducing *Salmonella* levels, its use presents some challenges, since 51% of PVP-SE2 genome encodes for proteins with unknown function. This means that some of these genes may encode for unknown toxic proteins or for proteins with other undesirable properties. Hence, another objective of this work was to delete, resorting to synthetic biology tools, genes with unknown and unnecessary functions from PVP-SE2 genome, making it completely safe. The first ORF present in PVP-SE2 genome is ORF_01, which was identified as a hypothetical protein with unknown functions, and so it was chosen to be deleted by BRED. Results showed that ORF_01 was successfully deleted from PVP-SE2 genome, and the mutation stability was confirmed until the 11th mutant phage generation. To this new phage the name PVP-SE2ΔOrf_01 was given, and its growth parameters and infection abilities were compared to the wild-type phage PVP-SE2. Deletion of Orf_01 was shown to influence the phage replication parameters, shortening its latent and rise periods, and also its burst size, but not the phage's infectivity, which was shown to infect as well as the wild-type phage planktonic cells in the exponential and stationary phases. These results show that, not only BRED is a suitable method to generate genetically modified phage genomes, but also that Orf_01 is not essential for PVP-SE2 replication and infection abilities.

Different bacteria are often found contaminating food processing facilities. Besides *Salmonella*, *E. coli*, another human pathogen, is commonly responsible for food related outbreaks, and it has been reported to form biofilms with *Salmonella* on food working surfaces and utensils. Hence, mono- and dual- species biofilms of *E. coli* and *S.* Enteritidis strains were studied in order to evaluate the relationships formed by these two species in a mixed consortium and how these interactions could impact the ability of two phages, DaICa (a newly isolated and sequenced phage) and φ135, isolated and characterized in 2010, to control these bacteria. Phage PVP-SE2 was not used in this study since it was not able to replicate in both *S.* Enteritidis strains used. Also, it was necessary to isolate, sequence, and annotate a new phage, named DaICa, since other phages in the CEB collection were also not able to infect both *E. coli* serotypes used. Mono- and dual-species biofilms were formed *in vitro* and the kinetics of biofilm formation were characterized. The results showed that both *E. coli* and *S.* Enteritidis strains presented higher numbers of viable cells in mono- than in dual-species biofilms, and confocal microscopy images revealed a spatial organization of strains in single species biofilms similar to their spatial distribution when forming mono-species

biofilms. Also, FTIR-ATR spectroscopy biofilm EPS analyses showed that EPSs spectra of dual-species biofilms can either be a mixture of both species EPS, or that the EPS of one strain predominates. *E. coli* and *S.* Enteritidis single and mixed biofilms were challenged by phages φ135 and DalCa, alone or in a cocktail. Single species biofilms suffered greater reductions in the number of viable cells than the mixed biofilms, for which the phage cocktail was used. Besides this, phages antibiofilm abilities were shown to be highly dependent on their infection characteristics, the bacterial growth parameters of their hosts, and the bacterial spatial distribution in biofilms, determined by CLSM. This study provided new insights regarding species-species interactions in dual-species biofilms and how this can influence the antibiofilm capacity of phages towards mixed biofilms.

In conclusion, the present work shows how important it is to continue studying the applicability and efficiency of phages in the control of pathogenic bacteria. The applicability of phages should not be restricted to the food industry, which was the main focus of this thesis, but also tested in other environments, like hospitals and industries in general. The recombinant phage obtained in this work shows that synthetic biology has come as a great help, since it is enabling researchers to improve phage's natural properties and to make them safer. The worked described herein showed the great potential of phages as biocontrol agents in industrial environments and food products. Biofilm structure and composition, and the polymicrobial nature of the biofilm pose an additional challenge to phages and impact their performance, and lastly, that synthetic biology tools can be used to increase safety and efficiency of phages

5.2 Future perspectives

This thesis has shed some light into the real capacity of phages to control *Salmonella* biofilms, but there is still the need to improve phage's antibiofilm abilities through genome engineering, and the necessity to better understand the relationship stablished between different species in mixed consortia, so phage control abilities can be improved. For example, not only *S.* Enteritidis is commonly related to foodborne outbreaks. Other *Salmonella* strains are responsible for illnesses and deaths, like *Salmonella* Newport, *Salmonella* Infantis, and others. Isolation of phages targeting these strains and creating a phage cocktail able to significantly reduce *Salmonella* numbers, either in the biofilm state or as superficially attached cells, would improve the chance of developing a phage-based product to successfully control a varied number of strains that can be present in a panoply of food products. Also, the combination of phages with other antimicrobial products, like disinfectants and weak acids, could improve the biofilm removal from surfaces.

The construction of PVP-SE2ΔOrf_01 was part of a plan to create a safe phage that encoded only the proteins necessary for its replication and infectivity. However, from the 31 ORFs found to have unknown functions, only one, Orf_01, was efficiently deleted by BRED, although the deletion of other ORFs was tried but without success. Although phage PVP-SE2ΔOrf_01 ability to infect *S.* Enteritidis planktonic cells was not affected by the absence of Orf_01 from its genome, this recombinant phage was not tested in biofilms. The use of phage PVP-SE2ΔOrf_01 to control *S.* Enteritidis biofilms should now be tested to confirm if PVP-SE2ΔOrf_01 has enhanced antibiofilm characteristics. Besides this, more genes with unknown function from PVP-SE2ΔOrf_01 should be attempted to be deleted for the creation of a more compact phage. However, the burst size attained should not be more reduced, otherwise the recombinant phage will have very low antimicrobial efficacy. In the future, other synthetic biology tools, like CRISPR/Cas, that greatly facilitates the selection of recombinant phages, thus shortening the time spent creating new gene deletions, should be chosen for phage genome editing. Besides this, the knowledge acquired about phage genome engineering should be applied to the creation of phages with enhanced performances, like broadening of the phage's host spectrum, the introduction of genes that encode for enzymes with known antibiofilm properties, and even addition of antimicrobial peptides.

Finally, the study of the interactions between species like *E. coli* and *Salmonella* in mixed populations, and how these interactions affect the structure of the dual-species biofilms and consequently the antibiofilm action of phages, should be deepened by the use of more

sophisticated methodologies like time-lapse microscopy imaging, flow cytometry and even spinning disk confocal microscopy imaging.